Technical Report ECOM-01870-180 May 1967

ANALYSIS OF AN APERTURE ANTENNA SYSTEM LOADED WITH AN INHOMOGENEOUS DIELECTRIC

C. E. C. Technical Report No. 7695-180

Contract No. DA 28-043-AMC-01870(E)

DA Project No. 1 PO 21101 AO42.01.02

Prepared by (Jesse Samuel)
J. Samuel Bitler

COOLEY ELECTRONICS LABORATORY

Department of Electrical Engineering
The University of Michigan
Ann Arbor, Michigan

for

U. S. Army Electronics Command, Fort Monmouth, N. J.

ABSTRACT

An analysis is made of an aperture system loaded with an inhomogeneous dielectric. The system consists of two parts. The first part is a section of rectangular waveguide extending from negative infinity along the z-axis to a distance z_0 back from an infinite, perfectly conducting ground plane, whose normal is also in the z direction. This section of waveguide is filled with a homogeneous dielectric. The second part is a section of rectangular of the same dimensions extending from z_0 to an aperture in the ground plane. This section of waveguide is filled with an inhomogeneous dielectric. The dielectric is characterized by a permeability and permittivity that varies exponentially with distance from the aperture.

At first the waveguide containing the inhomogeneous dielectric was considered to extend to negative infinity. A set of modes was found to satisfy Maxwell's equations and the required aperture symmetries when the field incident at the aperture was a conventional TE_{10} mode. The fields on the free-space side of the aperture were written in integral form using the free-space Green's function as a kernel and the aperture electric field was expanded in the waveguide modes. Application of the boundary condition on the tangential magnetic field resulted in an aperture reflection coefficient and the necessary equations to solve for the expansion coefficients.

Higher order modes at the aperture were considered as negligible at the interface between the homogeneous and inhomogeneous dielectric. A system reflection coefficient at this interface was calculated.

Numerical calculations were done by assuming waveguide dimensions of a width equal to 0.1 meter and a height equal to 0.05 meter. The frequency range was $0.86 \text{ GHz} < f < 1.39 \text{ GHz}$. Only the dominant mode was allowed to propagate in the system.

Aperture power reflection coefficient versus degree of inhomogeneity was calculated for various frequencies and values of aperture permeability and permittivity. The inhomogeneous material parameters were chosen from this data. A second set of curves assumed these inhomogeneous material parameters and calculated the lowest possible system

power reflection coefficient versus termination distance from the aperture of the inhomogeneous section into the homogeneous section. The balance of the system parameters was chosen from this data. A third set of curves assumed these system parameters and calculated the system power reflection coefficient versus frequency, for several resonant frequencies. This data was compared to a similar set calculated for a completely homogeneous system. The homogeneous system had the same general configuration as the inhomogeneous system except that its material parameters did not depend upon z. The aperture permeability and permittivity were assumed to be the same in both systems. The system power reflection versus frequency was considered as the measure of performance of the two systems.

With this as the criterion, the results show that at the lower frequency end the inhomogeneous system performs better than the homogeneous one. In the mid-frequency range, there was no appreciable difference in the performance of the systems. In the high-frequency range, the homogeneous system performed better than the inhomogeneous one.

ACKNOWLEDGMENTS

The author wishes to thank the members of his doctoral committee for their helpful comments and technical guidance. Special appreciation is due Professor D. M. Grimes for his help in preparing the final manuscript and Doctor V. H. Weston for his help with portions of the mathematical development.

Special gratitude is owed to Mrs. Jeanette Karnes, Mrs. Mary Belt, Miss Linda Beattie and Miss Heather Sawler for preparing this manuscript for publication.

Finally, the author is appreciative of the support given this work by the U. S. Army Electronics Command, Fort Monmouth, New Jersey.

TABLE OF CONTENTS

LIST OF TABLES

LIST OF SYMBOLS

Symbol	Meaning	First Appeared
x, y, z	rectangular coordinant variables	p. 3
$\hat{a}_x$, $\hat{a}_y$, $\hat{a}_z$	unit vectors	p. 3
z_0	termination distance	p. 3
∞	infinity	p. 3
μ	permeability	p. 3
ϵ	permittivity	p. 3
a	waveguide width	p. 3
b	waveguide height	p. 3
$\epsilon(z)$	permittivity as a function of z	eq. 1.1
$\mu(z)$	permeability as a function of z	eq. 1.2
C_ϵ	rate of change of permittivity	eq. 1.1
C_μ	rate of change of permeability	eq. 1.2
ϵ_0	free-space permittivity	p. 4
μ_0	free-space permeability	p. 4
TE	transverse electric	p. 4
TM	transverse magnetic	p. 4
LE	longitudinal electric	p. 4
E_x	x component of the electric field vector	p. 4
$\vec{E}$	electric field vector	eq. 2.1
$\vec{B}$	magnetic flux density vector	eq. 2.1
t	time	eq. 2.1
$\overline{H}$	magnetic field vector	eq. 2.2
$\overline{J}$	current density vector	eq. 2.2

LIST OF SYMBOLS (Cont.)

Symbol	Meaning	First Appeared
$\overline{D}$	electric flux density vector	eq. 2.2
ρ_t	time charge density	eq. 2.4
∇x	curl operator	p. .6
$\nabla \cdot$	divergence operator	p. 6
$\frac{\partial}{\partial}$	parital differential operator	p. 6
i	$\sqrt{-1}$	p. 6
ω	angular frequency	p. 6
∇^2	lapican operator	p. 7
∇	gradient operator	p. 7
E_y, E_z	components of the electric field vector	p. 7
H_x, H_y, H_z	components of the magnetic field vector	p. 7
$H_{\substack{x \\ y}}$	either the x or the y component of $\vec{H}$	eq. 2.23
$E_{\substack{x \\ y}}$	either the x or the y component of $\vec{E}$	eq. 2.28
φ, f(z), g(z)	scalar functions	eq. 2.29
$\Omega(x,y)$, $\psi(z)$	scalar functions	eq. 2.30
λ	separation constant	eq. 2.21
C_f	Either C_μ or C_ϵ as needed in text	p. 11
C_g	$C_\mu + C_\epsilon$	eq. 2.36
$k_g(0)$	aperture wave number	p. 11
R(z)	scalar function related to $\psi(z)$	p. 11
τ	variable	p. 11
ν_f	separation constant	p. 12
$H_p^{(1)}(x)$	Hankel function of the first kind of order p and argument x	eq. 2.40

LIST OF SYMBOLS (Cont.)

Symbol	Meaning	First Appeared
$H_p^{(2)}(x)$	Hankel function of the second kind of order p and argument x	eq. 2.41
$F_1(x,p)$	scalar function related to the Hankel functions	eq. 2.41
$\Gamma(m+\frac{1}{2})$	gamma function of argument $m+\frac{1}{2}$	eq. 2.42
m	summation index	eq. 2.42
T_{ν_f}	transmission coefficient	p. 13
Γ_{ν_f}	reflection coefficient	p. 13
k_x, k_y	separation constant	eq. 2.44
$A(k_x)$, $B(k_x)$, $C(k_y)$, $D(k_y)$	mode coefficients	eq. 2.44
$E_x^{(M)}$, $E_y^{(M)}$, $E_z^{(M)}$	electric field vector components for the TM modes	pp. 13, 14
A_{nm}	expansion coefficients	pp. 13, 14
n	summation index	pp. 13, 14
$H_x^{(M)}$, $H_y^{(M)}$, $H_z^{(M)}$	magnetic field vector	p. 14
$E_x^{(E)}$, $E_y^{(E)}$, $E_z^{(E)}$	electric field vector tangents for the TE modes	p. 14
B_{nm}	expansion coefficient	p. 14
$H_x^{(E)}$, $H_y^{(E)}$, $H_z^{(E)}$	magnetic field vector components for the TE	pp. 14, 15
η, ξ	aperture variables	p. 16
D(0)	constant	p. 16
$\chi_{nm}^{(M)}(Z)$	scalar function related to the TM modes	eq. 2.70
$\chi_{nm}^{(M)}(Z)$	scalar function related to the TE modes	eq. 2.72
$F_{nm}(0)$	constant related to aperture quantities	p. 19

LIST OF SYMBOLS (Cont.)

Symbol	Meaning	First Appeared
E_{nm}	expansion coefficient	p. 21
H_{nm}	expansion coefficient	eq. 2.90
$f(x,y)$	scalar function	eq. 2.90
ϵ_{nm}	1 or 2	eq. 2.92
δ	very small distance	p. 24
$\vec{M}_s$	magnetic surface current vector	eq. 2.97
$\hat{n}$	normal unit vector	eq. 2.97
$G(x, y, z, \eta, \xi)$	Green's function	eq. 2.98
$dS(\eta, \xi)$	differential surface vector	eq. 2.98
k	free-space wave number	eq. 2.98
$G_{nm}(0)$	scalar function related to aperture quantities	eq. 2.112
$I_{nm}^{(y)}$	integral	eq. 2.114
X, Y, Z	transformed rectangular variables	p. 27
R, Θ, Φ	spherical coordinate variables	p. 27
$s(k)$	surface	p. 28
$\Phi(k_x, k_y)$	scalar integral	p. 28
k_x^0, k_y^0	stationary phase points	p. 29
F_{nm}	expansion coefficient	p. 29
$h_{nm}(\Theta, \Phi)$	scalar function	p. 29
$\hat{a}_r, \hat{a}_\theta, \hat{a}_\phi$	unit spherical coordinate vector	eq. 2.131
P	Poynting vector	eq. 2.138
C_{nm}	constant related to $\chi_{nm}^{(E)}(0)$	p. 32
0^+	small aperture quantity	eq. 3.3

LIST OF SYMBOLS (Cont.)

Symbol	Meaning	First Appeared
D_{nm}	constant related to $\chi^{(E)}_{nm}(0)$ and $\chi^{(M)}_{nm}(0)$	p. 32
$\alpha, \beta, \gamma, \zeta$	summation indices	p. 32
$A^{(1)}_{n}, A^{(2)}_{\gamma}, A^{(3)}_{m}, A^{(4)}_{\delta}$	expansion coefficients	p. 34
$I^{\alpha\beta}_{nm}$	integral	eq. 3.17
$M_{\gamma\zeta}$	matrix elements	eq. 3.20
K	constant	p. 37
$\delta_{\gamma, \zeta}$	Kroneker delta	eq. 3.20
λ_0	free-space wave length	p. 39
N_{μ}, N_{ϵ}	constants related to C_{μ} and C_{ϵ}	p. 39
μ_r	relative permeability	p. 40
ϵ_r	relative permittivity	p. 40
μ_h	permeability in the homogeneous material	p. 41
ϵ_h	permittivity in the homogeneous material	p. 41
ρ	reflection coefficient	p. 41
y	quantity related to the admittance	p. 44
f_c	cut-off frequency of airguide	p. 47
G	normalized conductance	eq. 5.1
B	normalized susceptance	eq. 5.1
r_{μ}	ratio of permeabilities	eq. 5.2
R_{μ}	optimum value of r_{μ}	eq. 5.3
b_m	expansion coefficient	p. 94
K_c	cut-off wave number	p. 97

LIST OF SYMBOLS (Cont.)

Symbol	Meaning	First Appeared
H	constant related to the Hankel function	p. 97
$\epsilon_{nm}^{\alpha\beta}$	constant which depends upon n, m, α, β	p. 99
$K_{nm}^{\alpha\beta}$	constant related to $\epsilon_{nm}^{\alpha\beta}$	p. 100
$I, -I_8$	integrals	p. 101
x_0	particular value of x	p. 102
y_0	particular value of y	p. 102
B_k, A_k	limits of integration	p. 105
ω_i	weighting function	p. 106
x_i	Gaussian points	p. 106

LIST OF ILLUSTRATIONS

LIST OF ILLUSTRATIONS (cont.)

LIST OF APPENDICES

CHAPTER I

INTRODUCTION

With the general use of high-speed aircraft, missles, etc., it has become necessary to consider flush-mounted antennas that do not extend beyond the surface of the vehicle. These antennas may be any one of a number of possible designs, but they all must be backed by a cavity. There are strong limitations on physical size, frequency of operation, bandwidth, and efficiency of cavity-backed radiators. For the antenna to radiate effectively, the cavity size must be comparable to a wavelength at the radiated frequency which, except for very high frequencies, places a severe lower limit on the cavity size. For frequencies of less than 300 MHz, at least one dimension must be in excess of 1 meter.

One method of reducing the required size is to load, or fill, the cavity with a dielectric material which has a large mu-epsilon product. The reduction in the necessary cavity size is approximately the square root of the mu-epsilon product; since the electrical length is then larger than the physical length, a smaller cavity may be used. However, there are disadvantages of loading. In particular, there is a commensurate reduction in bandwidth and efficiency. The reduction in bandwidth results primarily from an unavoidable impedance mismatch at the aperture. For any one frequency, this mismatch may be removed by appropriate cancellation procedures, but such a technique is inherently narrowband. The larger the initial mismatch, the narrower the matched frequency range.

The reduction in efficiency results from the loss associated with any real material. The loss tangent of the dielectric material is independent of the antenna configuration; however, there are ways of reducing losses due to an effective loss tangent. If standing waves exist in the material, the loss is greater than it would be without them. Therefore, if the magnitude of the standing waves can be reduced in the material, then the efficiency is correspondingly higher. It is the impedance mismatch at the antenna aperture that generates the standing waves, so a better match at the aperture increases both the bandwidth and the efficiency.

The purpose of this investigation is to determine the radiative characteristics of a rectangular waveguide that is filled with an inhomogeneous dielectric. The question to be answered is whether a guide filled with a material whose permeability and permit-

tivity increase exponentially with distance can effect a better match to free-space than the same guide filled with a homogeneous material.

1.1 Review of the Literature

The use of dielectric materials to increase the efficiency of electrically small antennas has recieved much attention in the literature. A number of theoretical studies of loaded antennas have been made utilizing classical methods (Refs. 1-8) in coordinate systems for which the differential equations are separable; such as, the loop antenna loaded with a ferrite sphere (Refs. 2-7), cylinder (Ref. 1), or spheroid (Refs. 1,2), the biconical antenna loaded with a ferrite sphere (Refs. 3,8). These studies all show increases in radiation resistance at resonance which indicates the possibility of increased efficiency.

Radiation from waveguides and cavities (Refs. 9-24) has been treated using a number of different antenna shapes, geometries, and methods. Lewin (Ref. 9) derived a stationary expression for the impedance of an unloaded waveguide radiating into free-space. Cohen, Crowley, Levis (Ref. 14), and Adams (Ref. 21) solved a similar problem, but with dielectric loading. The impedance of an unloaded, rectangular waveguide opening through an infinite ground plane has been studied by other methods (Refs. 17, 18). Levine and Papas (Ref. 10) analyzed the admittance of an unloaded coaxial line opening through an infinite ground plane. Galejs (Refs. 11, 12) made a theoretical analysis of the dielectric-loaded, angular slot-antenna. Cohen (Ref. 14) studied transient phenomena to analyze the Q of the cavity antennas. A number of analyses of loaded cavity antennas have been made by using other techniques. For example, Tector (Ref. 20) made an experimental investigation of air-loaded cavity antennas. Adams (Ref. 21) treated the problem of radiation from a cavity-backed, slot-antenna that was loaded with an unbiased ferrite.

Radiation from ferrite-filled waveguides in which the ferrite is biased with a magnetic field has been treated by Angelakos, Korman, Tyras, and Held (Refs. 22, 23). Palais (Ref. 24) treated the case of a biased ferrite obstacle in the aperture of a rectangular waveguide. Further, integral transforms and Wiener-Hopf techniques have been applied to loaded and unloaded antennas (Refs. 25-30). However, in the case of loaded antennas, the material must be homogeneous.

The purpose of the inhomogeneous section of waveguide, which may be thought of as a taper or nonuniform section, is to match a homogeneous section to free-space

over as large a bandwidth as possible. Related problems using nonuniform transmission lines have been treated by various authors (Refs. 31-34). Walker and Wax (Ref. 31) treated the nonuniform line and reflection coefficient by deriving a first-order Riccati equation. Gurley (Ref. 32) treated the case of impedance matching with nonuniform lines. Klopfenstein (Ref. 33) and Collin (Ref. 34) refined and optimized the design of taper transmission lines.

1.2 Statement of the Problem

An open-end waveguide flanged by an infinite ground plane is studied. The waveguide is filled with a dielectric material with constant parameters μ and ϵ for $z = -\infty$ to a distance z_0 back from the aperture. The waveguide between z_0 and the aperture at $z = 0$ is filled with a dielectric whose parameters, μ and ϵ, depend upon distance from the aperture, (See Fig. 1.1). The variation in μ and ϵ is exponential with z but is independent of x and y. The material is assumed to be lossless. A TE_{10} mode is launched at (-) infinity, and the resulting field configurations are calculated.

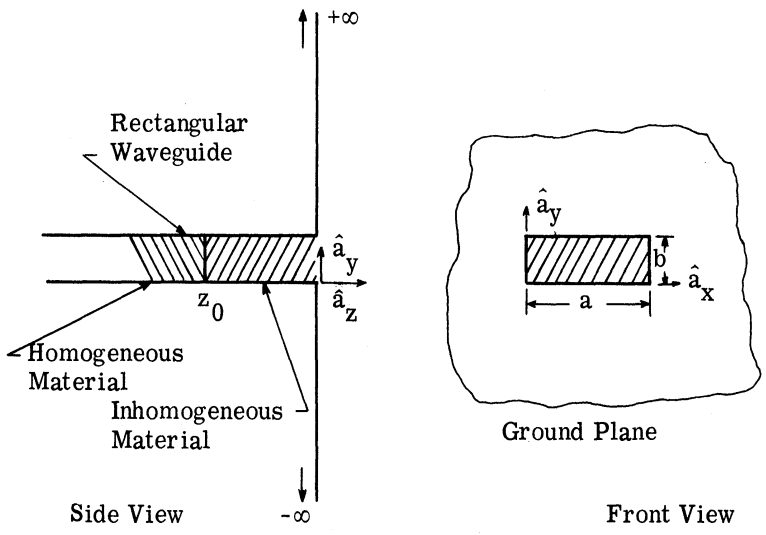

Fig. 1.1. Details of the antenna to be analyzed

The functional form of μ and ϵ was chosen to yield differential equations with solutions that can be written in closed form

$$\epsilon(z) = \epsilon(0)\, e^{C_\epsilon z} \tag{1.1}$$

$$\mu(z) = \mu(0)\, e^{C_\mu z} \tag{1.2}$$

The terms C_μ and C_ϵ are taken as real, positive constants. The terms $\epsilon(0)$ and $\mu(0)$ are arbitrary except that $\epsilon(0) / \epsilon_0 > 1$ and is real, and $\mu(0) / \mu_0 > 1$ and is real. It is further assumed that only the dominant mode propagates at all points in the wave guide.

Using these assumptions, Maxwell's equation can be solved in the inhomogeneous guide and yields the conventional rectangular waveguide TE and TM modes. However, there are other sets of conventional modes which do not exist because the material is inhomogeneous. To take advantage of the symmetry at the aperture, it is convenient to choose a particular linear combination of the TE and TM modes as a new set of modes. This set reduces to the longitudinal electric or LE modes in the limit as C_ϵ and C_μ go to zero. The LE modes contain all field components except E_x, and form a complete set for the type of symmetry in this antenna whenever the incident field contains no E_x. The electric field in the aperture is expanded in terms of the new set. The field $z > 0$ which uses the aperture electric field as its source is given in integral form.

The form of the fields guarantees continuity of the transverse electric fields through the aperture. Continuity of the transverse magnetic field is then imposed; an integral equation for the aperture field results.

The integral equation is solved in an approximate manner by expanding the aperture field in an infinite series and solving for the coefficients. The solution of the coefficients also yields an aperture reflection coeffiecient.

The interface at $z = z_0$ is treated by assuming that all higher order modes generated at the aperture decay to zero amplitude at the interface. Therefore, the boundary condition at the interface can be satisfied with TE_{10} modes only. This restricts possible mu-epsilon values in the homogeneous guide. Another reflection coefficient was found for this interface. This reflection coefficient can be thought of as an over-all or system coefficient.

Since the principle application is expected to be at frequencies normally cut off

in an air-filled waveguide, that assumption was used in this investigation. Numerical results were obtained by programming the 7090 computer.

CHAPTER II

SOLUTION OF MAXWELL'S EQUATIONS

2. 1 Maxwell's Equations in an Inhomogeneous Material

Maxwell's equations are given by

$$\nabla x\vec{E} = -\frac{\partial\vec{B}}{\partial t} \tag{2.1}$$

$$\nabla x\vec{H} = \vec{j} + \frac{\partial\vec{D}}{\partial t} \tag{2.2}$$

$$\nabla \cdot \vec{B} = 0 \tag{2.3}$$

$$\nabla \cdot \vec{D} = \rho_t \tag{2.4}$$

al is isotropic and linear, the following relations are valid

$$\vec{D} = \epsilon\vec{E} \tag{2.5}$$

$$\vec{B} = \mu\vec{H} \tag{2.6}$$

where ϵ and μ may be functions of position. If it is also assumed that the material is located in a source free region, then Maxwell's equations for each Fourier component with an $e^{-i\omega t}$ time dependence is written as follows

$$\frac{1}{\mu}(\nabla x\vec{E}) = i\omega\vec{H} \tag{2.7}$$

$$\frac{1}{\epsilon}(\nabla x\vec{H}) = -i\omega\vec{E} \tag{2.8}$$

$$\nabla \cdot (\epsilon\vec{E}) = 0 \tag{2.9}$$

$$\nabla \cdot (\mu\vec{H}) = 0 \tag{2.10}$$

By the proper manipulation of the above equations, and the use of appropriate vector identities, it is shown that

$$\nabla^2\vec{E} + \nabla[\frac{1}{\epsilon}(\nabla\epsilon) \cdot \vec{E}] + \omega^2 \mu\epsilon\vec{E} = \mu[\nabla(\frac{1}{\mu}) \times(\nabla\times\vec{E})] \tag{2.11}$$

$$\nabla^2\vec{H} + \nabla[\frac{1}{\mu}(\nabla\mu) \cdot \vec{H}] + \omega^2 \mu\epsilon\vec{H} = \epsilon[\nabla(\frac{1}{\epsilon}) \times(\nabla\times\vec{H})] \tag{2.12}$$

In rectangular coordinates, with the condition that μ and ϵ are functions of z only, Eqs. 2.11 and 2.12 reduce to

$$\nabla^2 E_x - (\frac{\partial}{\partial z} \ln \mu)\frac{\partial E_x}{\partial z} + \omega^2 \mu\epsilon E_x = -(\frac{\partial}{\partial z} \ln \mu\epsilon) \cdot \frac{\partial E_z}{\partial x} \tag{2.13}$$

$$\nabla^2 E_y - (\frac{\partial}{\partial z} \ln \mu)\frac{\partial E_y}{\partial z} + \omega^2 \mu\epsilon E_y = -(\frac{\partial}{\partial z} \ln \mu\epsilon) \cdot \frac{\partial E_z}{\partial y} \tag{2.14}$$

$$\nabla^2 E_z + (\frac{\partial}{\partial z} \ln \epsilon)\frac{\partial E_z}{\partial z} + (\frac{\partial^2}{\partial z^2} \ln \epsilon + \omega^2 \mu\epsilon) E_z = 0 \tag{2.15}$$

$$\nabla^2 H_x - (\frac{\partial}{\partial z} \ln \epsilon)\frac{\partial H_x}{\partial z} + \omega^2 \mu\epsilon H_x = -(\frac{\partial}{\partial z} \ln \mu\epsilon) \cdot \frac{\partial H_z}{\partial x} \tag{2.16}$$

$$\nabla^2 H_y - (\frac{\partial}{\partial z} \ln \epsilon)\frac{\partial H_y}{\partial z} + \omega^2 \mu\epsilon H_y = -(\frac{\partial}{\partial z} \ln \mu\epsilon) \cdot \frac{\partial H_z}{\partial y} \tag{2.17}$$

$$\nabla^2 H_z + (\frac{\partial}{\partial z} \ln \mu)\frac{\partial H_z}{\partial z} + (\frac{\partial^2}{\partial z^2} \ln \mu + \omega^2 \mu\epsilon) H_z = 0 \tag{2.18}$$

These equations are of particular interest because they illustrate the basic difference between homogeneous and inhomogeneous materials. The difference is that the transverse electric and magnetic fields are coupled to their longitudinal components with inhomogeneous material, not with homogeneous material. For example, consider a rectangular waveguide, filled with an inhomogeneous material as described above. Assume that the z coordinate is measured along the length of the guide. It is shown by Eqs. 2.13 and

2. 14 that when E_z is nonzero anywhere, then E_x and E_y must be nonzero somewhere. This means that the LE, (longitudinal electric), modes cannot exist as a complete set. However, the TE, (transverse electric), and TM, (transverse magnetic), modes still exist; and together they form a complete set.

2. 2 Fields in the Waveguide

The electromagnetic field in the waveguide is expressed as an infinite sum over an appropriate set of normal modes. The basic requirements of any set of normal modes is that: (1) it forms a complete set (all possible fields can be constructed with it) and (2) each member of the set satisfies both Maxwell's equations and the proper boundary conditions.

All field distributions for which $H_z = 0$ and all field distributions for which $E_z = 0$ can be expanded in a set of TM and TE modes respectively. From the principle of superposition, it follows that any field distribution can be expanded in a set of modes by taking a particular linear combination of the TM and TE modes. If the guide parameters change abruptly with position, then the particular linear combination of modes that describe the resulting field are determined by the nature of the discontinuity.

Still another reason for using a particular linear combination of TM and TE modes, as opposed to any other set, is shown in Eqs. 2. 13 through 2. 18. When $E_z = 0$, Eqs. 2. 13 and 2. 14 are second-order, linear, homogeneous differential equations. The equations are solved exactly and in closed-form for special functional forms of μ and ϵ, and similarly for Eqs. 2. 16 and 2. 17 when $H_z = 0$. If μ is of the same functional form as ϵ, then the solution of the TM and TE modes is further simplified. Only one of the four equations (Eqs. 2. 13, 2. 14, 2. 17, and 2. 18) needs to be solved, the other three are obtained from the first by relabeling the appropriate parameters.

2. 2. 1 Transverse Magnetic Modes.

For $H_z = 0$, Eqs. 2. 8 and 2. 10 reduce to

$$E_x = \frac{-i}{\omega\epsilon} \frac{\partial H_y}{\partial z} \tag{2. 19}$$

$$E_y = \frac{i}{\omega\epsilon} \frac{\partial H_x}{\partial z} \tag{2. 20}$$

$$E_z = \frac{i}{\omega\epsilon}\left[\frac{\partial H_y}{\partial x} - \frac{\partial H_x}{\partial y}\right] \tag{2.21}$$

$$\frac{\partial H_x}{\partial x} + \frac{\partial H_y}{\partial y} = 0 \tag{2.22}$$

where

$$\nabla^2 H_{\substack{x \\ y}} - \left(\frac{\partial}{\partial z} \ln \epsilon\right) \frac{\partial H_{\substack{x \\ y}}}{\partial z} + \omega^2 \mu\epsilon H_{\substack{x \\ y}} = 0 \tag{2.23}$$

2.2.2 Transverse Electric Modes. For $E_z = 0$, Eqs. 2.7 and 2.9 reduce to

$$H_x = \frac{i}{\omega\mu} \frac{\partial E_y}{\partial z} \tag{2.24}$$

$$H_y = \frac{-i}{\omega\mu} \frac{\partial E_x}{\partial z} \tag{2.25}$$

$$H_z = \frac{-i}{\omega\mu}\left[\frac{\partial E_y}{\partial x} - \frac{\partial E_x}{\partial y}\right] \tag{2.26}$$

$$\frac{\partial E_x}{\partial x} + \frac{\partial E_y}{\partial y} = 0 \tag{2.27}$$

where

$$\nabla^2 E_{\substack{x \\ y}} - \left(\frac{\partial}{\partial z} \ln \mu\right) \frac{\partial E_{\substack{x \\ y}}}{\partial z} + \omega^2 \mu\epsilon E_{\substack{x \\ y}} = 0 \tag{2.28}$$

and therefore the general form of differential equation to be solved is

$$\nabla^2 \phi - f(z) \frac{\partial \phi}{\partial z} + g(z)\phi = 0 \tag{2.29}$$

where

$$g(z) = \omega^2 \mu(z)\, \epsilon(z)$$

$$\phi = H_x \text{ or } H_y;\ f(z) = \frac{\partial}{\partial z} \ln \epsilon$$

$$\phi = E_x \text{ or } E_y;\ f(z) = \frac{\partial}{\partial z} \ln \mu$$

2.2.3 Solution of the Wave Equation for the TM and TE Modes. Equation 2.29 is separated into three differential equations, each one being a function of only one variable, by the standard separation of variable techniques. For example, let

$$\phi = \Omega(x, y)\psi(z) \tag{2.30}$$

then

$$\nabla^2 \Omega(x, y) + \lambda^2 \Omega(x, y) = 0 \tag{2.31}$$

$$\frac{d^2\psi}{dz^2} - f(z)\frac{d\psi}{dz} + [g(z) - \lambda^2]\psi = 0 \tag{2.32}$$

Notice that Eq. 2.31, which describes the field behavior in the transverse plane, is the same as if the material were homogeneous. Therefore no property of the transverse variables, such as orthogonality, etc., is affected by the inhomogenity of the material, when the material inhomogenity is dependent on the longitudinal direction only.

The functions $f(z)$ and $g(z)$ must be given before a solution of Eq. 2.32 can be obtained. Usually, Eq. 2.32 does not have a closed-form solution. Therefore, it is necessary to choose $\mu(z)$ and $\epsilon(z)$, so that closed-form solutions do exist and will yield useful results.

One such form of $\mu(z)$ and $\epsilon(z)$ is

$$\mu(z) = \mu(0)\, e^{C_\mu z} \tag{2.33}$$

$$\epsilon(z) = \epsilon(0)\, e^{C_\epsilon z} \tag{2.34}$$

where $\mu(0)$, C_μ, $\epsilon(0)$, and C_ϵ are arbitrary constants.

As will be shown, these forms are particularly useful because closed-form solutions exist.

In order to obtain the solution of Eq. 2.32 let $f(z) = C_f$, where $C_f = C_\epsilon$ when $\phi = H_x$ or H_y and $C_f = C_\mu$ when $\phi = E_x$ or E_y. Then

$$g(z) = \omega^2 \mu(0) \epsilon(0) e^{(C_\mu + C_\epsilon) z} \tag{2.35}$$

for either case, therefore

$$\frac{d^2}{dz^2}\psi - C_f \frac{d\psi}{dz} + [k_g^2(0) e^{\frac{1}{2}C_g z} - \lambda^2]\psi = 0 \tag{2.36}$$

where

$$k_g^2(0) = \omega^2 \mu(0) \epsilon(0)$$

$$C_g = C_\mu + C_\epsilon$$

Upon defining a quantity $R \equiv \psi(z)\, e^{-\frac{1}{2}C_f z}$, the resulting differential equation for $R(z)$ is

$$\frac{d^2 R}{dz^2} + [k_g^2(0) e^{C_g z} - (\lambda^2 + \tfrac{1}{4} C_f^2)] R = 0 \tag{2.37}$$

and upon defining a new variable

$$\tau = \frac{2k_g(0)}{C_g} e^{\frac{1}{2}C_g z}$$

the resulting differential equation with τ as the independent variable is

$$\tau^2 \frac{d^2 R}{d\tau^2} + \tau \frac{dR}{d\tau} + [\tau^2 - \nu_f^2] R = 0 \tag{2.38}$$

where

$$\nu_f^2 \equiv \frac{4\lambda^2 + C_f^2}{C_g^2}$$

Equation 2.38 is Bessel's equation and its solution is the Bessel function of order ν,

$$\psi(z) = e^{\frac{1}{2}C_f z} R_{\nu_f}\left(\frac{2k_g(0)}{C_g} e^{\frac{1}{2}C_g z}\right) \tag{2.39}$$

Equation 2.36 is a second-order differential equation with two independent solutions, which are necessary to satisfy boundary conditions in an appropriate linear combination of these solutions. An appropriate linear combination of these solutions are necessary to satisfy the boundary condition. The particular linear combination of solutions that describe propagation down the guide are the Hankel functions. This property can be shown from the asymptotic form of the Hankel functions given by Bateman, (Ref. 35).

$$H_p^{(1)}(x) = \frac{\sqrt{2}\, F_1(x, p)}{\pi(x^2 - p^2)^{\frac{1}{4}}} e^{i\left[\sqrt{x^2 - p^2} + p \sin^{-1}(p/x) - \frac{\pi}{2}(p + \frac{1}{2})\right]} \tag{2.40}$$

and

$$H_p^{(2)}(x) = \frac{\sqrt{2}\, F_1^*(x, p)}{\pi(x^2 - p^2)^{\frac{1}{4}}} e^{-i\left[\sqrt{x^2 - p^2} + p \sin^{-1}(p/x) - \frac{\pi}{2}(p + \frac{1}{2})\right]} \tag{2.41}$$

where

$$F_1(x, p) = \sum_{m=0}^{M-1} 2^m b_m \Gamma(m + \tfrac{1}{2})(-i)^m (x^2 - p^2)^{\frac{-m}{2}} + 0(x^{-M}) \tag{2.42}$$

The terms $x > p > 0$, and x is real.

b_m are given functions of x and p.

The Hankel functions, $H_p^{(1)}(x)$ and $H_p^{(2)}(x)$ are of the first and second kind, respectively. When $x > p$, $H_p^{(1)}(x)$ represents a positive traveling wave and $H_p^{(2)}(x)$ represents a negative traveling wave. A time dependence of $e^{-i\omega t}$ is assumed throughout. The function $\psi(z)$ is written in terms of the Hankel functions as

$$\psi(z) = e^{\frac{i}{2}C_f z}\left[T_{\nu_f} H_{\nu_f}^{(1)}\left(\frac{2k_g(0)}{C_g} e^{\frac{i}{2}C_g z}\right) + \Gamma_{\nu_f} H_{\nu_f}^{(2)}\left(\frac{2k_g(0)}{C_g} e^{\frac{i}{2}C_g z}\right)\right] \qquad (2.43)$$

where

T_{ν_f} is a constant of the system and plays the role of a transmission coefficient and

Γ_{ν_f} is a constant of the system, and plays the role of a reflection coefficient. They are determined by the nature of the discontinuity.

The solution of Eq. 2.31 is the same as it would be if the guide were homogeneous, and it is

$$\Omega(x,y) = [A(k_x)\sin k_x x + B(k_x)\cos k_x x][C(k_y)\sin k_y y + D(k_y)\cos k_y y] \qquad (2.44)$$

where

$$k_x^2 + k_y^2 = \lambda^2$$

The TM modes are found by combining Eqs. 2.19 through 2.22 with the solutions of the differential equations and the boundary conditions at the wall.

$$E_x^{(M)} = \sum_{n,m} i A_{nm} \left(\frac{1}{\omega\epsilon}\right)\left(\frac{n\pi}{a}\right) \cos\frac{n\pi x}{a} \sin\frac{m\pi y}{b} \frac{d\psi^{(M)}(z)}{dz} \qquad (2.45)$$

$$E_y^{(M)} = \sum_{n,m} i A_{nm} \frac{1}{\omega\epsilon}\left(\frac{m\pi}{b}\right) \sin\frac{n\pi x}{a} \cos\frac{m\pi y}{b} \frac{d\psi^{(M)}(z)}{dz} \qquad (2.46)$$

$$E_z^{(M)} = \sum_{n,m} i A_{nm} \frac{1}{\omega\epsilon} \left(\frac{n^2\pi^2}{a^2} + \frac{m^2\pi^2}{b^2}\right) \sin\frac{n\pi x}{a} \sin\frac{m\pi y}{b} \psi^{(M)}(z) \qquad (2.47)$$

$$H_x^{(M)} = \sum_{n,m} A_{nm} \left(\frac{m\pi}{b}\right) \sin\frac{n\pi x}{a} \cos\frac{m\pi y}{b} \psi^{(M)}(z) \qquad (2.48)$$

$$H_y^{(M)} = -\sum_{n,m} A_{nm} \left(\frac{n\pi}{a}\right) \cos\frac{n\pi x}{a} \sin\frac{m\pi y}{b} \psi^{(M)}(z) \qquad (2.49)$$

$$H_z^{(M)} = 0 \qquad (2.50)$$

where

$$\epsilon = \epsilon(0) \epsilon^{C_\epsilon z}$$

The TE modes are found by combining Eqs. 2.24 through 2.27 with the solutions of the differential equations and the boundary conditions at the wall.

$$E_x^{(E)} = \sum_{n,m} B_{nm} \left(\frac{m\pi}{b}\right) \cos\frac{n\pi x}{a} \sin\frac{m\pi y}{b} \psi^{(E)}(z) \qquad (2.51)$$

$$E_y^{(E)} = -\sum_{n,m} B_{nm} \left(\frac{n\pi}{a}\right) \sin\frac{n\pi x}{a} \cos\frac{m\pi y}{b} \psi^{(E)}(z) \qquad (2.52)$$

$$E_z^{(E)} = 0 \qquad (2.53)$$

$$H_x^{(E)} = -i \sum_{n,m} B_{nm} \left(\frac{1}{\omega\mu}\right)\left(\frac{n\pi}{a}\right) \sin\frac{n\pi x}{a} \cos\frac{m\pi y}{b} \frac{d\psi^{(E)}}{dz} \qquad (2.54)$$

$$H_y^{(E)} = -i \sum_{n,m} B_{nm} \left(\frac{1}{\omega\mu}\right)\left(\frac{m\pi}{b}\right) \cos\frac{n\pi x}{a} \sin\frac{m\pi y}{b} \frac{d\psi^{(E)}}{dz} \qquad (2.55)$$

$$H_z^{(E)} = i \sum_{n,m} B_{nm} \left(\frac{1}{\omega\mu}\right)\left(\frac{n^2\pi^2}{a^2} + \frac{m^2\pi^2}{b^2}\right) \cos\frac{n\pi x}{a} \cos\frac{m\pi y}{b} \psi^{(E)} \qquad (2.56)$$

where

$$\mu = \mu(0)\, e^{C_\mu z}$$

2.2.4 A Set of Modes in which the Aperture Fields are Expanded. As previously stated, the normal modes that must be used in the expansion of fields in the waveguide are a linear combination of the TM and TE modes.

The TE_{10} wave that is incident from the left in Fig. 2.1 does not have an electric field component in the $\hat{a}_x$ direction. Now the fields in the transverse plane are symmetric about the lines $x = a/2$ and $y = b/2$. Therefore, if the incident field has no component in the x direction, there can be no x directed component in the radiated field.

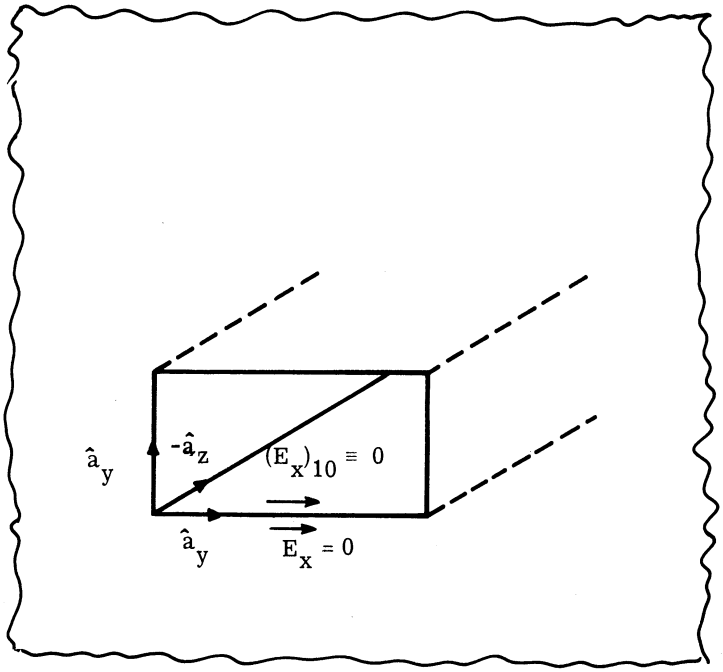

Fig. 2.1 Details of the aperture

According to Eq. 2.100, there will be an x directed electric field in the far field, unless $E_x(\eta, \xi) = 0$ throughout the aperture of the guide. Therefore, we conclude that the proper linear combination of TM and TE modes has no electric field component in the $\hat{a}_x$ direction. All other field components will exist.

The solution is now specialized to the case where there is no x directed electric field incident upon the aperture. When the aperture is taken as $z = 0$, the relation between the coefficient A_{nm} and B_{nm} is

$$B_{nm}\left(\frac{m\pi}{b}\right)\psi^{(E)}(0) + i\,A_{nm}\frac{1}{\omega\epsilon(0)}\,\frac{n\pi}{a}\,\frac{d}{dz}\psi^{(M)}(0) = 0 \tag{2.57}$$

and so

$$A_{nm} = B_{nm}\,i\,\frac{\omega\epsilon(0)\frac{m\pi}{b}}{\frac{n\pi}{a}}\,\frac{\psi^{(E)}(0)}{\frac{d\psi^{(M)}(0)}{dz}} \tag{2.58}$$

This can be simplified by defining

$$D(0) \equiv \frac{\epsilon(0)\psi^{(E)}(0)}{\frac{d\psi^{(M)}(0)}{dz}}$$

with the result

$$A_{nm} = B_{nm}\,\frac{i\omega\left(\frac{m\pi}{b}\right)}{\left(\frac{n\pi}{a}\right)}\,D(0) \tag{2.59}$$

A set of modes which represent propagation of energy down the guide and contain the proper symmetry in the aperture are

$$E_x = -\sum_{n,m} B_{nm}\left(\frac{m\pi}{b}\right)\cos\frac{n\pi x}{a}\,\sin\frac{m\pi y}{b}\left[\psi^{(E)}(z) - \frac{D(0)}{\epsilon}\,\frac{d\psi^{(M)}(z)}{dz}\right] \tag{2.60}$$

$$E_y = + \sum_{n,m} B_{nm} \left(\frac{a}{n\pi}\right) \sin\frac{n\pi x}{a} \cos\frac{m\pi y}{b} \left[\frac{n^2\pi^2}{a^2} \psi^{(E)}(z) + \frac{m^2\pi^2}{b^2} \frac{D(0)}{\epsilon} \frac{d\psi^{(M)}}{dz}(z)\right] \quad (2.61)$$

$$E_z = + \sum_{n,m} B_{nm} \left(\frac{m\pi/b}{n\pi/a}\right) \left(\frac{n^2\pi^2}{a^2} + \frac{m^2\pi^2}{b^2}\right) \sin\frac{n\pi x}{a} \sin\frac{m\pi y}{b} \frac{D(0)}{\epsilon} \psi^{(M)}(z) \quad (2.62)$$

$$H_x = + i \sum_{n,m} B_{nm} \left(\frac{a}{n\pi}\right) \sin\frac{n\pi x}{a} \cos\frac{m\pi y}{b} \left[\frac{1}{\omega\mu} \frac{n^2\pi^2}{a^2} \frac{d\psi^{(E)}(z)}{dz} - \frac{m^2\pi^2}{b^2} \omega D(0) \psi^{(M)}(z)\right] \quad (2.63)$$

$$H_y = + i \sum_{n,m} B_{nm} \left(\frac{m\pi}{b}\right) \cos\frac{n\pi x}{a} \sin\frac{m\pi y}{b} \left[\frac{1}{\omega\mu} \frac{d\psi^{(E)}(z)}{dz} + \omega D(0) \psi^{(M)}(z)\right] \quad (2.64)$$

$$H_z = - i \sum_{n,m} B_{nm} \left(\frac{n^2\pi^2}{a^2} + \frac{m^2\pi^2}{b^2}\right) \cos\frac{n\pi x}{a} \cos\frac{m\pi y}{b} \left(\frac{1}{\omega\mu}\right) \psi^{(E)}(z) \quad (2.65)$$

where

$$\epsilon \equiv \epsilon(0)\, e^{C_\epsilon z}$$

and

$$\mu \equiv \mu(0)\, e^{C_\mu z}$$

In order to arrive at the final form of the normal modes, the proper functional form of $\psi^{(E)}(z)$ and $\psi^{(M)}(z)$ must be determined from Eq. 2.43. Combining Eq. 2.43 with the boundary condition gives

$$\psi^{(M)}(z) = e^{\frac{1}{2} C_\epsilon z} \left\{ T^{(M)}_{\nu_\epsilon} H^{(1)}_{\nu_\epsilon} \left[\frac{2k_g(0)}{C_g} e^{\frac{1}{2} C_g z}\right] + \Gamma^{(M)}_{\nu_\epsilon} H^{(2)}_{\nu_\epsilon} \left[\frac{2k_g(0)}{C_g} e^{\frac{1}{2} C_g z}\right] \right\} \quad (2.66)$$

where

$$\nu_\epsilon \equiv \frac{\sqrt{4\left(\frac{n^2\pi^2}{a^2}+\frac{m^2\pi^2}{b^2}\right)+C_\epsilon^2}}{C_\epsilon + C_\mu}$$

and

$$\psi^{(E)}(z) = e^{\frac{1}{2}C_\mu z}\left\{T^{(E)}_{\nu_\mu} H^{(1)}_{\nu_\mu}\left[\frac{2k_g(0)}{C_g} e^{\frac{1}{2}C_g z}\right] + \Gamma^{(E)}_{\nu_\mu} H^{(2)}_{\nu_\mu}\left[\frac{2k_g(0)}{C_g} e^{\frac{1}{2}C_g z}\right]\right\} \quad (2.67)$$

where

$$\nu_\mu \equiv \frac{\sqrt{4\left(\frac{n^2\pi^2}{a^2}+\frac{m^2\pi^2}{b^2}\right)+C_\mu^2}}{C_\epsilon + C_\mu}$$

The incident wave is characterized by $n = 1$, $m = 0$. Since it is partially reflected at the aperture, there is both a forward and a backward traveling wave. Any other modes that are present will be generated at the discontinuity and will travel in the backward direction only. For this reason

$$\psi^{(M)}(z) = e^{\frac{1}{2}C_\epsilon z}\Gamma^{(M)}_{\nu_\epsilon} H^{(2)}_{\nu_\epsilon}\left[\frac{2k_g(0)}{C_g} e^{\frac{1}{2}C_g z}\right] \quad (2.68)$$

and

$$\psi^{(E)}(z) = e^{\frac{1}{2}C_\mu z}\left\{T^{(E)}_{0_\mu} H^{(1)}_{0_\mu}\left[\frac{2k_g(0)}{C_g} e^{\frac{1}{2}C_g z}\right] + \Gamma^{(E)}_{0_\mu} H^{(2)}_{0_\mu}\left[\frac{2k_g(0)}{C_g} e^{\frac{1}{2}C_g z}\right] + \Gamma^{(E)}_{\nu_\mu} H^{(2)}_{\nu_\mu}\left[\frac{2k_g(0)}{C_g} e^{\frac{1}{2}C_g z}\right]\right\} \quad (2.69)$$

where the subscript 0 implies the zeroth order mode, i. e., n = 1, m = 0.

The function $\chi(z)$ is defined as

$$\chi^{(M)}_{nm}(z) \equiv e^{\frac{1}{2}C_\epsilon z} H^{(2)}_{\nu_\epsilon}\left[\frac{2k_g(0)}{C_g} e^{\frac{1}{2}C_g z}\right] \tag{2.70}$$

$$\chi^{(E)}_{10}(z) \equiv e^{\frac{1}{2}C_\mu z}\left\{ H^{(1)}_{0_\mu}\left[\frac{2k_g(0)}{C_g} e^{\frac{1}{2}C_g z}\right] + \frac{\Gamma^{(E)}_{0_\mu}}{T^{(E)}_{0_\mu}} H^{(2)}_{0_\mu}\left[\frac{2k_g(0)}{C_g} e^{\frac{1}{2}C_g z}\right]\right\} \tag{2.71}$$

$$\chi^{(E)}_{nm}(z) \equiv e^{\frac{1}{2}C_\mu z} H^{(2)}_{\nu_\mu}\left[\frac{2k_g(0)}{C_g} e^{\frac{1}{2}C_g z}\right] \tag{2.72}$$

All quantities involving $\psi^{(M)}(z)$ and $\psi^{(E)}(z)$ are written in terms of $\chi^{(M)}(z)$ and $\chi^{(E)}(z)$.

$$\psi^{(M)}(z) = \Gamma^{(M)}_{\nu_\epsilon} \chi_{nm}(z) \tag{2.73}$$

$$\psi^{(E)}(z) = T^{(E)}_{0_\mu} \chi^{(E)}_{10}(z) + \Gamma^{(E)}_{\nu_\mu} \chi^{(E)}_{nm}(z) \tag{2.74}$$

$$D(0)\frac{d\psi^{(M)}(z)}{dz} = \Gamma^{(E)}_{\nu_\mu} \frac{\epsilon(0)\chi^{(E)}_{nm}(0)}{\frac{d}{dz}\chi^{(M)}_{nm}(0)} \frac{d}{dz}\chi^{(M)}(z) \tag{2.75}$$

Define

$$F_{nm}(0) = \frac{\epsilon(0)\chi^{(E)}_{nm}(0)}{\frac{d}{dz}\chi^{(M)}_{nm}(0)}$$

then

$$D(0)\frac{d\psi^{(M)}(z)}{dz} = \Gamma^{(E)}_{\nu\mu} F_{nm}(0)\frac{d}{dz}\chi^{(M)}(z) \tag{2.76}$$

and

$$D(0)\,\psi^{(M)}(z) = \Gamma^{(E)}_{\nu\mu} F_{nm}(0)\,\chi^{(M)}(z) \tag{2.77}$$

therefore

$$E_x = -\sum_{n,m}{}' B_{nm}\left(\frac{m\pi}{b}\right)\Gamma^{(E)}_{\nu\mu}\cos\frac{n\pi x}{a}\sin\frac{m\pi y}{b}\left[\chi^{(E)}_{nm}(z) - \frac{F_{nm}(0)}{\epsilon}\frac{d}{dz}\chi^{(M)}_{nm}(z)\right] \tag{2.78}$$

$$E_y = B_{10}\frac{\pi}{a}T^{(E)}_{0\mu}\sin\frac{\pi x}{a}\chi^{(E)}_{10}(z) + \sum_{n,m}{}' B_{nm}\left(\frac{a}{n\pi}\right)\Gamma^{(E)}_{\nu\mu}\sin\frac{n\pi x}{a}\cos\frac{m\pi y}{b} \tag{2.79}$$

$$\left[\frac{n^2\pi^2}{C^2}\chi^{(E)}_{nm}(z) + \frac{m^2\pi^2}{b^2}\frac{F_{nm}(0)}{\epsilon}\frac{d}{dz}\chi^{(M)}_{nm}(z)\right]$$

$$E_z = \sum_{n,m}{}' B_{nm}\frac{\left(\frac{m\pi}{b}\right)}{\left(\frac{n\pi}{a}\right)}\Gamma^{(E)}_{\nu\mu}\left(\frac{n^2\pi^2}{a^2}+\frac{m^2\pi^2}{b^2}\right)\sin\frac{n\pi x}{a}\sin\frac{m\pi x}{b}\frac{F_{nm}(0)}{\epsilon}\chi^{(M)}_{nm}(z) \tag{2.80}$$

$$H_x = iB_{10}\left(\frac{\pi}{a}\right)T^{(E)}_{0\mu}\frac{1}{\omega\mu}\sin\frac{\pi x}{a}\frac{d}{dz}\chi^{(E)}_{10} + i\sum_{n,m}{}' B_{nm}\left(\frac{a}{n\pi}\right)\Gamma^{(E)}_{\nu\mu}\sin\frac{n\pi x}{a}\cos\frac{m\pi y}{b} \tag{2.81}$$

$$\left[\frac{1}{\omega\mu}\frac{n^2\pi^2}{a^2}\frac{d}{dz}\chi^{(E)}_{nm} - \frac{m^2\pi^2}{b^2}\omega F_{nm}(0)\,\chi^{(M)}_{nm}(z)\right] \tag{2.82}$$

$$H_y = i\sum_{n,m}{}' B_{nm}\left(\frac{m\pi}{b}\right)\Gamma^{(E)}_{\nu\mu}\cos\frac{n\pi x}{a}\sin\frac{m\pi y}{b}\left[\frac{1}{\omega\mu}\frac{d}{dz}\chi^{(E)}_{nm}(z) + \omega F_{nm}(0)\chi^{(M)}_{nm}(z)\right]$$

$$H_z = -iB_{10}\frac{\pi^2}{a^2}T_{0\mu}^{(E)}\frac{1}{\omega\mu}\cos\frac{\pi x}{a}\chi_{10}^{(E)} - i\sum_{n,m}{}' B_{nm}$$

$$\Gamma_{\nu\mu}^{(E)}\left(\frac{n^2\pi^2}{a^2}+\frac{m^2\pi^2}{b^2}\right)\cos\frac{n\pi x}{a}\cos\frac{m\pi y}{b}\frac{1}{\omega\mu}\chi_{nm}^{(E)}(z) \qquad (2.83)$$

Next, let

$$B_{10}\frac{\pi^2}{a^2}T_{0\mu}^{(E)} \equiv E_{10}$$

$$B_{nm}\Gamma_{\nu\mu}^{(E)} \equiv E_{nm}$$

and multiply each of the equations by $\frac{n\pi}{a}$.

The resulting expressions for the fields in the waveguide are

$$E_x = -\sum_{n,m}E_{nm}\left(\frac{n\pi}{a}\right)\left(\frac{m\pi}{b}\right)\cos\frac{n\pi x}{a}\sin\frac{m\pi y}{b}\left[\chi_{nm}^{(E)}(z) - \frac{F_{nm}(0)}{\epsilon}\frac{d}{dz}\chi_{nm}^{(M)}(z)\right] \qquad (2.84)$$

$$E_y = E_{10}\sin\frac{\pi x}{a}\chi_{10}^{(E)}(z) + \sum_{n,m}E_{nm}\sin\frac{n\pi x}{a}\cos\frac{m\pi y}{b}\left[\frac{n^2\pi^2}{a^2}\chi_{nm}^{(E)}(z) + \frac{m^2\pi^2}{b^2\epsilon}F_{nm}(0)\frac{d}{dz}\chi_{nm}^{(M)}(z)\right] \qquad (2.85)$$

$$E_z = \sum_{n,m}{}' E_{nm}\left(\frac{m\pi}{b}\right)\left(\frac{n^2\pi^2}{a^2}+\frac{m^2\pi^2}{b^2}\right)\sin\frac{n\pi x}{a}\sin\frac{m\pi y}{b}\frac{F_{nm}(0)}{\epsilon}\chi_{n,m}^{(M)}(z) \qquad (2.86)$$

$$H_x = iE_{10}\frac{1}{\omega\mu}\sin\frac{\pi x}{a}\frac{d}{dz}\chi_{10}^{(E)}(z) + i\sum_{n,m}{}' E_{nm}\sin\frac{n\pi x}{a}\cos\frac{m\pi y}{b}\left[\frac{1}{\omega\mu}\frac{n^2\pi^2}{a^2}\frac{d}{dz}\chi_{nm}^{(E)}(z) - \frac{m^2\pi^2}{b^2}\omega F_{nm}(0)\chi_{nm}^{(M)}(z)\right] \qquad (2.87)$$

$$H_y = i\sum_{n,m}{}' E_{nm}\left(\frac{n\pi}{a}\right)\left(\frac{m\pi}{b}\right)\cos\frac{n\pi x}{a}\sin\frac{m\pi y}{b}\left[\frac{1}{\omega\mu}\frac{d}{dz}\chi^{(E)}_{n,m}(z) + \omega F_{nm}(0)\chi^{(M)}_{nm}(z)\right] \quad (2.88)$$

$$H_z = -iE_{10}\left(\frac{\pi}{a}\right)\frac{1}{\omega\mu}\cos\frac{\pi x}{a}\chi^{(E)}_{10} - i\sum_{nm}{}' E_{nm}\left(\frac{n\pi}{a}\right)\left(\frac{n^2\pi^2}{a^2}+\frac{m^2\pi^2}{b^2}\right)\frac{1}{\omega\mu}$$

$$\cos\frac{n\pi x}{a}\cos\frac{m\pi y}{b}\chi^{(E)}_{nm}(z) \quad (2.89)$$

where the primes indicate that the term $n = 1,\ m = 0$ is omitted from the sum.

2.2.5 Selection Rules. Selection rules for the expansion coefficient is determined from the symmetry relationships in the aperture. The symmetry of the total H_z field is determined by the symmetry of the aperture and the impressed field. Since the aperture is symmetric in both the x and y directions about the lines $x = \frac{a}{2}$ and $y = \frac{b}{2}$, the symmetry in the x direction is given by the H_z field of the TE_{10} mode. That is, H_z is an odd function of x with respect to the line $x = \frac{a}{2}$, but is an even function of y with respect to the line $y = \frac{b}{2}$.

The total H_z in the aperture is expressed as a Fourier series

$$H_z(z=0) = \sum_{n,m}^{\infty} H_{nm}\cos\frac{n\pi x}{a}\cos\frac{m\pi y}{b} = f(x,y) \quad (2.90)$$

where f(x, y) is written to display the symmetry relation shown above. The integral over the aperture is

$$\int_0^a\int_0^b dx\,dy\sum_{n',m'}^{\infty} H_{n'm'}\cos\frac{n'\pi x}{a}\cos\frac{m'\pi y}{b}\cos\frac{n\pi x}{a}\cos\frac{m\pi y}{b} = \int_0^a\int_0^b dx\,dy\,f(x,y)\cos\frac{n\pi x}{a}\cos\frac{m\pi y}{b} \quad (2.91)$$

and after ultilizing orthogonality of the trigonometric functions

$$H_{nm}\,\epsilon_{nm}\left(\frac{ab}{4}\right) = \int_0^a\int_0^b dx\,dy\,f(x,y)\cos\frac{n\pi x}{a}\cos\frac{m\pi y}{b} \quad (2.92)$$

$$\epsilon_{nm} = \begin{cases} 2 \text{ if } n = 0, \ m \neq 0 \\ 2 \text{ if } m = 0, \ n \neq 0 \\ 1 \text{ otherwise} \end{cases}$$

The expression for H_{nm} is simplified by substituting

$$\eta = x - \frac{a}{2} \qquad \xi = y - \frac{b}{2}$$

to become

$$H_{nm} = \frac{4}{ab} \frac{1}{\epsilon_{nm}} \int_{-\frac{a}{2}}^{\frac{a}{2}} \int_{-\frac{b}{2}}^{\frac{b}{2}} d\eta \, d\xi \, f(\eta + \frac{a}{2}, \xi + \frac{b}{2}) \cos\left[\frac{n\pi(y + \frac{a}{2})}{a}\right] \cos\left[\frac{m\pi(\xi + \frac{b}{2}}{b}\right] \tag{2.93}$$

where

$$f(\eta + \frac{a}{2}, \xi + \frac{b}{2}) = -f(-\eta + \frac{a}{2}, \xi + \frac{b}{2})$$

$$f(\eta + \frac{a}{2}, \xi + \frac{b}{2}) = f(\eta + \frac{a}{2}, -\xi + \frac{b}{2})$$

finally

$$\int_{-\frac{a}{2}}^{\frac{a}{2}} d\eta \, f(\eta + \frac{a}{2}, \xi + \frac{b}{2}) \cos\left[\frac{n\pi(\eta + \frac{a}{2})}{2}\right] = 0 \text{ if } n \text{ is even} \tag{2.94}$$

$$\int_{-\frac{b}{2}}^{\frac{b}{2}} d\xi \, f(\eta + \frac{a}{2}, \xi + \frac{b}{2}) \cos\left[\frac{m\pi(\xi + \frac{b}{2})}{2}\right] = 0 \text{ if } m \text{ is odd} \tag{2.95}$$

and

$$H_{nm} = 0 \begin{cases} n \text{ even} \\ \\ m \text{ odd} \end{cases} \tag{2.96}$$

2.3 Free-Space Fields

The electromagnetic fields external to the guide, i.e., for $z > 0$, are found by using a combination of the equivalence principle and image theory. According to the equivalence principle the aperture is considered as a perfect conductor on which magnetic surface currents are flowing. They are related to the original field by

$$\vec{M}_s = \vec{E} x \hat{n} \tag{2.97}$$

where $\hat{n}$ is the unit vector normal to the surface.

Consider that the magnetic currents are displaced a distance δ away from the ground plane. The boundary conditions on the ground plane are satisfied if an image current of the same magnitude and direction is placed a distance δ behind the ground plane, and then the ground plane is removed. Let the distance δ go to zero so the original magnetic current is of double magnitude.

Using this image technique, the physical conductor is no longer considered to be present, and the free space Green's function can be used to describe the fields.

According to Harrington (Ref. 36) by using the integral form of the free space Green's function, the electric field is written

$$\vec{E}(x,y,z) = -\nabla x \int_{\text{aperture}} G(x,y,z,\eta,\xi)\, \vec{E}(\eta,\xi) \times d\vec{S}(\eta,\xi) \tag{2.98}$$

where

x, y, z are the field variables

η, ξ are the source variables

The term $G(x, y, z, \eta, \xi)$ is twice the free-space Green's function and is written in integral form

$$G(x, y, z, \eta, \xi) = \frac{i}{4\pi^2} \int_{-\infty}^{\infty} dk_x \int_{-\infty}^{\infty} dk_y \frac{e^{i\left[k_x(x-\eta) + k_y(y-\xi) + \sqrt{k^2 - (k_x^2 + k_y^2)}\, z\right]}}{\sqrt{k^2 - (k_x^2 + k_y^2)}} \quad (2.99)$$

where

$$k^2 = \omega^2 \mu_0 \epsilon_0 = \left(\frac{2\pi}{\lambda_0}\right)^2$$

The subscript 0 denotes free-space quantities, for example,

$$\frac{1}{\sqrt{\mu_0 \epsilon_0}} = 3 \times 10^8 \text{ m/sec}$$

$\sqrt{k^2 - (k_x^2 + k_y^2)}$ must be chosen sc

ıereas in the interval, $k^2 < (k_x^2$

Using Eqs. 2.98 and 2.99 and $dS(\eta, \xi) = dS(\eta, \xi)\hat{a}_z$, the electromagnetic fields are written

$$E_x(x, y, z) = -\int_{\text{aperture}} \frac{\partial G(x, y, z, \eta, \xi)}{\partial z} E_x(\eta, \xi)\, dS(\eta, \xi) \quad (2.100)$$

$$E_y(x, y, z) = -\int_{\text{aperture}} \frac{\partial G(x, y, z, \eta, \xi)}{\partial z} E_y(\eta, \xi)\, dS(\eta, \xi) \quad (2.101)$$

$$E_z(x, y, z) = \int_{\text{aperture}} \left[\frac{\partial G(x, y, z, \eta, \xi)}{\partial x} E_x(\eta, \xi) + \frac{\partial G(x, y, z, \eta, \xi)}{\partial y} E_y(\eta, \xi)\right] dS(\eta, \xi) \quad (2.102)$$

$$H_x(x, y, z) = \frac{-i}{\omega \mu_0} \int_{\text{aperture}} \left\{ \frac{\partial^2 G(x, y, z, \eta, \xi)}{\partial x\, \partial y} E_x(\eta, \xi) + \left[\frac{\partial^2 G(x, y, z, \eta, \xi)}{\partial y^2} + \frac{\partial^2 G(x, y, z, \eta, \xi)}{\partial z^2}\right] E_y(\eta, \xi) \right\} dS(\eta, \xi) \quad (2.103)$$

$$H_y(x,y,z) = \frac{i}{\omega\mu_0} \int_{\text{aperture}} \left\{ \left[\frac{\partial^2 G(x,y,z,\eta,\xi)}{\partial x^2} + \frac{\partial^2 G(x,y,z,\eta,\xi)}{\partial z^2} \right] E_x(\eta,\xi) + \frac{\partial^2 G(x,y,z,\eta,\xi)}{\partial x\,\partial y} E_y(\eta,\xi) \right\} dS(\eta,\xi) \tag{2.104}$$

$$H_z(x,y,z) = \frac{-i}{\omega\mu_0} \int_{\text{aperture}} \left[\frac{\partial^2 G(x,y,z,\eta,\xi)}{\partial y\,\partial z} E_x(\eta,\xi) - \frac{\partial^2 G(x,y,z,\eta,\xi)}{\partial x\,\partial z} E_y(\eta,\xi) \right] dS(\eta,\xi) \tag{2.105}$$

Appendix A contains proof that Eqs. 2.100 through 2.105 satisfy both Maxwell's equations and the proper boundary conditions.

Equations 2.100 through 2.105 are valid for any aperture field, but for this problem $E_x(\eta,\xi) = 0$. Thus, the fields for $(z > 0)$, as a function of the electric field in the aperture are

$$E_x = 0 \tag{2.106}$$

$$E_y = -\int_{\text{aperture}} \frac{\partial G(x,y,z,\eta,\xi)}{\partial z} E_y(\eta,\xi)\, d\eta\, d\xi \tag{2.107}$$

$$E_z = \int_{\text{aperture}} \frac{\partial G(x,y,z,\eta,\xi)}{\partial y} E_y(\eta,\xi)\, d\eta\, d\xi \tag{2.108}$$

$$H_x = \frac{-i}{\omega\mu_0} \int_{\text{aperture}} \left[\frac{\partial^2 G(x,y,z,\eta,\xi)}{\partial y^2} + \frac{\partial^2 G(x,y,z,\eta,\xi)}{\partial z^2} \right] E_y(\eta,\xi)\, d\eta\, d\xi \tag{2.109}$$

$$H_y = \frac{i}{\omega\mu_0} \int_{\text{aperture}} \frac{\partial^2 G(x,y,z,\eta,\xi)}{\partial x\,\partial y} E_y(\eta,\xi)\, d\eta\, d\xi \tag{2.110}$$

$$H_z = \frac{+i}{\omega\mu_0} \int_{\text{aperture}} \frac{\partial^2 G(x,y,z,\xi)}{\partial x\,\partial z} E_y(\eta,\xi)\, d\eta\, d\xi \tag{2.111}$$

2.4 Far Field Form of the Radiated Fields

Those portions of the field that are in proportion to $\frac{1}{R}$ are found in terms of the expansion coefficients of the guide modes. Integration by the method of stationary phase will

be used. To begin, the aperture field is

$$E_y(\eta, \xi) = \sum_{n,m} E_{nm} \sin\frac{n\pi\eta}{a} \cos\frac{m\pi\xi}{b} g_{nm}(0) \tag{2.112}$$

where

$$g_{nm}(0) = \frac{n^2\pi^2}{a^2} \chi_{nm}^{(E)}(z) + \frac{m^2\pi^2}{b^2} \frac{F_{nm}^{(0)}}{\epsilon} \frac{d}{dz} \chi_{nm}^{(m)}(z) \Bigg|_{z = 0}$$

for

$$n, m \neq 1, 0$$

and

$$g_{10}(0) = \chi_{10}^{(E)}(z) \Big|_{z = 0}$$

Therefore

$$E_y = \sum_{n,m} E_{nm}\, g_{nm}(0) \frac{1}{4\pi^2} I_{nm}^{(y)} \tag{2.113}$$

where

$$I_{nm}^{(y)} = \int_{\text{aperture}} d\eta\, d\xi \int_{-\infty}^{\infty} dk_x\, dk_y \sin\frac{n\pi\eta}{a} \cos\frac{m\pi\xi}{b} e^{i\left[k_x(x - \eta) + k_y(y - \xi) + \sqrt{k^2 - (k_x^2 + k_y^2)}\, z\right]} \tag{2.114}$$

The integration over the aperture is done using conventional methods. When the selection rules, which are derived in Section 2.2.3, are used and the following change of variables is made

$$X = (x - \frac{a}{2}) = R \sin\theta \cos\phi \tag{2.115}$$

$$Y = (y - \frac{b}{2}) = R \sin\theta \sin\phi \tag{2.116}$$

$$Z = z = R \cos\theta \tag{2.117}$$

the result is

$$I_{nm}^{(y)} = -4\left(\frac{n\pi}{a}\right) \int_{-\infty}^{\infty} dk_x\, dk_y \frac{k_y \sin\left(\frac{k_y b}{2}\right) \cos\left(\frac{k_x a}{2}\right)}{\left(k_x^2 - \frac{n^2\pi^2}{a^2}\right)\left(k_y^2 - \frac{m^2\pi^2}{b^2}\right)} \tag{2.118}$$

$$e^{iR\left[k_x \sin\theta \cos\phi + k_y \sin\theta \sin\phi + \sqrt{k^2 - (k_x^2 + k_y^2)}\cos\theta\right]}$$

where

$$\arg\sqrt{k^2 - (k_x^2 + k_y^2)} = \begin{cases} 0 & \text{for } k_x^2 + k_y^2 < k^2 \\ \frac{\pi}{2} & \text{for } k_x^2 + k_y^2 > k^2 \end{cases}$$

approximation that only those terms in proportion to $\frac{1}{R}$ remain, i.e., the far field approximation, is now made. As R increases without limit, the integral goes to zero exponentially for $k_x^2 + k_y^2 > k^2$, so the limits of integration are changed so that at all points $k_x^2 + k_y^2 \leq k^2$, with the result that

$$I_{nm}^{(y)} = -4\left(\frac{n\pi}{a}\right) \int_{s(k)} dk_x dk_y\, \Phi(k_x, k_y)\, e^{iR\left[k_x \sin\theta \cos\phi + k_y \sin\theta \sin\phi + \sqrt{k^2 - (k_x^2 + k_y^2)}\cos\theta\right]} \tag{2.119}$$

where

$$\Phi(k_x, k_y) = \frac{k_y \sin\left(\frac{k_y b}{2}\right) \cos\left(\frac{k_x a}{2}\right)}{\left(k_x^2 - \frac{n^2\pi^2}{a^2}\right)\left(k_y^2 - \frac{m^2\pi^2}{b^2}\right)} \tag{2.120}$$

s(k) is the surface interior to the circle $k_x^2 + k_y^2 = k^2$.

Equation 2.119 is in the form of the integral that is evaluated by the Method of Stationary Phase in Appendix E. After making comparisons, the result is

$$I_{nm}^{(y)} = -4\left(\frac{n\pi}{a}\right)\left(\frac{-2\, i\pi k \cos\theta}{R}\right)\Phi\,(k_x^0, k_y^0)\, e^{ikR} \tag{2.121}$$

where

$$k_x^0 = k \sin\theta \cos\phi \tag{2.122}$$

$$k_y^0 = k \sin\theta \sin\phi \tag{2.123}$$

and

$$\lim_{R \to \infty} E_y = \frac{-e^{ikR}}{R} \sum_{n,m} F_{nm} \cos\theta \sin\theta \sin\phi\, h_{nm}(\theta, \phi) \tag{2.124}$$

where

$$F_{nm} \equiv 2i\pi k^2 \left(\frac{n\pi}{a}\right) f_{nm}(0)\, E_{nm} \tag{2.125}$$

and

$$h_{nm}(\theta, \phi) \equiv \frac{\sin\left(\frac{kb}{2} \sin\theta \sin\phi\right) \cos\left(\frac{ka}{2} \sin\theta \cos\phi\right)}{\left(k^2 \sin^2\theta \cos^2\phi - \frac{n^2\pi^2}{a^2}\right)\left(k^2 \sin^2\theta \sin^2\phi - \frac{m^2\pi^2}{b^2}\right)} \tag{2.126}$$

When a similar process is carried out for the other field components they become

$$E_z = \frac{e^{ikR}}{R} \sum_{n,m} F_{nm} \sin^2\theta \sin^2\phi\, h_{nm}(\theta, \phi) \tag{2.127}$$

$$H_x = \frac{k}{\omega\mu_0} \frac{e^{ikR}}{R} \sum_{n,m} F_{nm}(1 - \sin^2\theta \cos^2\phi) \sin\theta \sin\phi\, h_{nm}(\theta, \phi) \tag{2.128}$$

$$H_y = -\frac{k}{\omega\mu_0} \frac{e^{ikR}}{R} \sum_{n,m} F_{nm} \sin^3\theta \cos\phi \sin^2\phi\, h_{nm}(\theta, \phi) \tag{2.129}$$

$$H_z = -\frac{k}{\omega\mu_0} \frac{e^{ikR}}{R} \sum_{n,m} F_{nm} \sin^2\theta \cos\theta \sin\phi \cos\phi\, h_{nm}(\theta, \phi) \tag{2.130}$$

On the free-space side of the antenna, it is more convenient to use spherical coordinates than rectangular coordinates. Unit vectors in the two systems are related in Eq. 2.131.

$$\begin{bmatrix} \hat{a}_r \\ \hat{a}_\theta \\ \hat{a}_\phi \end{bmatrix} = \begin{bmatrix} \sin\theta\cos\phi & \sin\theta\sin\phi & \cos\theta \\ \cos\theta\cos\phi & \cos\theta\sin\phi & -\sin\theta \\ -\sin\phi & \cos\phi & 0 \end{bmatrix} \begin{bmatrix} \hat{a}_x \\ \hat{a}_y \\ \hat{a}_z \end{bmatrix} \tag{2.131}$$

The radiated field, written in terms of spherical coordinates is

$$E_r = 0 \tag{2.132}$$

$$E_\theta = -\frac{e^{ikR}}{R} \sum_{n,m} F_{nm} \sin\theta \sin^2\phi \, h_{nm}(\theta,\phi) \tag{2.133}$$

$$E_\phi = \frac{e^{ikR}}{R} \sum_{n,m} F_{nm} \cos\theta \sin\theta \sin\phi \cos\phi \, h_{nm}(\theta,\phi) \tag{2.134}$$

$$H_r = 0 \tag{2.135}$$

$$H_\theta = -\sqrt{\frac{\epsilon_0}{\mu_0}} E_\phi \tag{2.136}$$

$$H_\phi = \sqrt{\frac{\epsilon_0}{\mu_0}} E_\theta \tag{2.137}$$

The relationship between the transverse electric and magnetic fields as shown in Eqs. 2.136 and 2.137 is, of course, necessary for any finite source. This provides an internal check on the formulation of the free-space fields. The above fields display all of the boundary conditions and required symmetries. The power radiated is calculated by integration of the Poynting vector.

$$\text{Power} = P = \frac{1}{2} \int (\vec{E} \times \vec{H}^*) \cdot d\vec{S} \tag{2.138}$$

where the integration is carried over the half sphere, and in the limit as the radius of the sphere becomes infinite.

Plots of the Poynting vector on the $\phi = 0$ and $\phi = \frac{\pi}{2}$ planes are given in Figs. 5.26 through 5.29 for various material parameters and frequencies.

CHAPTER III

CALCULATION OF REFLECTION COEFFICIENT

3.1 Reflection Coefficient in the Aperture

The continuity of the transverse electric and magnetic fields at the aperture interface is used to determine the set of expansion coefficients E_{nm}. Continuity of the transverse electric fields is assured by Eqs. 2.107 and 2.108. Therefore, the mathematical constraint can be placed on either of the transverse magnetic fields.

From Eq. 2.85, $E_y(\eta, \xi, 0)$ is written

$$E_y(\eta, \xi, 0) = E_{10} C_{10} \sin \frac{\pi \eta}{a} + \sum_{n,m}{}' E_{nm} C_{nm} \sin \frac{n\pi\eta}{a} \cos \frac{m\pi\xi}{b} \tag{3.1}$$

where

$$C_{10} \equiv \chi_{10}^{(E)}(0)$$

$$C_{nm} \equiv \left(\frac{n^2\pi^2}{a^2} + \frac{m^2\pi^2}{b^2}\right) \chi_{nm}^{(E)}(0)$$

The term C_{10} includes the reflection coefficient of the dominant mode and therefore, it must be determined.

Using the integral form of Green's function, Eq. 2.109 is written,

$$H_x(x,y,z) = \frac{1}{4\pi^2 \omega \mu_0} \int_0^a d\eta \int_0^b d\xi \int_{-\infty}^{\infty} dk_x\, dk_y \left[\frac{(k_x^2 - k^2)}{\sqrt{k^2 - (k_x^2 + k_y^2)}} \right.$$
$$\left. \cdot\, e^{i[k_x(x-\eta) + k_y(y-\xi) + \sqrt{k^2 - (k_x^2 + k_y^2)}\, z]} E_y(\eta, \xi, 0) \right] \tag{3.2}$$

Therefore, H_x on the right side of the aperture and H_x on the left side of the aperture is written in terms of E_{nm}. The determination of E_{nm} follows by equating the

two expressions for H_x in the aperture. In the limit as z approaches zero Eq. 3.2 becomes

$$H_x(x, y, 0) = \frac{1}{4\omega\mu_0\pi^2} \int_0^a d\eta \int_0^b d\xi \int_{-\infty}^{\infty} \frac{dk_x dk_y (k_x^2 - k^2)}{\sqrt{k^2 - (k_x^2 + k_y^2)}}$$

$$e^{i[k_x(x-\eta) + k_y(y-\xi) + \sqrt{k^2 - (k_x^2 + k_y^2)}\, 0^+]} \left(E_{10}C_{10} \sin\frac{\pi\eta}{a} + \sum_{n,m}{}' E_{nm}C_{nm} \sin\frac{n\pi\eta}{a} \cos\frac{m\pi\xi}{b} \right) \tag{3.3}$$

The term 0^+ represents a positive infinitesimal value of z. Due to the choice of the branch cuts in Section 2.3, Eq. 3.3 is absolutely convergent.

In the aperture Eq. 2.87 becomes

$$H_x(x, y, 0) = E_{10}D_{10} \sin\frac{\pi x}{a} + \sum_{n,m}{}' E_{nm}D_{nm} \sin\frac{n\pi x}{a} \cos\frac{m\pi y}{b} \tag{3.4}$$

where

$$D_{10} \equiv i \frac{1}{\omega\mu(0)} \frac{d}{dz} \chi_{10}^{(E)}(0)$$

$$D_{nm} \equiv \frac{i}{\omega\mu(0)} \frac{n^2\pi^2}{a^2} \frac{d}{dz} \chi_{nm}^{(E)}(0) - i\omega F_{nm}(0) \frac{m^2\pi^2}{b^2} \chi_{nm}^{(M)}(0)$$

By equating Eq. 3.3 and 3.4, an integral relation for the determination of E_{nm} is obtained.

$$E_{10}D_{10} \sin\frac{\pi x}{a} + \sum_{n,m}{}' E_{nm}D_{nm} \sin\frac{n\pi x}{a} \cos\frac{m\pi y}{b}$$

$$= \frac{1}{4\omega\mu_0\pi^2} \int_0^a d\eta \int_0^b d\xi \int_{-\infty}^{\infty} \frac{dk_x dk_y (k_x^2 - k^2)}{\sqrt{k^2 - (k_x^2 + k_y^2)}} e^{i[k_x(x-\eta) + k_y(\eta-\xi)]} \tag{3.5}$$

$$\left[E_{10}C_{10} \sin\frac{\pi\eta}{a} + \sum_{\alpha,\beta}{}' E_{\alpha\beta}C_{\alpha\beta} \sin\frac{\alpha\pi\eta}{a} \cos\frac{\beta\pi\xi}{b} \right]$$

Since this expression is valid only in the aperture, the range of x and y is restricted to that of η and ξ, i.e.,

$$0 \leq x \leq a \qquad 0 \leq y \leq b$$

$$0 \leq \eta \leq a \qquad 0 \leq \xi \leq b$$

Within the aperture, $e^{i[k_x(x-\eta) + k_y(y-\xi)]}$ is expanded in a product of Fourier series; one for each of the four factors. Each of them is extended beyond the aperture as a periodic function with the proper symmetry, as demanded by the Fourier series. Let

$$e^{ik_x x} = \sum_{n=1} a_n^{(1)} \sin \frac{n\pi x}{a} \qquad 0 \leq x \leq a \tag{3.6}$$

$$e^{-ik_x \eta} = \sum_{\gamma=1} a_\gamma^{(2)} \sin \frac{\gamma\pi\eta}{a} \qquad 0 \leq \eta \leq a \tag{3.7}$$

$$e^{ik_y y} = + \sum_{m=0} a_m^{(3)} \cos \frac{m\pi y}{b} \qquad 0 \leq y \leq b \tag{3.8}$$

$$e^{-ik_y \xi} = + \sum_{\zeta=0} a_\zeta^{(4)} \cos \frac{\delta\pi\xi}{b} \qquad 0 \leq \xi \leq b \tag{3.9}$$

The Fourier coefficients are

$$a_n^{(1)} = \frac{(\frac{2}{a})(\frac{n\pi}{a})\left[(-1)^n e^{ik_x a} - 1\right]}{k_x^2 - \frac{n^2\pi^2}{a^2}} \tag{3.10}$$

$$a_\gamma^{(2)} = \frac{(\frac{2}{a})(\frac{\gamma\pi}{a})\left[(-1)^\gamma e^{-ik_x a} - 1\right]}{k_x^2 - \frac{\gamma^2\pi^2}{a^2}} \tag{3.11}$$

$$a_0^{(3)} = \frac{-i}{k_y b}\left(e^{ik_y b} - 1\right) \tag{3.12}$$

$$a_m^{(3)} = \frac{-(\frac{2}{b})(ik_y)\left[(-1)^m e^{ik_y b} - 1\right]}{k_y^2 - \frac{m^2\pi^2}{b^2}} \tag{3.13}$$

$$a_0^{(4)} = \frac{i}{k_y b}\left[e^{-ik_y b} - 1\right] \tag{3.14}$$

$$a_\zeta^{(4)} = \frac{(\frac{2}{b})(ik_y)\left[(-1)^\zeta e^{-ik_y b} - 1\right]}{k_y^2 - \frac{\delta^2\pi^2}{b^2}} \tag{3.15}$$

Since the integral in Eq. 3.5 is absolutely convergent, the order of integration can be interchanged by using the orthogonality relationships between the trigonometric functions, and then Eq. 3.5 becomes

$$E_{10}D_{10}\sin\frac{\pi x}{a} + \sum_{\substack{n=1\\m=0}}^{\infty}{}' E_{nm}D_{nm}\sin\frac{n\pi x}{b}\cos\frac{m\pi y}{b} =$$

$$+\frac{1}{4\omega\mu_0\pi^2}\int_{-\infty}^{\infty}\frac{dk_x dk_y (k_x^2 - k^2)}{\sqrt{k^2 - (k_x^2 + k_y^2)}}\sum_{\substack{n=1\\m=0}}^{\infty} a_n^{(1)} a_m^{(3)}\sin\frac{n\pi x}{a}\cos\frac{m\pi y}{b} \tag{3.16}$$

$$\left[E_{10}C_{10}a_1^{(2)}a_0^{(4)}(\frac{ab}{2}) + \sum_{\substack{\alpha=1\\\beta=0}}^{\infty}{}' E_{\alpha\beta}C_{\alpha\beta}\epsilon_{\alpha\beta}a_\alpha^{(2)}a_\beta^{(4)}\frac{ab}{4}\right]$$

where

$$\epsilon_{\alpha\beta} = \begin{cases} 0 & \text{when } \alpha = 0 \\ 2 & \text{when } \beta = 0 \\ 1 & \text{otherwise} \end{cases}$$

Define

$$I_{nm}^{\alpha\beta} \equiv \int_{-\infty}^{\infty} \frac{dk_x dk_y (k_x^2 - k^2)}{\sqrt{k^2 - (k_x^2 + k_y^2)}} a_n^{(1)} a_\alpha^{(2)} a_m^{(3)} a_\beta^{(4)} \tag{3.17}$$

and with it, Eq. 3.16 becomes

$$E_{10}D_{10} \sin\frac{\pi x}{a} + \sum_{\substack{n=1 \\ m=0}}^{\infty\prime} E_{nm}D_{nm} \sin\frac{n\pi x}{a} \cos\frac{m\pi y}{b} - \frac{1}{4\omega\mu_0\pi^2} \sum_{\substack{n=1 \\ m=0}}^{\infty} \sin\frac{n\pi x}{a} \cos\frac{m\pi y}{b}$$

$$\left[\left(\frac{ab}{2}\right) E_{10}C_{10}I_{nm}^{10} + \sum_{\substack{\alpha=1 \\ \beta=0}}^{\infty\prime} \left(\frac{ab}{4}\right) E_{\alpha\beta} C_{\alpha\beta} \epsilon_{\alpha\beta} I_{nm}^{\alpha\beta} \right] = 0 \tag{3.18}$$

The trigonometric functions are linearly independent, which implies that the coefficient of each function must be separately zero. In the limit as k_x and k_y go to infinity

$$I_{nm}^{\alpha\beta} \to \int \frac{dk_x dk_y \, e^{i\sqrt{k^2 - (k_x^2 + k_y^2)}\, 0^+}}{k_x^2 k_y^2 \sqrt{k^2 - (k_x^2 + k_y^2)}}$$

Therefore, the limit $0^+ = 0$ can now be taken.

The evaluation of $I_{nm}^{\alpha\beta}$ is in the limit of $0^+ = 0$ and is discussed in Appendix C. The boundary conditions at the aperture yield the relation that must be satisfied by the reflection coefficient

$$E_{nm}D_{nm} - \frac{ab}{16\omega\mu_0\pi^2} \sum_{\substack{\alpha=1 \\ \beta=0}}^{\infty} E_{\alpha\beta}C_{\alpha\beta}\epsilon_{\alpha\beta} I_{nm}^{\alpha\beta} = 0 \tag{3.19}$$

Define the new summation indices γ, ζ so that there is a one to one correspondence between γ for each nm pair and ζ for each $\alpha\beta$ pair. This ordering process is such that $\frac{n^2\pi^2}{a^2} + \frac{m^2\pi^2}{b^2}$ becomes progressively larger as γ increases. The matrix elements of the resulting null matrix are

$$M_{\gamma\zeta} = D_\gamma \delta_{\gamma\zeta} - \frac{ab}{16\omega\mu\pi^2} C_\zeta \epsilon_\zeta I^\zeta_\gamma \tag{3.20}$$

The only unknown quantities in Eq. 3.20 are D_1 and C_1, both of which contain an unknown reflection coefficient. Define

$$K \equiv \frac{16\omega\mu_0\pi^2}{ab}$$

and then

$$M_{\gamma\zeta} = KD_\gamma \delta_{\gamma,\zeta} - C_\zeta \epsilon_\zeta I^\zeta_\gamma \tag{3.21}$$

so the determinant of the matrix is of the form

$$\begin{bmatrix} KD_1 - C_1\epsilon_1 I_1^1 & - C_2\epsilon_2 I_1^2 & - C_3\epsilon_3 I_1^3 \cdots & - C_n\epsilon_n I_1^n \\ - C_1\epsilon_1 I_2^1 & KD_2 - C_2\epsilon_2 I_2^2 & - C_3 I_3 I_2^3 \cdots & \cdot \\ - C_1\epsilon_1 I_3^1 & \cdot & \cdot & \cdot \\ \cdot & \cdot & \cdot & \cdot \\ \cdot & \cdot & \cdot & \cdot \\ \cdot & \cdot & \cdot & \cdot \\ - C_1\epsilon_1 I_n^1 & \cdot & \cdot & \cdot \\ & & & \cdot \end{bmatrix} = 0 \tag{3.22}$$

All the unknown quantities occur in the first row, and there is a common unknown quantity in each element of the row, so the determinant may be written in the form

$$(\epsilon_1 C_1)\begin{bmatrix} \frac{KD_1}{\epsilon_1 C_1} - I_1^1 & -C_2\epsilon_2 I_1^2 & -C_3\epsilon_3 I_1^3 \cdots -\epsilon_n \epsilon_n I_1^n \\ -I_2^1 & KD_2 - C_2\epsilon_2 I_2^2 & \cdots \\ -I_3^1 & \cdots & \cdots \\ \vdots & & \\ -I_n^1 & \cdots & \cdots \end{bmatrix} = 0 \qquad (3.23)$$

C_1^c is proportional to the electric field of the dominant mode. If C_1 were zero, it would correspond physically to a short circuit. Therefore, the new determinant must be zero, but the unknown in the new determinant appears only in the first element.

The matrix can be rewritten in a lower triangularized form as

$$\begin{bmatrix} \left(\frac{KD_1}{\epsilon_1 C_1} - I_1^1 - M'_{11}\right) & 0 & 0 & 0 \cdots 0 \\ M'_{21} & M'_{22} & 0 & 0 \cdots \\ M'_{31} & M'_{32} & M'_{33} & \cdots \\ \vdots & \vdots & \vdots & \vdots \\ M'_{n1} & \cdots & \cdots & \cdots \end{bmatrix} \qquad (3.24)$$

where $M'_{\alpha\beta}$ is a function of $M_{\gamma\zeta}$, except for M_{11}.

Since the determinant of the lower triangular matrix is just the product of its diagonal elements, the value of C_1 and D_1 that yields the original determinant zero is

$$\frac{D_1}{C_1} = (M_{11} + I_1)\frac{\epsilon_1}{K} \qquad (3.25)$$

$M_{\alpha\beta}$ is never zero.

Since Eq. 3.25 is complex, it contains enough information to evaluate both the real and the imaginary parts of the reflection coefficient.

With the determination of the reflection coefficient, the system of Eq. 3.19 is

unique. Therefore, the expansion coefficient E_{nm} is determined by using Cramer's Rule. The term E_{10} is still arbitrary.

3.1.1 Inhomogeneous Material Parameters. It is convenient to define new material parameters that are normalized with respect to the free-space wave numbers, and to discuss the limit of their values.

$$\omega = \frac{k}{\sqrt{\mu_0 \epsilon_0}} ; \quad \lambda_0 = \frac{2\pi}{k}$$

Define the quantities N_μ and N_ϵ so that

$$C_\mu \lambda_0 = N_\mu ; \quad C_\epsilon \lambda_0 = N_\epsilon$$

$$\therefore C_\mu = \frac{k N_\mu}{2\pi} \tag{3.26}$$

$$C_\epsilon = \frac{k N_\epsilon}{2\pi} \tag{3.27}$$

$$C_g = \frac{k}{2\pi} (N_\mu + N_\epsilon) \tag{3.28}$$

$$k_g(0) = \omega \sqrt{\mu(0)\, \epsilon(0)} = k \sqrt{\frac{\mu(0)\, \epsilon(0)}{\mu_0 \epsilon_0}} = k \sqrt{\mu_r(0)\, \epsilon_r(0)} \tag{3.29}$$

The terms $\mu(0)$ and $\epsilon(0)$ must be chosen so that the lowest mode will propagate at the aperture, but all others will be cut-off.

The cut-off condition is assumed to be when the argument of the Hankel function is equal to its order.

$$\therefore \quad \underbrace{\frac{\sqrt{\frac{4\pi^2}{a^2} + C_f^2}}{C_g}}_{\substack{\uparrow \\ n = 1,\ m = 0}} < \frac{2k_g(0)}{C_g} < \underbrace{\frac{\sqrt{\frac{16\pi^2}{a^2} + C_f^2}}{C_g}}_{\substack{\uparrow \\ n = 2,\ m = 0}} \tag{3.30}$$

Thus

$$\frac{\pi^2}{a^2k^2} + \frac{N_f^2}{16\pi^2} < \frac{\mu(0)\,\epsilon(0)}{\mu_0\,\epsilon_0} < \frac{4\pi^2}{a^2k^2} + \frac{N_f^2}{16\pi^2} \tag{3.31}$$

Only the case of $k^2 < \frac{\pi^2}{a^2}$ is treated here. If N_f is too large, then either μ or ϵ will be less than one at distances near the aperture. For estimating various magnitudes

$$\frac{\pi^2}{a^2k^2} < \frac{\mu(0)\,\epsilon(0)}{\mu_0\,\epsilon_0} < \frac{4\pi^2}{a^2k^2} \tag{3.32}$$

The first limitation is for numerical convenience. If $\mu_r(0)\,\epsilon_r(0)$ is not too near either limit, then the asymptotic forms for the Hankel functions are used in the aperture.

A more fundamental limitation is the distance back from the aperture for which traveling waves can exist. Define z_0 to be such a distance.

Then

$$\frac{2k_g(0)}{C_g}\, e^{-\frac{1}{2}C_g z_0} = \frac{\sqrt{\frac{4\pi^2}{a^2} + C_f^2}}{C_g}$$

or

$$\frac{z_0}{\lambda_0} = \frac{\ln\left[\dfrac{4\mu_r(0)\,\epsilon_r(0)}{\dfrac{4\pi^2}{a^2k^2} + \dfrac{N_f^2}{4\pi^2}}\right]}{N_\mu + N_\epsilon} \tag{3.33}$$

Thus, it is clearly shown that in the limit as $N_\mu + N_\epsilon \to 0$, (homogeneous case), the distance back from the aperture for which the traveling waves are cut-off is infinite providing $k > \frac{\pi}{a\sqrt{\mu_r\,\epsilon_r}}$. This is the condition for propagation of the TE_{10} mode in a homogeneous guide.

$$\therefore \quad 0 < \frac{z_0}{\lambda_0} \lesssim \frac{1.39}{N_\mu + N_\epsilon} \tag{3.34}$$

3.2 Reflection Coefficient in the Homogeneous Guide

The inhomogeneous guide must be terminated at some point before the dominant mode is cut-off. In the case of $\mu\epsilon$ increasing with distance back from the aperture, the guide must be terminated before the higher order modes are able to propagate.

Consider the junction between a homogeneous guide and the inhomogeneous guide. It is possible to match boundary conditions at this interface with a TE_{10} mode only. Assume that the evanescent modes due to the aperture have completely decayed and that only the TE_{10} mode is necessary to match boundary conditions at the interface. Proceed until a contradiction is encountered.

In the homogeneous guide, the TE_{10} mode is

$$E_y = A_1 \sin\frac{\pi x}{a}\left(e^{i\kappa z} + \rho e^{-i\kappa z}\right) \tag{3.35}$$

$$H_x = \frac{i}{\omega\mu_h} A_1 \sin\frac{\pi x}{a}\frac{\partial}{\partial z}\left(e^{i\kappa z} + \rho e^{-i\kappa z}\right) \tag{3.36}$$

$$H_z = -i\, A_1 \frac{\pi}{a\omega\mu_h} \cos\frac{\pi x}{a}\left(e^{i\kappa z} + \rho e^{-i\kappa z}\right) \tag{3.37}$$

where

$$\kappa = \sqrt{\omega^2 \mu_h \epsilon_h - \frac{\pi^2}{a^2}}$$

μ_h is the permeability of the homogeneous guide

ϵ_h is the permittivity of the homogeneous guide

ρ is a complex reflection coefficient

In the inhomogeneous guide, the corresponding equations for the TE_{10} mode are

$$E_y = E_{10} \sin \frac{\pi x}{a} \chi_{10}^{(E)}(z) \tag{3.38}$$

$$H_x = \frac{i}{\omega \mu} E_{10} \sin \frac{\pi x}{a} \frac{\partial}{\partial z} \chi_{10}^{(E)}(z) \tag{3.39}$$

$$H_z = \frac{-i\pi}{a\omega \mu} E_{10} \cos \frac{\pi x}{a} \chi_{10}^{(E)}(z) \tag{3.40}$$

The boundary conditions at the interface are

a) $E_{tangential}$ must be continuous

b) $H_{tangential}$ must be continuous

c) B_{normal} must be continuous

Using Eqs. 3.35 through 3.40 and the boundary conditions a through c, the following condition must be satisfied

$$\begin{bmatrix} \left(e^{i\kappa z} + \rho e^{-i\kappa z}\right) - C_{10}(z) \\ \frac{-\kappa}{\omega \mu_h} \left(e^{i\kappa z} - \rho e^{-i\kappa z}\right) - D_{10}(z) \end{bmatrix} = 0 \tag{3.41}$$

whereas

$$C_{10}(z) \equiv \chi_{10}^{(E)}(z)$$

$$D_{10}(z) \equiv \frac{i}{\omega \mu} \frac{\partial}{\partial z} \chi_{10}^{(E)}(z)$$

Thus, for a given set of material parameters

$$\rho = -e^{2i\kappa z} \left\{ \frac{D_{10}(z) + C_{10}(z) \frac{\kappa}{\omega \mu_h}}{D_{10}(z) - C_{10}(z) \frac{\kappa}{\omega \mu_h}} \right\} \tag{3.42}$$

A set of conditions for μ_h and ϵ_h where the power reflection coefficient is a minimum are obtained. The power reflection coefficient is given by $|\rho|^2$.

$$|\rho|^2 = \rho\rho^* = \frac{|D_{10}(z)|^2 + \frac{\kappa^2}{\omega^2\mu_h^2}|C_{10}(z)|^2 + \frac{2\kappa}{\omega\mu_h}\mathrm{Re}D_{10}(z)\,C_{10}^*(z)}{|D_{10}(z)|^2 + \frac{\kappa^2}{\omega^2\mu_h^2}|C_{10}(z)|^2 - \frac{2\kappa}{\omega\mu_h}\mathrm{Re}D_{10}(z)\,C_{10}^*(z)} \tag{3.43}$$

The conditions for $\frac{\partial|\rho|^2}{\partial\epsilon_h} = 0$ and $\frac{\partial|\rho|^2}{\partial\epsilon_h} = 0$ are met by setting

$$\frac{\kappa}{\omega\mu_h} = \frac{|D_{10}(z)|}{|C_{10}(z)|} \tag{3.44}$$

Therefore, the minimum power reflection coefficient in the homogeneous guide is

$$|\rho|^2_{\min} = \frac{|D_{10}(z)|^2 + \frac{|D_{10}(z)|}{|C_{10}(z)|}\,\mathrm{Re}\,D_{10}(z)\,C_{10}^*(z)}{|D_{10}(z)|^2 - \frac{|D_{10}(z)|}{|C_{10}(z)|}\,\mathrm{Re}\,D_{10}(z)\,C_{10}^*(z)} \tag{3.45}$$

It follows that, $\mathrm{Re}D_{10}(z)\,C_{10}^*(z) < 0$, thus $|\rho|^2$ is always less than 1.

It is not always possible to choose values of μ_h and ϵ_h that satisfy Eq. 3.44. The following constraints must also satisfy μ_h and ϵ_h

$$\frac{\pi^2}{a^2k^2} < \frac{\mu_h\epsilon_h}{\mu_0\epsilon_0} < \frac{4\pi^2}{a^2k^2} \tag{3.46}$$

$$\mu_h' \geq 1 \text{ and } \epsilon_h' \geq 1$$

The magnitude of the transverse admittance is related to $\frac{|D_{10}(z)|}{|C_{10}(z)|}$. Let

$$y \equiv \frac{|D_{10}(z)|}{|C_{10}(z)|}$$

$$\frac{k}{\omega\mu_h} = \frac{\omega^2\mu_h\epsilon_h - \frac{\pi^2}{a^2}}{\omega\mu_h} = \frac{k^2\mu_r\epsilon_r - \frac{\pi^2}{a^2}}{k\frac{\mu_0}{\epsilon_0}\mu_r} = y \qquad (3.47)$$

where

$$\mu_r = \frac{\mu_h}{\mu_0} \quad , \quad \epsilon_r = \frac{\epsilon_h}{\epsilon_0}$$

$$\therefore \mu_r^2 = \frac{k^2\mu_r\epsilon_r - \frac{\pi^2}{a^2}}{k^2(\frac{\mu_0}{\epsilon_0})y^2} \qquad (3.48)$$

From Eq. 3.48, μ_r can be calculated for a given $\mu_r\epsilon_r$ product and a given y. The minimum value of $\mu_r\epsilon_r$ is found by using the constraint, $\mu_r \geq 1$.

$$\therefore \mu_r\epsilon_r \geq (\frac{\mu_0}{\epsilon_0})y^2 + \frac{\pi^2}{a^2k^2} \qquad (3.49)$$

In order for the TE_{10} mode to propagate, $\mu_r\epsilon_r > \frac{\pi^2}{a^2k^2}$. The additional term $\frac{\mu_0}{\epsilon_0}y^2$ is the constraint term for minimum power reflection coefficient.

The upper limit on $\mu_r\epsilon_r$ is established from the requirement that $\epsilon_r \geq 1$. If $\epsilon_r \geq 1$, then $\mu_r \leq \mu_r\epsilon_r$ or,

$$(\mu_r\epsilon_r)^2 \leq \frac{k^2\mu_r\epsilon_r - \frac{\pi^2}{a^2}}{k^2(\frac{\mu_0}{\epsilon_0})y^2} \qquad (3.50)$$

Therefore

$$\mu_r \epsilon_r \geq \frac{1 \pm \sqrt{1 - \frac{4\pi^2}{a^2 k^2} \left(\frac{\mu_0}{\epsilon_0}\right) y^2}}{2 \left(\frac{\mu_0}{\epsilon_0}\right) y^2} \tag{3.51}$$

But $\mu_r \epsilon_r < \frac{4\pi^2}{a^2 k^2}$ so that only the TE_{10} mode may propagate. Thus for $y < \frac{\sqrt{3}}{2} \frac{ak}{2\pi} \sqrt{\frac{\epsilon_0}{\mu_0}}$, the (-) sign must be taken.

So far the range of y where minimum power reflection coefficient is possible, has not been mentioned. From Eq. 3.51, it is apparent that

$$y \leq \frac{ak}{2\pi} \frac{\epsilon_0}{\mu_0} \tag{3.52}$$

In the limit as y goes to zero, Eq. 3.51 becomes

$$\lim_{y \to 0} \mu_r \epsilon_r = \frac{\pi^2}{a^2 k^2} \tag{3.53}$$

Equation 3.53 is still compatible with Eq. 3.49 in the limit as y goes to zero.

Therefore, the necessary condition for minimum power reflection coefficient in the homogeneous guide, for a given antenna configuration, is

$$0 < \frac{|D_{10}(z)|}{|C_{10}(z)|} < \frac{ak}{2\pi} \sqrt{\frac{\epsilon_0}{\mu_0}} \tag{3.54}$$

$$\frac{\pi^2}{a^2 k^2} + \left(\frac{\mu_0}{\epsilon_0}\right) \left|\frac{D_{10}(z)}{C_{10}(z)}\right|^2 < \mu_r \epsilon_r < \frac{1 \pm \sqrt{1 - \frac{4\pi^2}{a^2 k^2} \left(\frac{\mu_0}{\epsilon_0}\right) \left|\frac{D_{10}(z)}{C_{10}(z)}\right|^2}}{2 \left(\frac{\mu_0}{\epsilon_0}\right) \left|\frac{D_{10}(z)}{C_{10}(z)}\right|^2} \tag{3.55}$$

$$\mu_r \epsilon_r < \frac{4\pi^2}{a^2 k^2} \tag{3.56}$$

If these conditions are met, then μ_r and ϵ_r are determined from

$$\mu_r = \frac{\sqrt{k^2 \mu_r \epsilon_r - \frac{\pi^2}{a^2}}}{k\sqrt{\frac{\mu_0}{\epsilon_0}}\,\frac{|D_{10}|}{|C_{10}|}} \tag{3.57}$$

and

$$|\rho|^2_{min} = \frac{|D_{10}(z)|^2 + \frac{|D_{10}(z)|}{|C_{10}(z)|}\,\mathrm{Re}\, D_{10}(z)\, C_{10}^*(z)}{|D_{10}(z)|^2 - \frac{|D_{10}(z)|}{|C_{10}(z)|}\,\mathrm{Re}\, D_{10}(z)\, C_{10}^*(z)} \tag{3.58}$$

CHAPTER IV

NUMERICAL ANALYSIS

4. 1 Computer Subroutine

Numerical analysis of the antenna system was accomplished via the 7090 IBM digital computer. The waveguide dimensions were fixed at $a = 0.1$ meter and $b = 0.05$ meter. These dimensions corresponded to a cut-off free-space wave number of 10π in an air-filled waveguide, or $f_c = 1.5$ GHz.

The computer program was written in several parts; each part was self-contained enough to be written as an external function. The purpose being:

1) It is far more convenient to write and correct several smaller programs than one larger one.
2) Not all external functions are needed for various types of required output.
3) The external functions could be punched on binary cards and so need not be translated whenever a change in the main program is needed needed.

The following external functions were written:

A. Hankel functions
B. REI and IMI
C. REINT, IMINT
D. MATRIX
E. GAMMA
F. CSLE
G. RHO
H. RADPOR

A. The Hankel function subroutine has eight parts consisting of the real and imaginary parts of the required Hankel functions and their derivatives. The functions were

derived from an asymptotic series for large argument and order as given by Bateman (Ref. 35). See Appendix B for a discussion of this series and the errors involved. The various Hankel functions are used in almost every other subroutine.

B. REI and IMI are subroutines which evaluate the real and imaginary parts of the integrals defined in Appendix C. A university subroutine for numerical integration was used for the evaluation of the integral in the various regions of integration. See Appendix D for a discussion of this subroutine and the errors involved.

C. The integrals are functions of k only; whereas all other quantities which are calculated depend upon the material parameters. Thus, to save computer time, a program was written which used REI and IMI to calculate two matrices (REINT and IMINT) and punch the results on cards. These cards were then used as input data for the balance of the program.

D. The matrix Eq. 3. 22 is needed in lower triangular form to determine the aperture reflection coefficient, but it is also needed in its standard form to determine the expansion coefficient. Usually the expansion coefficients are not needed for each value of reflection coefficient. It was decided to write an external function whose only requirement was to have the matrix Eq. 3. 22 as its output. This output could then be used for either the calculation of the reflection coefficient or the calculation of the expansion coefficients. This subroutine was called MATRIX and uses REINT, IMINT, and the material parameters as its input. Its output is the real and imaginary parts of the matrix Eq. 3. 22 which are called REM and IMM.

E. GAMMA is the subroutine which utilizes MATRIX to calculate the aperture reflection coefficient. The calculation is accomplished by lower triangularization as described in Section 3. 1. Its output is the real and imaginary parts of the aperture reflection coefficient REGAM and IMGAM.

F. CSLE is the subroutine which utilizes MATRIX and GAMMA to calculate the expansion coefficients. They are calculated by using Cramer's Rule. Whenever determinants are to be evaluated the method of lower triangularization is used. This subroutine has both the real and imaginary parts of the expansion coefficients and the y directed aperture electric field as its output.

G. RHO is the subroutine which calculates the reflection coefficient in the homogeneous waveguide and the equivalent circuit of the inhomogeneous waveguide and aperture. The method of calculation is given in Section 3. 2.

H. As a check on the method of integration by Stationary Phase as described in Appendix E, and to determine the relative importance of the higher-order modes, it is necessary to calculate the total power radiated by integration of the Poynting Vector. RADPOR is the subroutine which accomplishes this purpose. The method of numerical integration is the same as that described in Appendix D.

4. 2 Numerical Checks on Over-All Accuracy

Various numerical checks are made to test assumptions and regions of validity of approximations.

The aperture reflection coefficient was calculated for various matrix sizes, first without using the selection rules derived in Section 2. 2. 5 and then the reflection coefficient was computed again with the selection rules. The results are given below:

Matrix Size	Re Γ	Im Γ	$N_\mu = N_\epsilon = 1.5$
5	-0. 1518	-0. 5428	$\mu(0) = \epsilon(0) = 2.4$
10	-0. 1515	-0. 5426	k = 25
20	-0. 1514	-0. 5422	

Table 4. 1 Aperture voltage reflection coefficient vs. matrix size

When the selection rules are used, the 20 x 20 matrix reduces to 7 x 7. This 7 x 7 matrix was found to give exactly the same value of aperture reflection coefficient.

When various quantities are calculated in the waveguide as a function of the distance back from the aperture, the approximations used in the Hankel functions begin to break down. The errors in the Hankel functions are unbounded as cut-off for the dominant mode is reached. This error is first detected in the power flow down the guide. The power remains nearly constant until cut-off is almost reached, and then breaks sharply upward. Thus, keeping track of the power flow at all points in the waveguide provides a check to ensure that

the region of validity for the Hankel functions is not violated.

One of the most important tests for the accuracy of the calculations is the comparison of the power radiated by the aperture antenna to the power incident in the homogeneously loaded waveguide. Power dissipation in the waveguide and in the material which loads the waveguide cannot occur in this idealized formulation of the problem; the total radiated power must equal the net power incident in the uniform waveguide. The radiated power is computed by the integration of the Poynting vector over a hemispherical surface of infinite radius centered at the aperture. Assuming unit incident power in the uniform waveguide, the net power is $1 - |\rho|^2$ which should approximate the radiated power very closely. A comparison of these two quantities computed numerically shows agreement to within two percent.

The program consists first of computing the reflection coefficient Γ and the power flow in the inhomogeneous guide. The guide was then terminated in a homogeneous guide 0.01 meter back from the aperture. The μ and ϵ of the homogeneous guide was taken to be the same as in the inhomogeneous guide at the interface. The reflection coefficient and power flow in the homogeneous guide were computed. The expansion coefficients were computed and used to evaluate the total power radiated via integration of the Poynting vector in the far-field.

In order to determine the effect of the higher order modes, the radiated power was calculated three times for each set of data. The first assuming only the dominant mode, the second assuming the dominant mode and the first cut-off mode, and the third assuming the dominant mode and the first two cut-off modes.

A value of $\mu(0)\epsilon(0) = 4.0$ was chosen so that $k = 18$ through $k = 29$ could be used. However, while the mode for $k = 18$ was not cut off, it was too close to cut-off for the approximation in the Hankel functions to be valid. If $\mu(0)\epsilon(0)$ were larger than 4.0, then the lowest cut-off mode for $k = 29$ could propagate. The results are shown in Table 4.2. All power is normalized to the input power in the homogeneous guide. Percent error figures refer to the difference between the input power and the power radiated.

As k moves further from its upper or lower limits the effect of the higher-order modes are less. This is to be expected. The accuracy for $k = 29$ is not as good as for $k = 25$; $k = 25$ is much better than $k = 21$. This is explained by reference to Fig. 4.1.

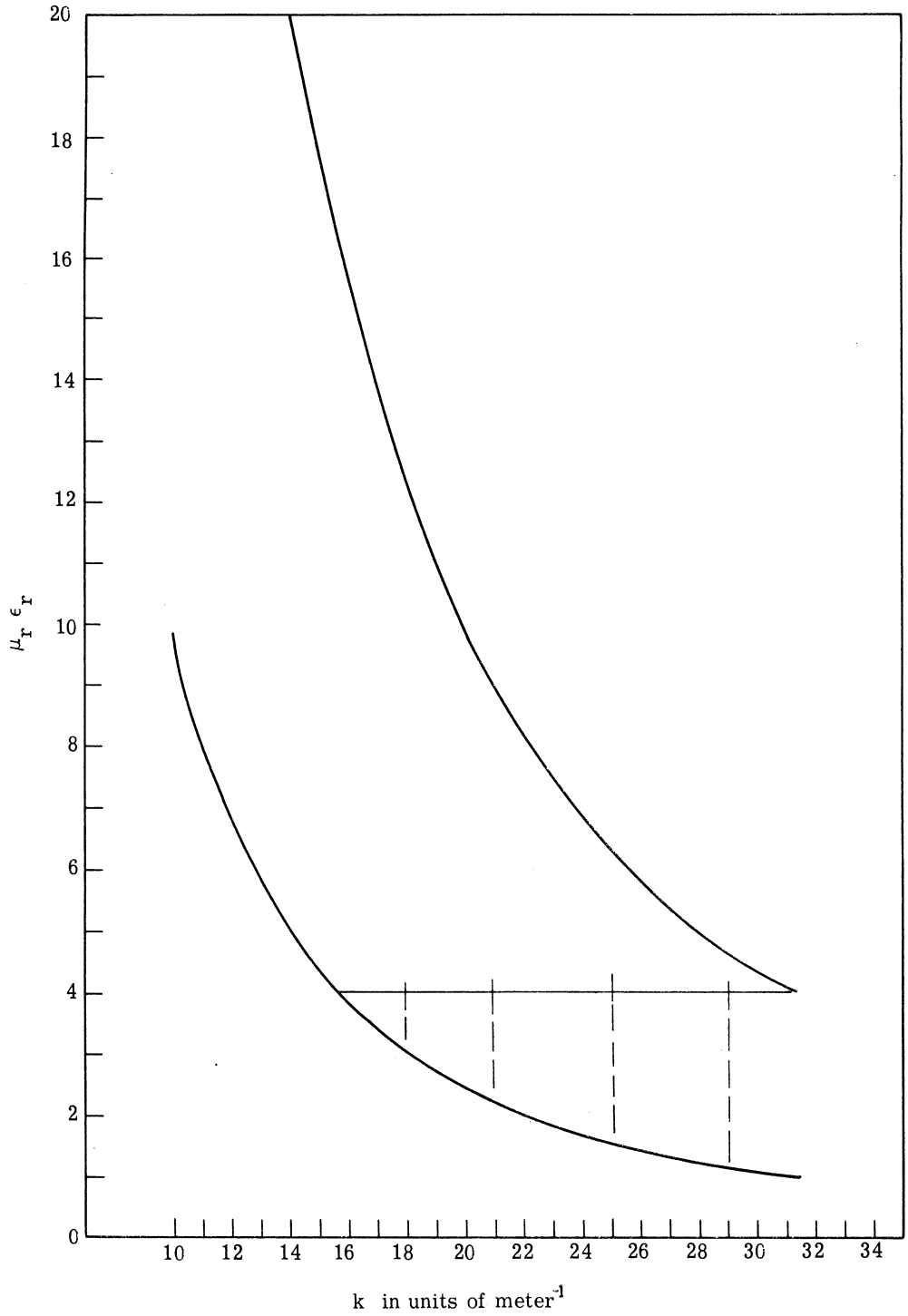

Fig. 4. 1. Range of relative permeability and permittivity for propagation of the dominate mode only

Number of Modes	k	P_H	P_{IH}	P_R	% Error	$N_\mu = N_\epsilon = 1.0$
1	21.0	1.0	0.9993	2.406	140.6%	$\mu(0) = \epsilon(0) = 2.0$
2	21.0	1.0	0.9993	1.930	93.0%	
3	21.0	1.0	0.9993	0.984	1.6%	
1	25.0	1.0	1.0	0.987	1.3%	
2	25.0	1.0	1.0	0.997	0.3%	
3	25.0	1.0	1.0	0.998	0.2%	
1	29.0	1.0	1.0	0.991	0.9%	
2	29.0	1.0	1.0	0.991	0.9%	
3	29.0	1.0	1.0	0.988	1.2%	

Table 4.2 Effect of higher-order modes

Whenever the operating point moves closer to the lower limit, the error in the Hankel function which represents the propagating modes becomes larger. But as the operating point moves closer to the upper limit, the larger the error comes from the Hankel function which represents the cut-off modes. A re-examination of the data shows that it is the higher-order mode that dominates the over-all inaccuracy of k = 29. The propagating mode does represent the entire field better than for k = 25.

This test run indicates that the solution to the problem and the computer programs adequately represent the physics of the problem.

CHAPTER V

EVALUATION OF AN INHOMOGENEOUS SYSTEM

5.1 Introduction

Investigation of the antenna system is divided into three parts: 1) the determination of whether the inhomogeneity is of any help in reducing the aperture power reflection coefficient and, if so, under what conditions, 2) the selection of material parameters, and 3) the comparison of system power reflection coefficient versus frequency between an inhomogeneous, and a homogeneous system.

The homogeneous system has the same geometry as the inhomogeneous system except that $N_\mu + N_\epsilon = 0$ at all points in the homogeneous system. This type of system is considered by Adams, (Ref. 21). In most cases, the permeability and permittivity of the inhomogeneous system is the same as used by Adams.

The choice of data points is shown in Fig. 5.1 which allows the determination of the maximum and minimum values of μ and ϵ in the aperture for a given free-space wave number. The dotted vertical lines represent the chosen frequencies and the solid horizontal lines represent the $\mu_r\epsilon_r$ products that are used by Adams and are also in this in this report. The intersections of the dotted and solid lines represent the selection of frequencies and $\mu_r\epsilon_r$ products. Selection of particular value of μ and ϵ for a given $\mu\epsilon$ product are also based in part on Adams' work.

5.2 Aperture Power Reflection Coefficient in a Homogeneous Guide

Adams produced a set of curves for the aperture admittance when a homogeneous guide is radiating through an aperture in an infinite ground plane. The results of this study are compared with Adams.

Although Adams considers only the special case of $\epsilon_r = \mu_r$, his results can be easily extended to an arbitrary ratio, μ_r/ϵ_r, keeping the product $\mu_r\epsilon_r$ constant. This is accomplished by multiplying the conductance and susceptance by the ratio of the permeabilities $\mu_{actual}/\mu_{figure}$

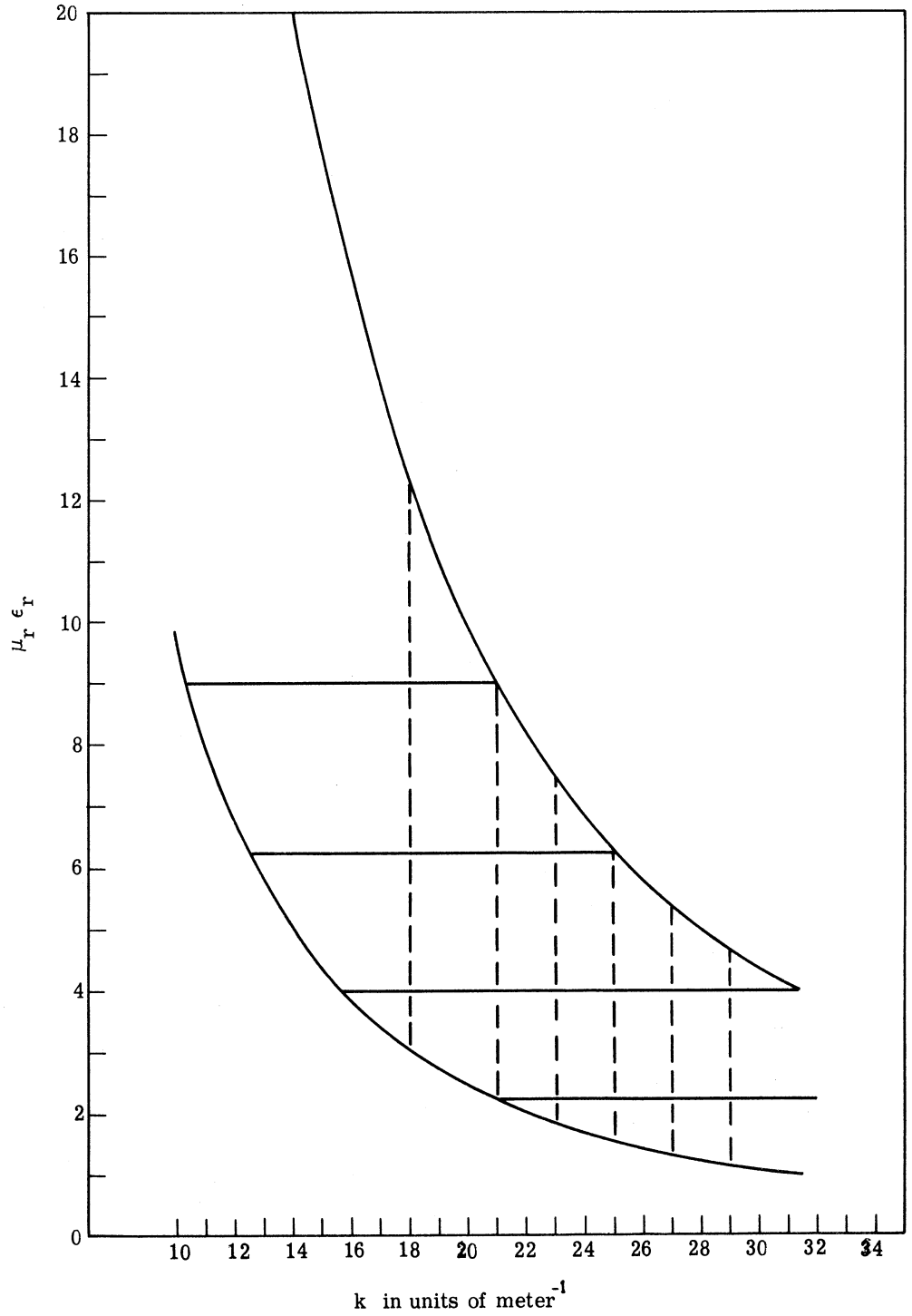

Fig. 5.1. Range of relative permeability and permittivity for propagation of the dominate mode only

In this study the figure of merit for the antenna system in the power reflection coefficient is represented by the magnitude squared of the voltage reflection coefficient, Γ. The power reflection coefficient is calculated from the aperture admittance.

$$|\Gamma|^2 = \frac{(1-G)^2 + B^2}{(1+G)^2 + B^2} \tag{5.1}$$

The term G is the normalized conductance and B is the normalized susceptance. These are read directly from Adam's curves for the special case of $\mu_r = \epsilon_r$. The more general case, but still keeping the product $\mu_r \epsilon_r$ constant, is

$$|\Gamma|^2 = \frac{(1 - r_\mu G)^2 + (r_\mu B)^2}{(1 + r_\mu G)^2 + (r_\mu B)^2} \tag{5.2}$$

where $r_\mu = \mu_{actual} / \mu_{figure}$. The term $|\Gamma|^2$ may be minimized with respect to r_μ. The value of r_μ for which $|\Gamma|^2$ is a minimum is R_μ

$$R_\mu = \frac{1}{\sqrt{G^2 + B^2}} \tag{5.3}$$

and

$$|\Gamma|^2_{min} = \frac{1 - R_\mu G}{1 + R_\mu G} \tag{5.4}$$

For Eqs. 5.3 and 5.4 to be valid, $\mu_{actual} = R_\mu \mu_{figure}$ must be less than $(\epsilon_r \mu_r)_{figure}$; otherwise ϵ_r would be less than one. When this constraint is not met, the power reflection coefficient is calculated from Eq. 5.2. The aperture power reflection coefficient must reduce to the results from Adams' work in the limit as $N_\mu + N_\epsilon$ goes to zero, for all cases when $\mu_r(0)\epsilon_r(0)$ in the aperture is equal to the $\mu_r \epsilon_r$. Thus, the main criteria for evaluating the inhomogeneous guide is a plot of the power reflection coefficient

k	μ/μ_0	ϵ/ϵ_0	$\lvert\Gamma\rvert^2$	$\lvert\Gamma\rvert^2$ Min Possible
18	4.90	1.84	0.581	Yes
18	3.865	1.617	0.555	Yes
21	6.055	1.032	0.307	Yes
21	3.534	1.132	0.362	Yes
23	6.25	1.0	0.161	No
23	4.0	1.0	0.191	No
25	4.0	1.0	0.0927	No
27	2.25	1.0	0.0308	No
27	4.0	1.0	0.0662	No
29	2.112	1.065	0.0	Yes
29	4.0	1.0	0.0266	No

Table 5.1. Optimum values of aperture permeability and permittivity

versus $N_\mu + N_\epsilon$, where the points for $N_\mu + N_\epsilon = 0$ are determined from Adams' work. In all cases only the dominate mode propagates.

Those parts of Adams' curves applicable to this study are reproduced in Figs. 5.2 through 5.5. A list of minimum power reflection coefficients for selected frequencies calculated from these curves are given in Table 5.1.

5.3 Selection of Material Parameters in the Inhomogeneous System

The material parameters in the inhomogeneous guide are determined from plots of the aperture power reflection coefficient versus $N_\mu + N_\epsilon$ for the frequencies, and $\mu_r(0)\epsilon_r(0)$ values as shown on Fig. 5.1. For $k = 18$ and $k = 25$ several different values of $\mu_r(0)$ and $\epsilon_r(0)$ were used. For the rest of the frequencies only values of $\mu_r(0)$ and $\epsilon_r(0)$ near optimum, as given in Table 5.1, were used. If the plots have a minimum value for $N_\mu + N_\epsilon \neq 0$, then the inhomogeneity has reached the aperture power reflector coefficient. $N_\mu + N_\epsilon$ is a measure of the inhomogeneity of the material and is defined as follows:

$$\mu(z)\epsilon(z) = \mu(0)\epsilon(0)e^{\frac{k}{2\pi}(N_\mu + N_\epsilon)z} \tag{5.5}$$

As the limit $N_\mu + N_\epsilon$ goes to zero, the material becomes homogeneous, and the aperture power reflection coefficient goes smoothly over to the corresponding coefficient computed from Adams' work. The curves that do not extend to $N_\mu + N_\epsilon = 0$ are computed for $\mu\epsilon$ products other than those used by Adams. From curves of this type, the advantage or disadvantage of the inhomogeneity with respect to the aperture power reflection coefficient is apparent.

Figures 5.6, 5.7 and 5.8 are plots of the aperture power reflection coefficient versus $N_\mu + N_\epsilon$ for $k = 18$. Figure 5.6 indicates that generally there is no advantage to using an inhomogeneous material in the waveguide. The exceptions are for

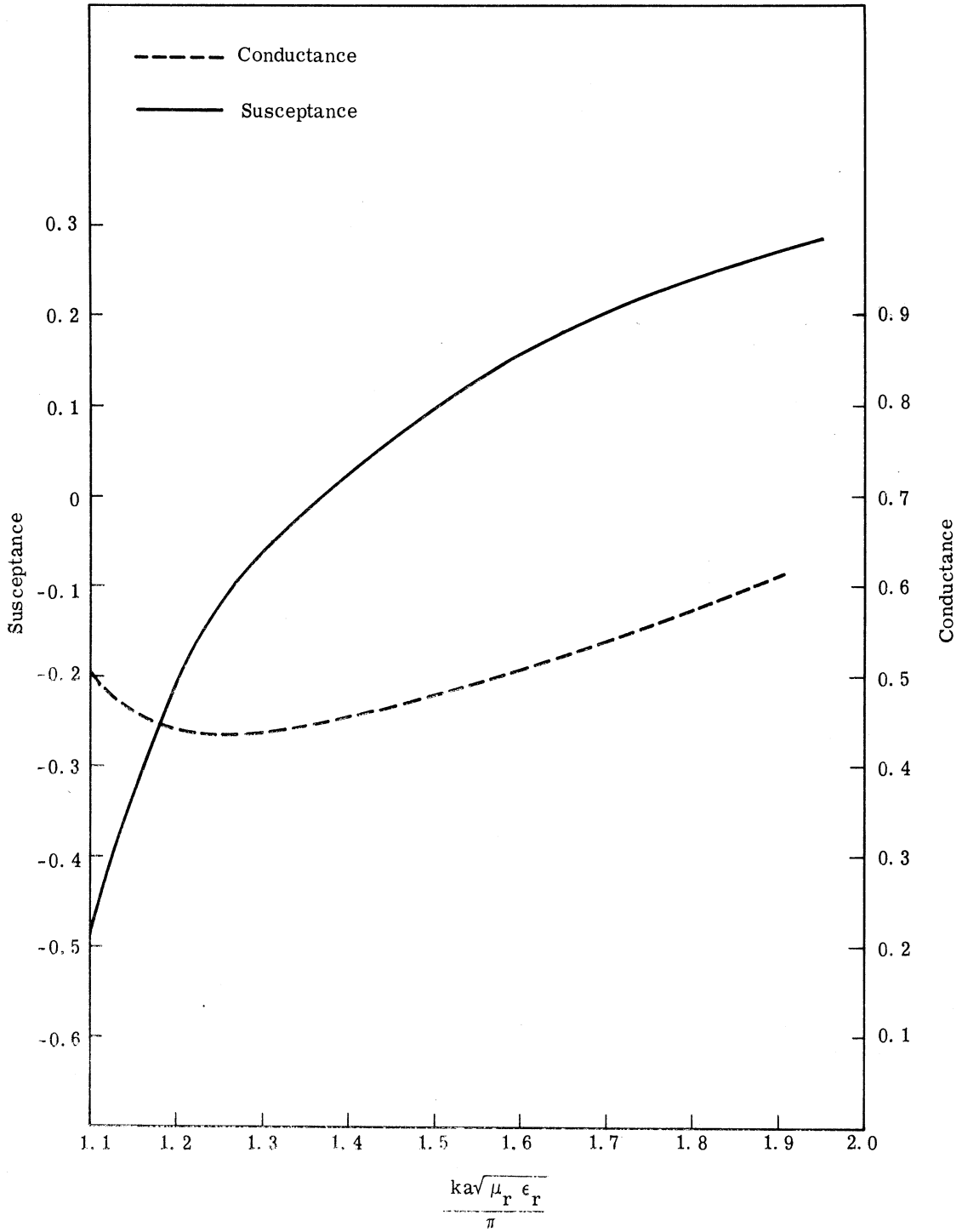

Fig. 5.2. Normalized aperture admittance of a waveguide radiator $\mu_r = \epsilon_1 = 1.5$

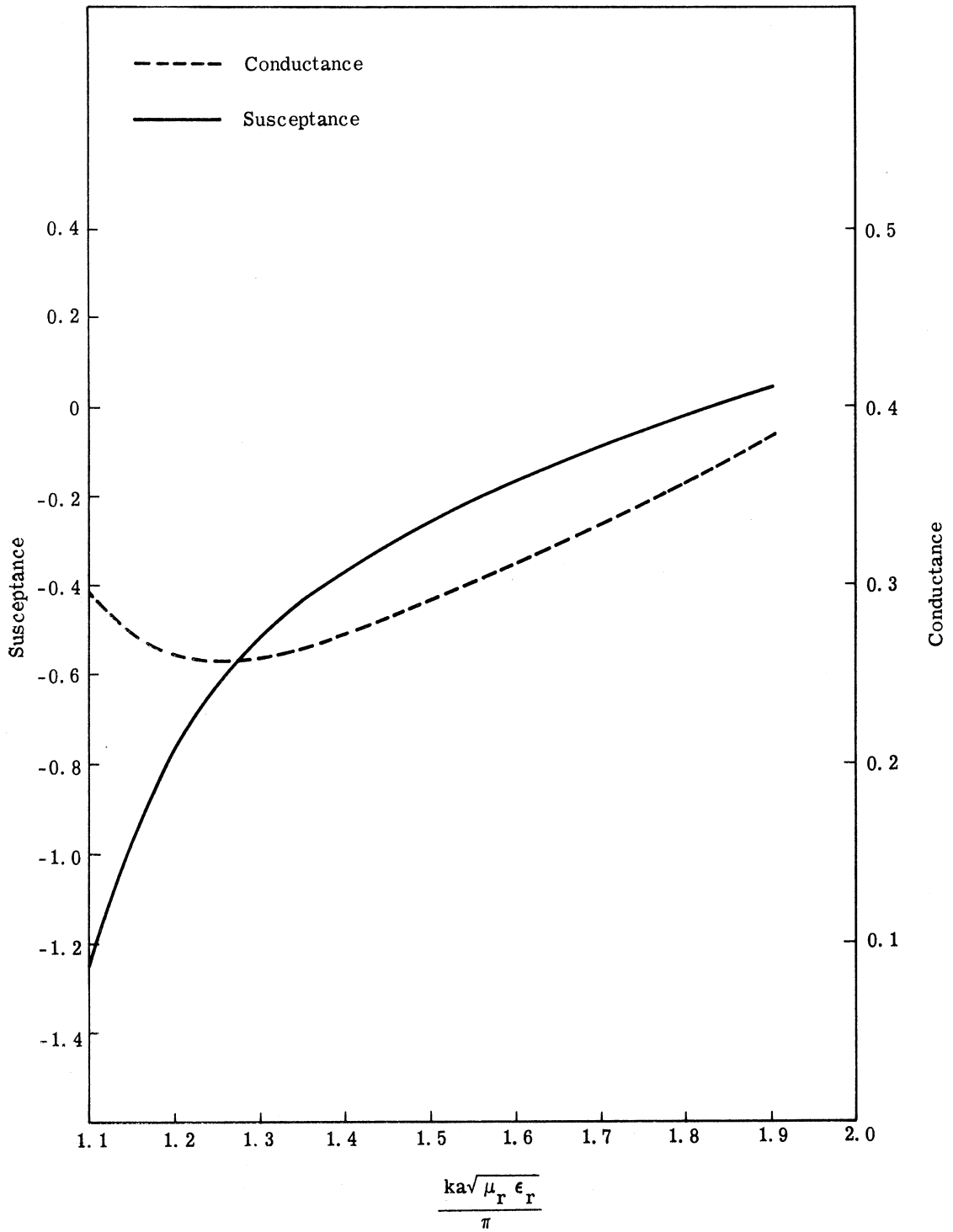

Fig. 5.3. Normalized aperture admittance of a loaded waveguide radiator $\mu_r = \epsilon_r = 2.0$

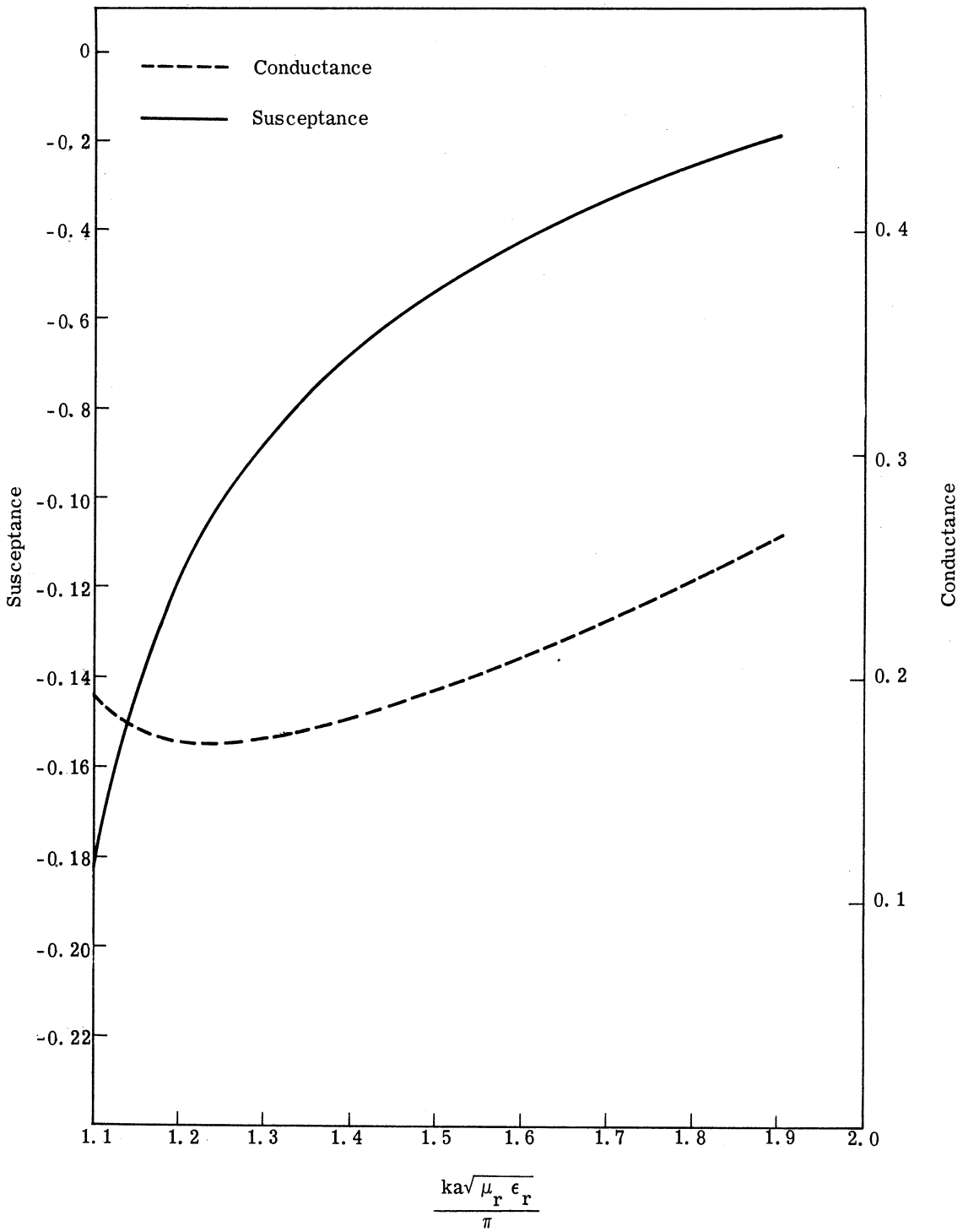

Fig. 5.4. Normalized aperture admittance of a loaded waveguide radiator $\mu_r = \epsilon_r = 2.5$

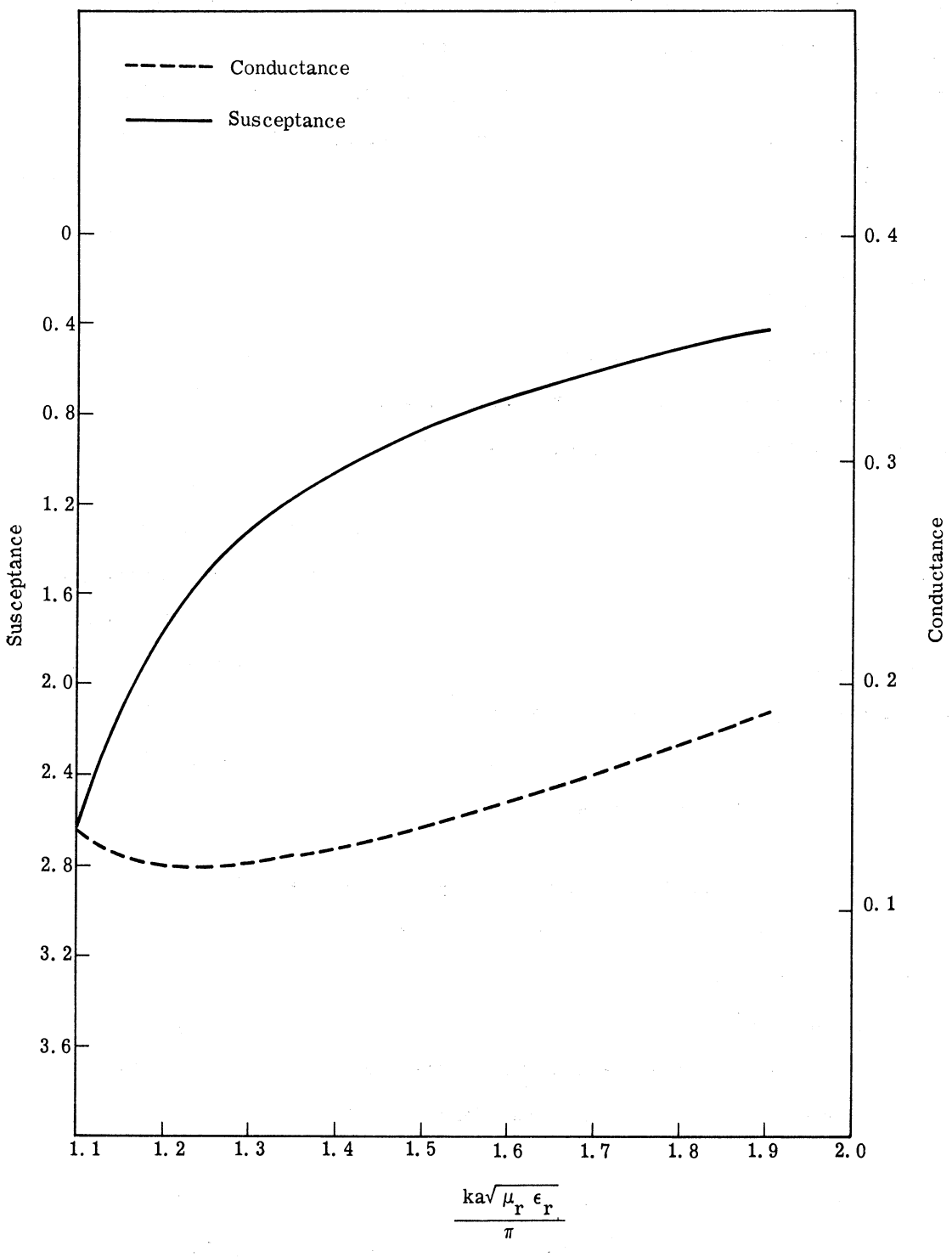

Fig. 5.5. Normalized aperture admittance of a loaded waveguide radiator $\mu_r = \epsilon_r = 3.0$

$\mu_r(0) = \epsilon_r(0) = 2.5$, and $\mu_r(0) = \epsilon_r(0) = 3.0$. However, Fig. 5.7 shows that for $\mu_r(0)$ near the optimum, as shown in Table 5.1, there is a definite advantage in the inhomogeneous guide. Figures 5.6 and 5.7 represent the case of either μ or ϵ being held constant. Figure 5.8 shows that the more general case of both μ and ϵ being variable. For k = 18, $\mu_r(0)\epsilon_r(0) = 9$, the minimum power reflection coefficient occurs for $\mu_r(0) = 4.5$, $\epsilon_r(0) = 2.0$, which is very near the optimum. The optimum, $\mu_r(0) = 4.9$, $\epsilon_r(0) = 1.84$ would yield a very small improvement.

The optimum values of μ and ϵ were chosen for k = 21. These results are shown in Fig. 5.9. It is noted that a substantial improvement is made through the inhomogeneity of the material, especially for $N_\mu = 0$.

For k = 23, it was impossible to use the optimum $\mu_r(0)$ because the optimum value of $\mu_r(0)$ was larger than the $\mu_r(0)$, $\epsilon_r(0)$ product, which forced $\epsilon_r(0)$ to be less than one. Figure 5.10 shows the results for k = 23. For both curves, $\epsilon_r = 1.0$. Therefore, it is not possible to have $N_\epsilon \neq 0$. It is seen from the figure that there is no improvement and the aperture power reflection coefficient is increased by the inhomogeneity. This follows the pattern shown in Fig. 5.6 which shows that there is no improvement when the value of $\mu_r(0)$ is not close to its optimum value.

Figures 5.11 and 5.12 represent a family of curves for k = 25. The same conditions prevail for k = 25 with respect to the optimum value of $\mu_r(0)$ as in k = 23, since the optimum value of $\mu_r(0)$ is too large for the given $\mu_r(0)\epsilon_r(0)$ product. The pattern of no improvement due to the inhomogeneity when $\mu_r(0)$ is not close to optimum, is again clearly seen. Also, the larger the value of $\mu_r(0)$, the lower the aperture power reflection coefficient, indicating that the optimum value is larger.

Figures 5.13 and 5.14 represent k = 27 and k = 29. Optimum values of $\mu_r(0)$ were not possible for k = 27. The optimum value of $\mu_r(0)$ was possible for k = 29, but the optimum value gave a power reflection coefficient of zero. Thus, any

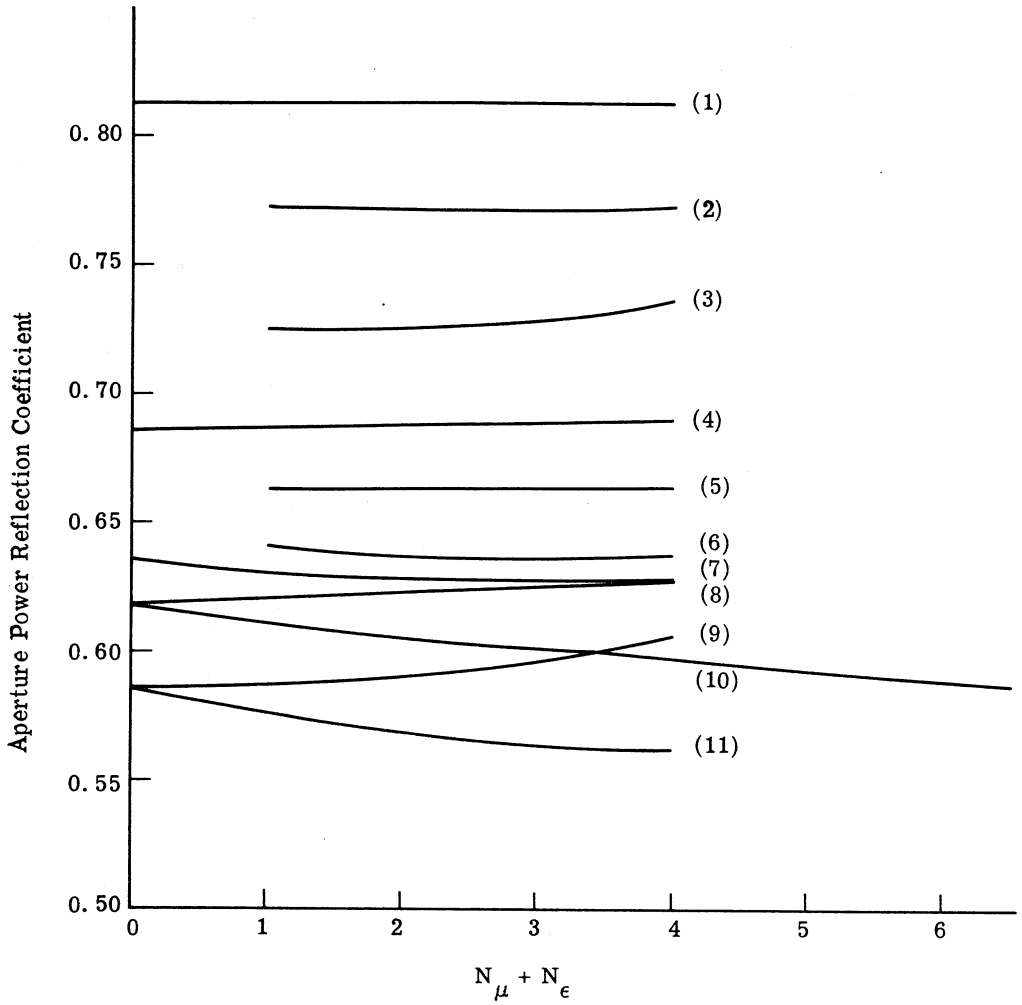

1) $\mu_r(0) = 1.0,\ \epsilon_r(0) = 9.0,\ N_\mu = 0$

2) $\mu_r(0) = 1.0,\ \epsilon_r(0) = 7.0,\ N_\mu = 0$

3) $\mu_r(0) = 1.0,\ \epsilon_r(0) = 5.5,\ N_\mu = 0$

4) $\mu_r(0) = 2.0,\ \epsilon_r(0) = 4.5,\ N_\epsilon = 0$

5) $\mu_r(0) = 2.5,\ \epsilon_r(0) = 4.0,\ N_\epsilon = 0$

6) $\mu_r(0) = 11.5,\ \epsilon_r(0) = 1.0,\ N_\epsilon = 0$

7) $\mu_r(0) = 9.0,\ \epsilon_r(0) = 1.0,\ N_\epsilon = 0$

8) $\mu_r(0) = 3.0,\ \epsilon_r(0) = 3.0,\ N_\epsilon = 0$

9) $\mu_r(0) = 2.5,\ \epsilon_r(0) = 2.5,\ N_\epsilon = 0$

10) $\mu_r(0) = 2.5,\ \epsilon_r(0) = 3.0,\ N_\mu = 0$

11) $\mu_r(0) = 2.5,\ \epsilon_r(0) = 2.5,\ N_\mu = 0$

Fig. 5.6. Aperture power reflection coefficient vs. $N_\mu + N_\epsilon$ for k = 18

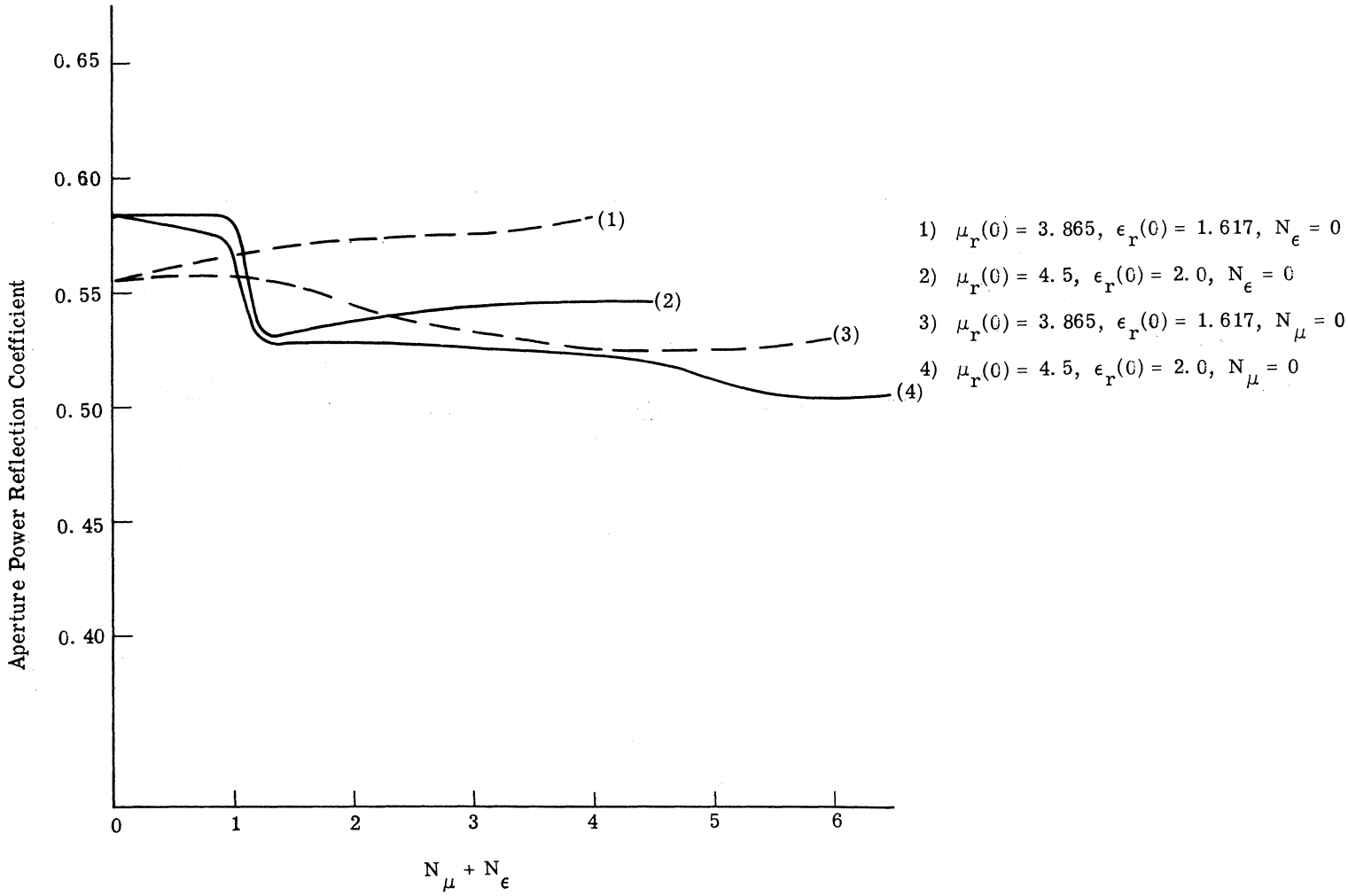

Fig. 5.7. Aperture power reflection coefficient vs. $N_\mu + N_\epsilon$ for k = 18

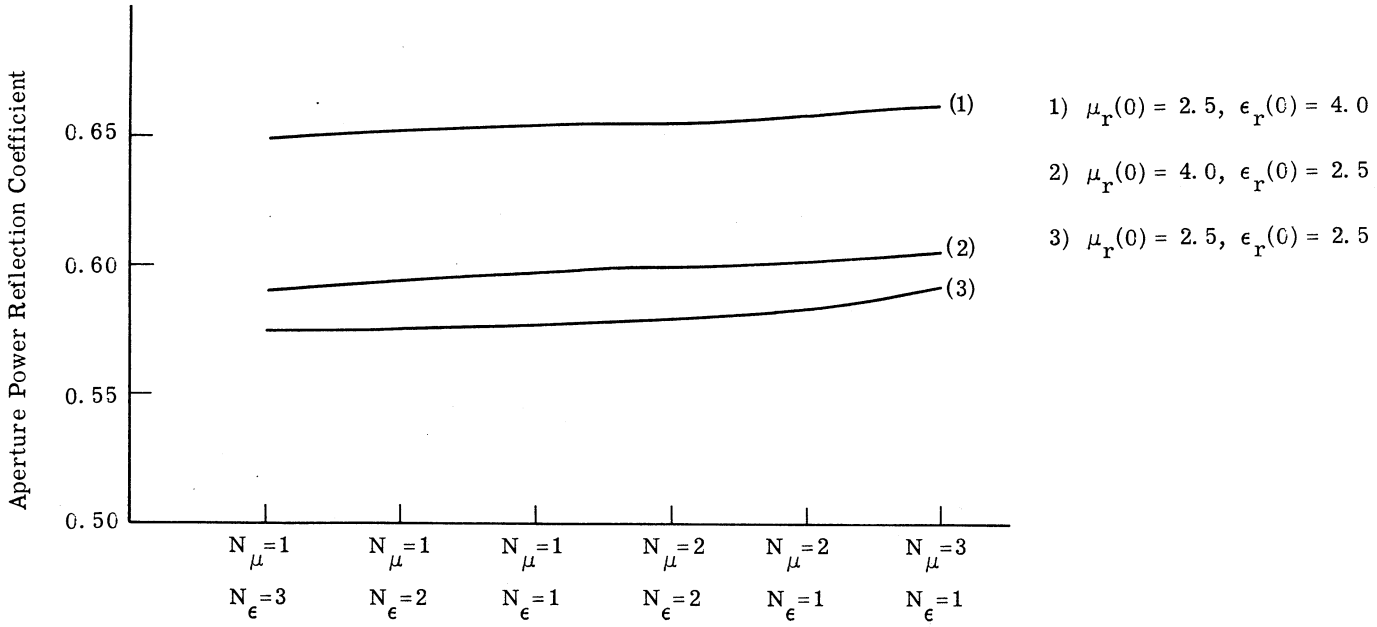

Fig. 5.8. Aperture power reflection coefficient vs. $N_\mu + N_\epsilon$ for k = 18

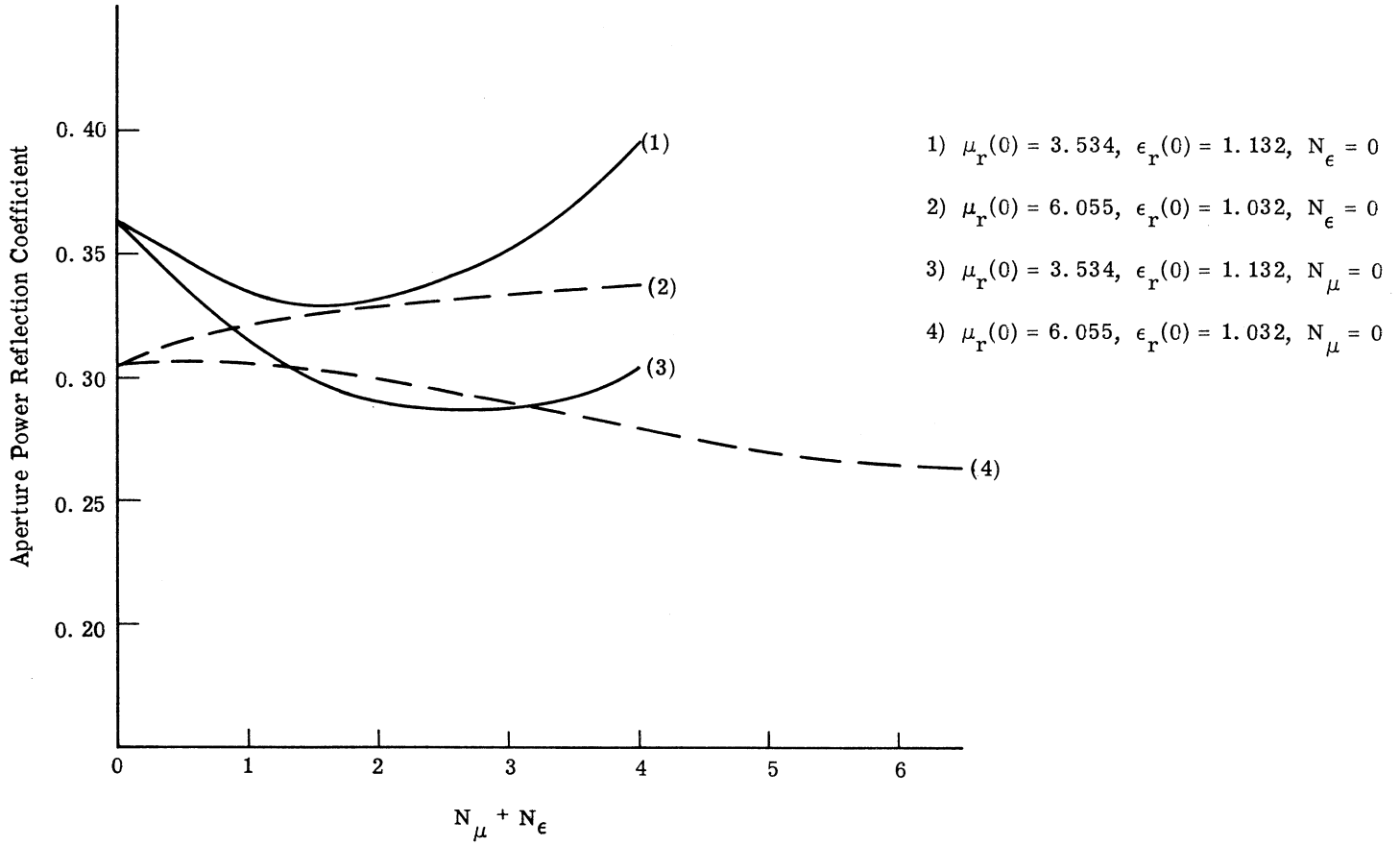

Fig. 5.9. Aperture power reflection coefficient vs. $N_\mu + N_\epsilon$ for k = 21

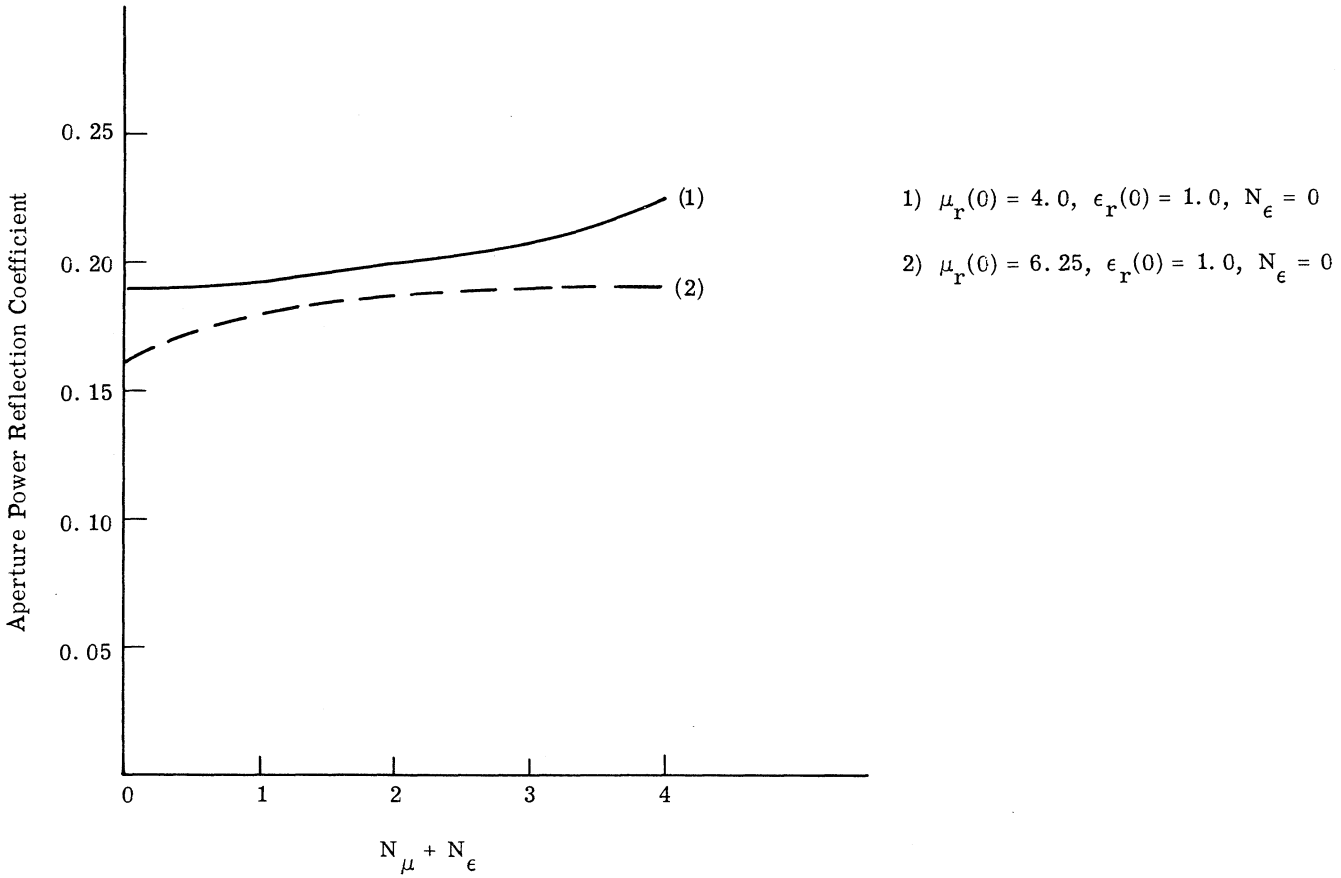

Fig. 5.10. Aperture power reflection coefficient vs. $N_\mu + N_\epsilon$ for k = 23

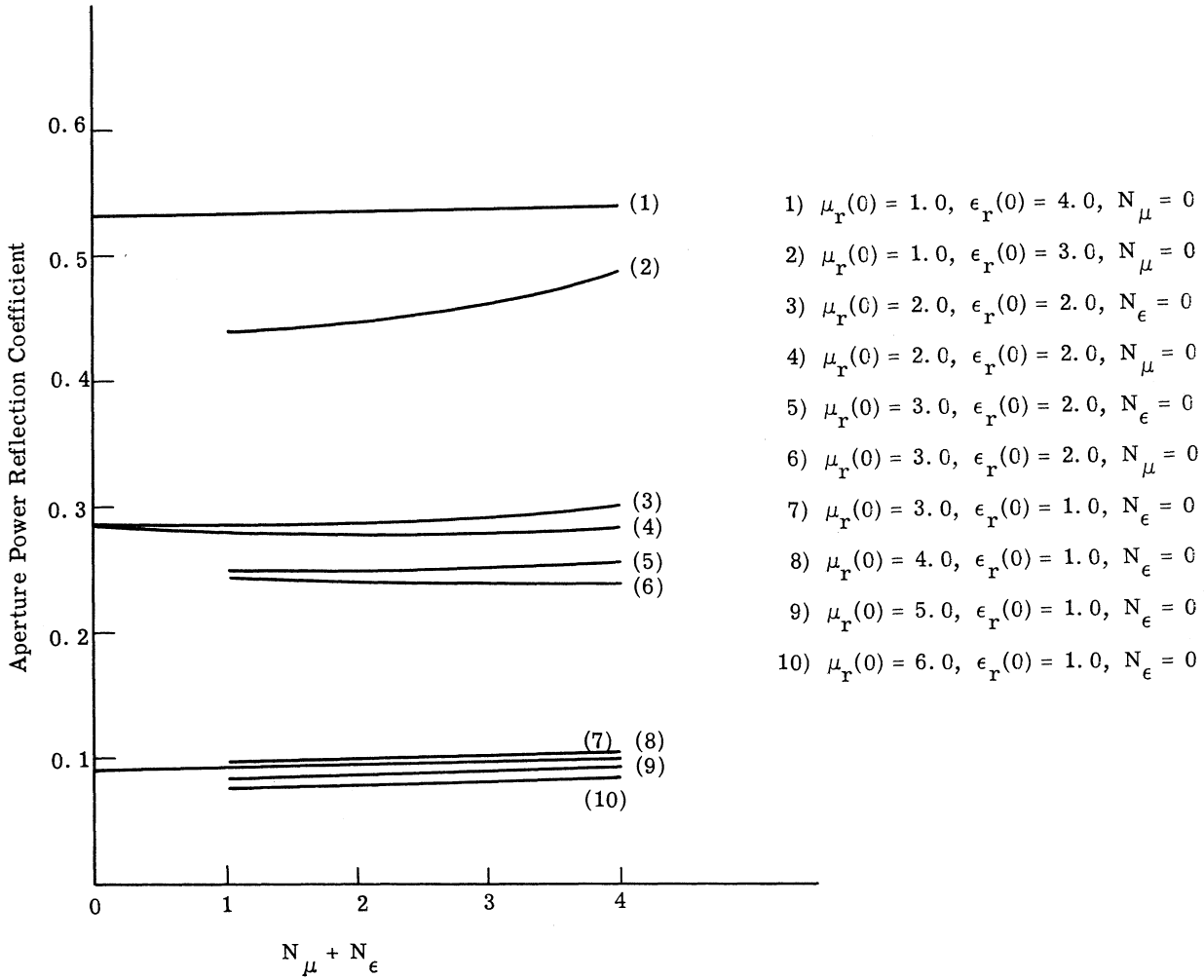

Fig. 5.11. Aperture power reflection coefficient vs. $N_\mu + N_\epsilon$ for k = 25

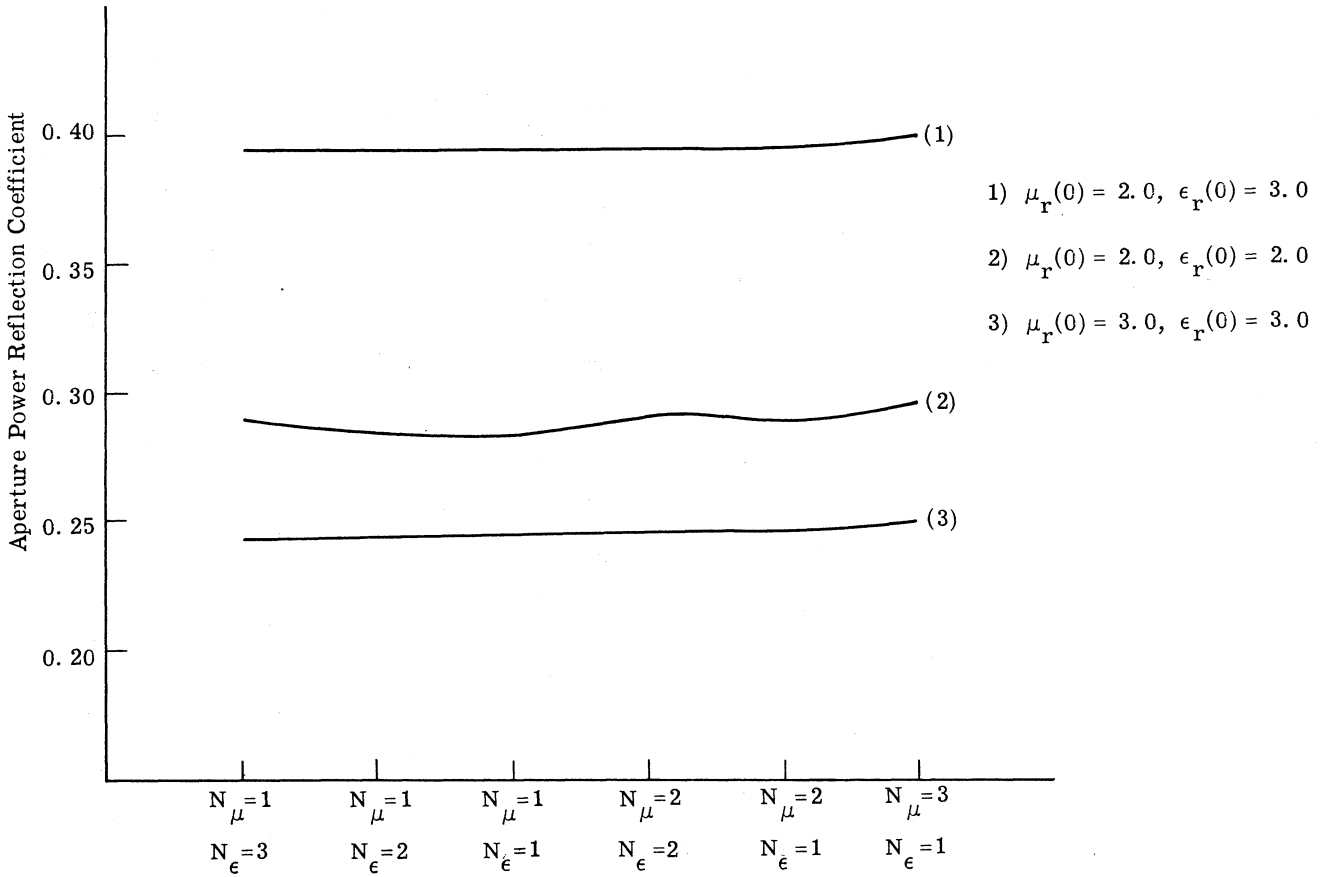

Fig. 5.12. Aperture power reflection coefficient vs. $N_\mu + N_\epsilon$ for k = 25

changes that are made raises the coefficient.

Figure 5.15 is a composite of the previous figures, using the lowest aperture power reflection for each frequency. There is a distinct advantage to using an inhomogeneous material for k less than or equal to 21. However, it is necessary in each case that a value of $\mu_r(0)$ near the optimum be used, or the advantage is reduced to zero and may become a disadvantage. It is also noted that the greatest improvement is always when N_ϵ is greater than N_μ. The impedance of the guide is proportional to

$$\sqrt{\frac{\mu}{\epsilon}} = \sqrt{\frac{\mu_r(0)}{\epsilon_r(0)}}\ e^{\frac{-k}{4\pi}(N_\mu - N_\epsilon)\,|z|} \tag{5.6}$$

The term $|z|$ is the magnitude of z measured from the aperture. Thus the guide impedance increases as $|z|$ increases, whenever $N_\epsilon > N_\mu$. This impedance behavior parallels that of a flared waveguide.

5.4 Selection of Termination Distance and Material Parameters in the Homogeneous Section

The best power match from a homogeneous guide is made when the imaginary part of the admittance is closest to zero. When the aperture admittance is different from the characteristic admittance of the guide, the magnitude of the admittance as a function of position from the aperture varies between maximum and minimum values. This occurs even when the imaginary part of the admittance is zero. The greater the mismatch at the aperture, the greater the maximum value and the smaller the minimum value.

The inhomogeneous guide must be terminated at either a maximum or minimum admittance value, and the material parameters of the homogeneous guide must be selected so that its characteristic admittance is equal to that of the inhomogeneous guide. The material parameters necessary to effect a power match when the admittance is near its maximum value will also allow the higher order modes to propagate, unless the mismatch is very slight. On the other hand, the material parameters necessary to effect a power match when the admittance is near its minimum value will make the guide nearly cut-off.

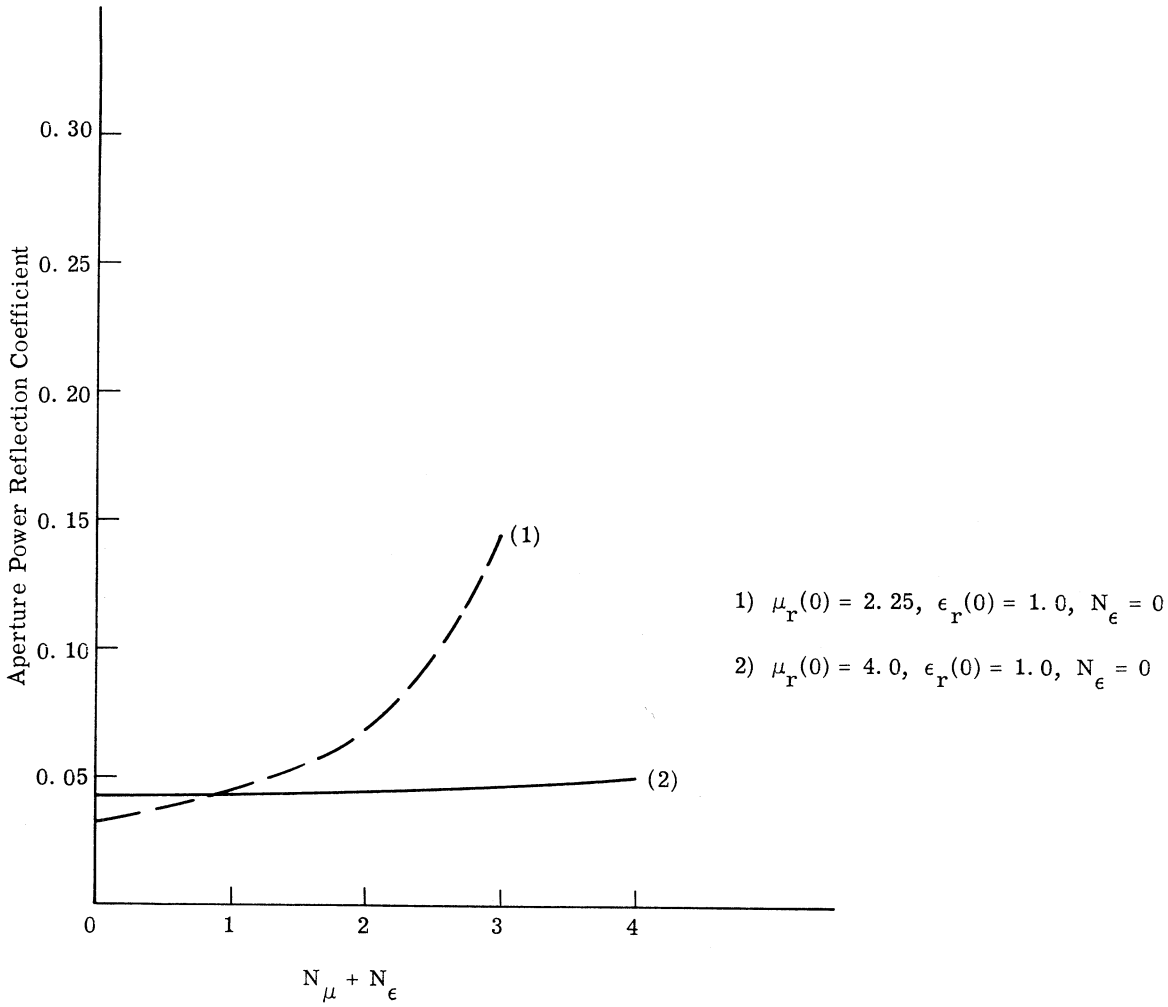

Fig. 5. 13. Aperture power reflection coefficient vs. $N_\mu + N_\epsilon$ for k = 27

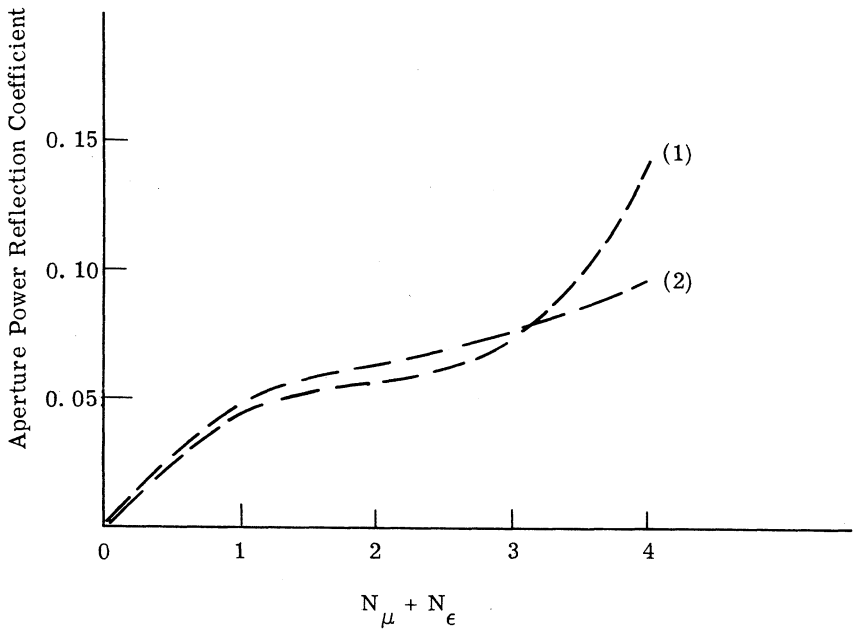

1) $\mu_r(0) = 2.112$, $\epsilon_r(0) = 1.065$, $N_\epsilon = 0$

2) $\mu_r(0) = 2.112$, $\epsilon_r(0) = 1.065$, $N_\mu = 0$

Fig. 5. 14. Aperture power reflection coefficient vs. $N_\mu + N_\epsilon$ for k = 27

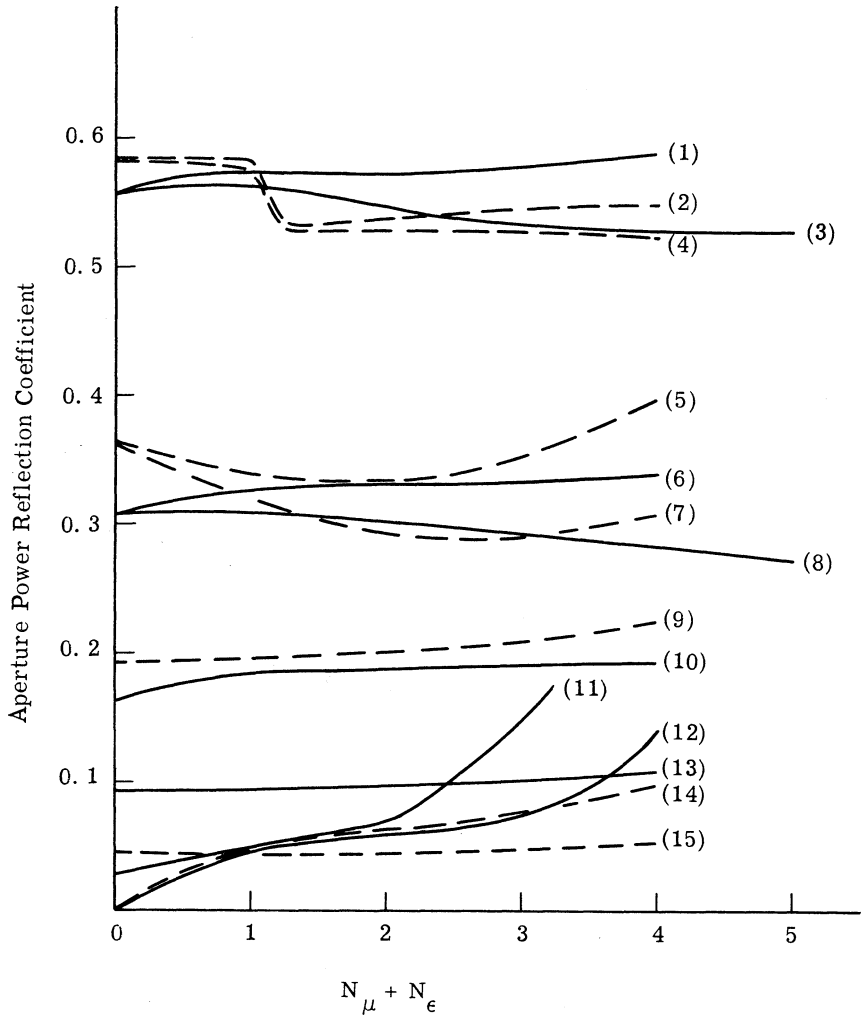

1) k = 18, $\mu_r(0) = 3.865$, $\epsilon_r(0) = 1.617$, $N_\epsilon = 0$

2) k = 18, $\mu_r(0) = 4.5$, $\epsilon_r(0) = 2.0$, $N_\epsilon = 0$

3) k = 18, $\mu_r(0) = 3.865$, $\epsilon_r(0) = 1.617$, $N_\mu = 0$

4) k = 18, $\mu_r(0) = 4.5$, $\epsilon_r(0) = 2.0$, $N_\mu = 0$

5) k = 21, $\mu_r(0) = 3.534$, $\epsilon_r(0) = 1.132$, $N_\epsilon = 0$

6) k = 21, $\mu_r(0) = 6.055$, $\epsilon_r(0) = 1.0322$, $N_\epsilon = 0$

7) k = 21, $\mu_r(0) = 3.534$, $\epsilon_r(0) = 1.132$, $N_\mu = 0$

8) k = 21, $\mu_r(0) = 6.055$, $\epsilon_r(0) = 1.0322$, $N_\mu = 0$

9) k = 23, $\mu_r(0) = 4.0$, $\epsilon_r(0) = 1.0$, $N_\epsilon = 0$

10) k = 23, $\mu_r(0) = 6.25$, $\epsilon_r(0) = 1.0$, $N_\epsilon = 0$

11) k = 27, $\mu_r(0) = 4.0$, $\epsilon_r(0) = 1.0$, $N_\epsilon = 0$

12) k = 29, $\mu_r(0) = 2.112$, $\epsilon_r(0) = 1.065$, $N_\epsilon = 0$

13) k = 25, $\mu_r(0) = 4.0$, $\epsilon_r(0) = 1.0$, $N_\epsilon = 0$

14) k = 29, $\mu_r(0) = 2.112$, $\epsilon_r(0) = 1.065$, $N_\mu = 0$

15) k = 27, $\mu_r(0) = 2.25$, $\epsilon_r(0) = 1.0$, $N_\epsilon = 0$

Fig. 5.15. Aperture power reflection coefficient vs. $N_\mu + N_\epsilon$ for selected values of k

That is, the homogeneous guide must be such that the resonant frequency is very nearly cut-off. A very unsymmetrical bandpass character results.

The passband may be made more symmetrical by adding an intermediate tuning element. Since the purpose of this discussion is to determine the relative advantages of an inhomogeneous section over a homogeneous section, the tuning element will not be considered.

The procedure for selecting the material parameters is : (a) select the value of $\mu_r(0)$, $\epsilon_r(0)$, N_μ and N_ϵ from Fig. 5.15, that gives the lowest aperture power reflection coefficient, and (b) use these values and calculate the minimum possible power reflection coefficient in a homogeneous guide versus the distance from the aperture for which the inhomogeneous guide can be terminated. Calculation of the minimum homogeneous or system power reflection coefficient is discussed in Section 3.2. Because the homogeneous guide is nearly cut off at resonance, it is important to consider the maximum bandwidth as a function of the termination distance.

Figures 5.16 through 5.21 represent the minimum value of power reflection coefficient in the homogeneous guide versus the distance from the aperture for which the inhomogeneous guide is terminated. The lower and upper limits of frequency, along with the maximum and minimum values of $\mu_r\epsilon_r$ in the homogeneous guide at resonance, are plotted on the same figures. These curves enable selection of the proper distance from the aperture to terminate the inhomogeneous section and also selection of the proper value of $\mu_r\epsilon_r$.

Figures 5.16 and 5.17 are related to the curves in Fig. 5.7. The minimum value of aperture power reflection coefficient for k = 18 is for $\mu_r(0) = 4.5$, $\epsilon_r(0) = 2.0$, $N_\mu = 0$, $N_\epsilon = 6$. This set of data was used for Fig. 5.16. A zero power reflection coefficient is possible when the inhomogeneous guide is terminated at $z = -0.016$ meters. This case is not too significant because of the limited bandwidth. At resonance, the minimum usable frequency corresponds to k = 17.8 and a maximum of k = 21. The reason for the upper limit is the ability of the higher order modes to propagate. From the standpoint of bandwidth, a more significant case is given by the other minimum value of aperture power reflection coefficient. That is for $\mu_r(0) = 3.865$, $\epsilon_r(0) = 1.617$, $N_\mu = 0$ and $N_\epsilon = 5.0$. Figure 5.17 was calculated from this data. For this case the minimum frequency is the same, but the upper limit has been raised to correspond to

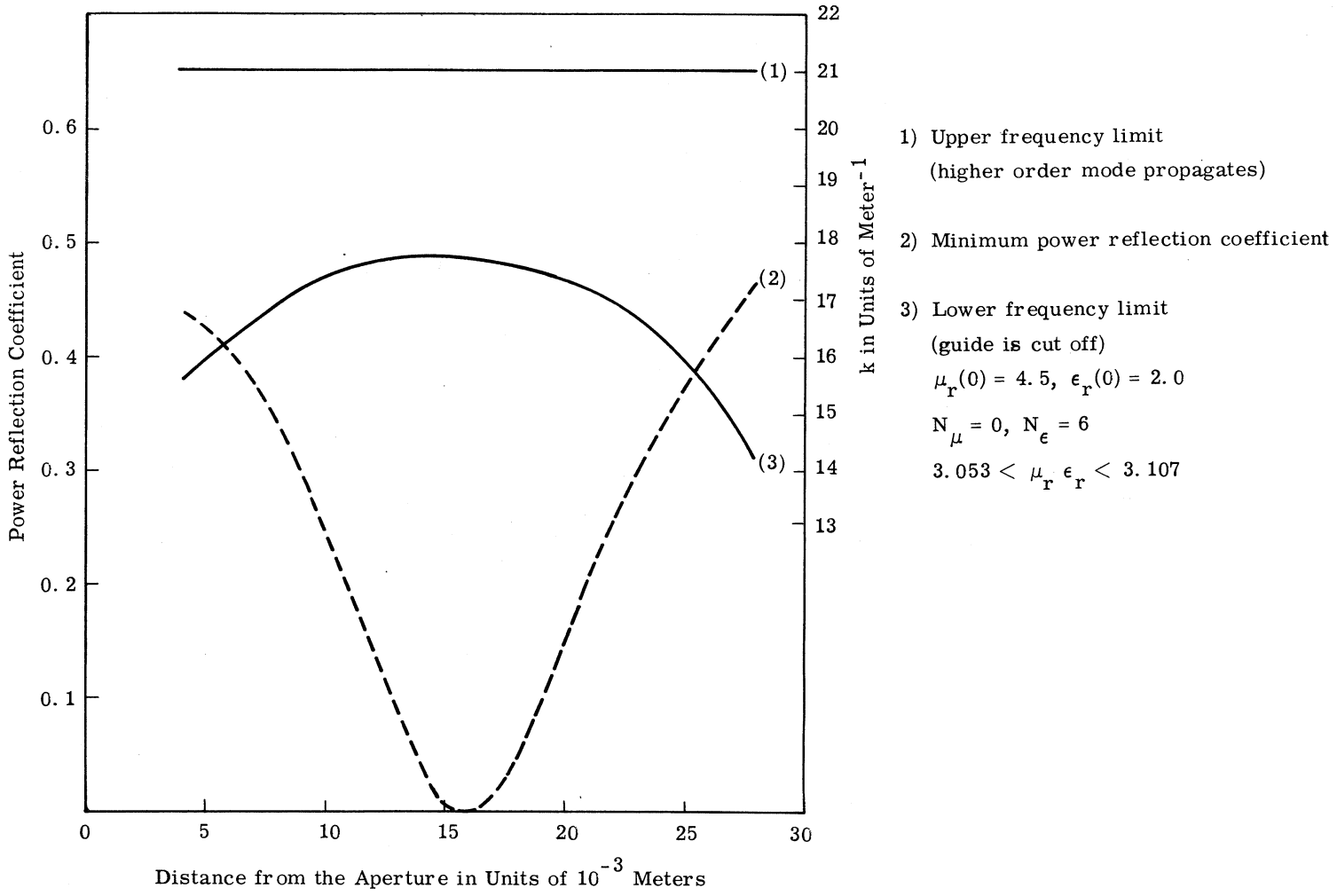

Fig. 5.16. Minimum overall power reflection coefficient and bandwidth vs. termination distance from the aperture for k = 18

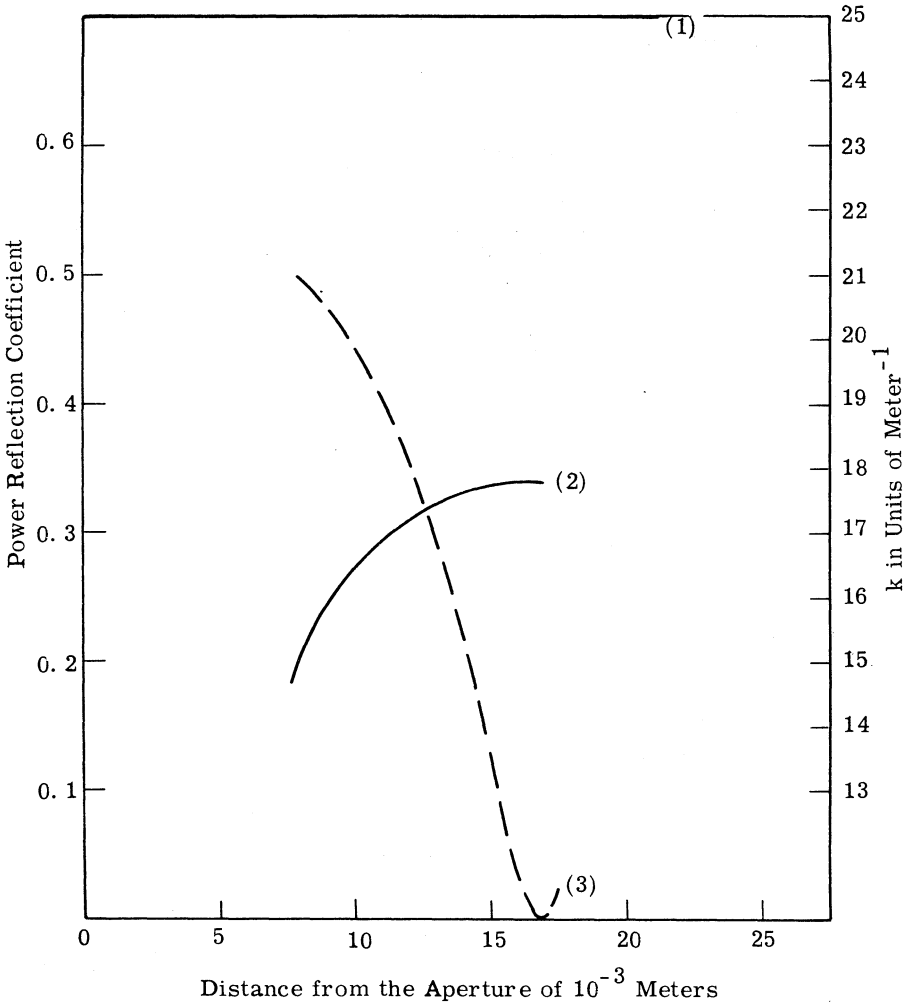

1) Upper frequency limit
(higher order mode propagates)

2) Lower frequency limit
(guide is cut off)

3) Minimum power reflection coefficient
$\mu_r(0) = 3.865$, $\epsilon_r(0) = 1.617$
$N_\mu = 0$, $N_\epsilon = 5$
$3.05 < \mu_r \epsilon_r < 3.10$

Fig. 5.17. Minimum overall power reflection coefficient and bandwidth vs. termination distance from the aperture for k = 18

k = 25. A zero power reflection coefficient for this set of data occurs if the inhomogeneous guide is terminated at z = -0.0169 meters and if $3.05 \leq \mu_r \epsilon_r \leq 3.1$ is used in the homogeneous guide.

The minimum aperture power reflection coefficient for k = 21, as shown in Fig. 5.15, occurs for $\mu_r(0) = 6.055$, $\epsilon_r(0) = 1.032$, $N_\mu = 0$, and $N_\epsilon = 6.5$. This set of data does not give significant results because $\epsilon_r(0)$ is very close to one. In order to have a small aperture reflection coefficient, it is necessary to use large values of N_ϵ; however, when large values of N_ϵ are used, $\epsilon_r(z)$ decays to less than unity very near the aperture, which is not a physically realizable situation. The other minimum is for $\mu_r(0) = 3.534$, $\epsilon_r(0) = 1.132$, $N_\mu = 0$, and $N_\epsilon = 2.75$. This data was used to calculate Fig. 5.18. However, the same problem exists in this data as exists for $\epsilon_r(0) = 1.032$, but it is less severe. Although it is impossible to terminate in a perfect match before $\epsilon_r(z)$ is less than one, it is possible to go back far enough to have a power reflection coefficient less than 0.2. Other material parameters can be used to make it possible to terminate in a perfect match, but they would all result in a larger aperture power reflection coefficient. One advantage of not terminating in a perfect match, is that the lower frequency curve is extended. In this case the lower frequency limit is extended to a frequency corresponding to k = 20.2; whereas, if it were possible to terminate on a perfect match, the lower frequency limit would correspond to a k closer to 21.

The rest of the frequencies are not as significant because the aperture power reflection coefficient in the inhomogeneous guide is not as small as is possible in a homogeneous guide.

The curve in Fig. 5.10 for $\mu_r(0) = 4.0$, $\epsilon_r(0) = 1.0$ was used, even though the curve for $\mu_r(0) = 6.25$, $\epsilon_r(0) = 1.0$ gave a smaller aperture power reflection coefficient. The reason for this choice was bandwidth. Due to the higher value of $\mu_r(0)\epsilon_r(0)$, the upper limit of usable frequency before the higher order modes begin to propogate corresponds to k = 25, the lower limit corresponds to about k = 22.8. Therefore the upper curve on Fig. 5.10 was used with $N_\epsilon = 0$ and $N_\mu = 2.0$ to calculate Fig. 5.19. For k = 23, a zero power reflection coefficient is possible if the inhomogeneous guide is terminated at z = -0.0154 meters and for a $\mu_r \epsilon_r$ range in the homogeneous guide of $1.886 \leq \mu_r \epsilon_r \leq 1.942$.

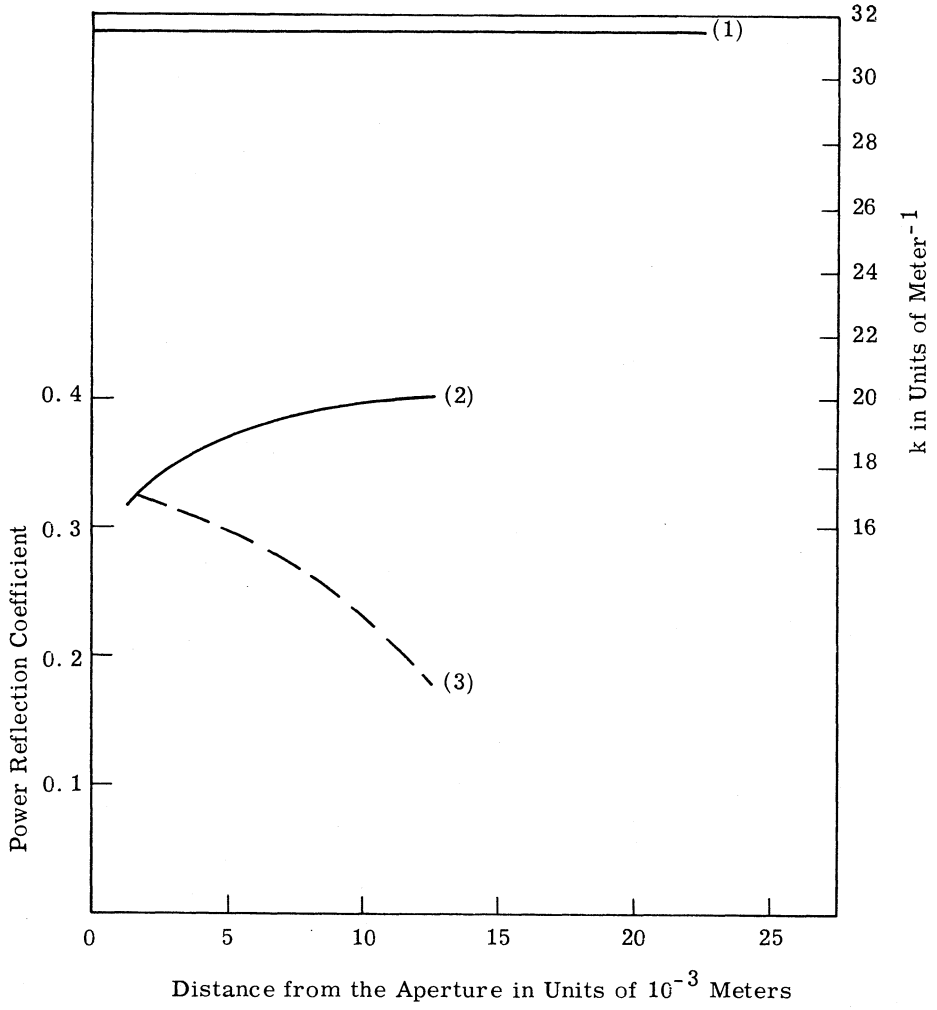

1) Upper frequency limit
(higher order mode propagates)

2) Lower frequency limit
(guide is cut off)

3) Minimum power reflection coefficient
$\mu_r(0) = 3.534$, $\epsilon_r(0) = 1.132$
$N_\mu = 0$, $N_\epsilon = 2.75$
$2.27 < \mu_r \epsilon_r < 2.42$

Fig. 5.18. Minimum overall power reflection coefficient and bandwidth vs. termination distance from the aperture for k = 21

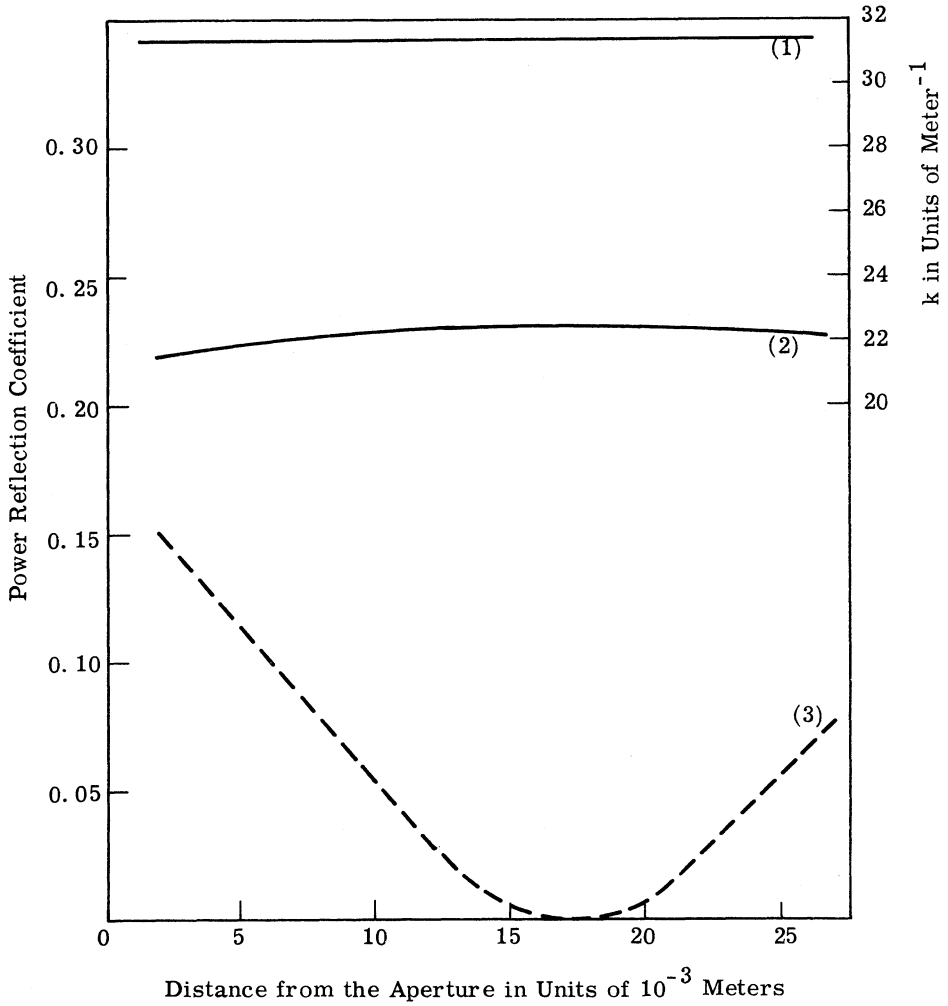

1) Upper frequency limit
(higher order mode propagates)

2) Lower frequency limit
(guide is cut off)

3) Minimum power reflection coefficient
$\mu_r(0) = 4.0$, $\epsilon_r(0) = 1.0$
$N_\mu = 2.0$, $N_\epsilon = 1.0$
$1.886 < \mu_r \epsilon_r < 1.942$

Fig. 5.19. Minimum overall power reflection coefficient and bandwidth vs. termination distance from the aperture for k = 23

Figure 20 shows that for $k = 25$ a zero power reflection coefficient is possible if the inhomogeneous guide is terminated at $z = -0.0125$ meters and a range of $(1.623 \leq \mu_r \epsilon_r \leq 1.707)$ in the homogeneous guide. $N_\mu = 2.0$ and $N_\epsilon = 0$ for Fig. 5.20.

For $k = 27$, Fig. 5.13 shows that the minimum value of the aperture power reflection coefficient occurs for $\mu_r(0)\epsilon_r(0) = 2.25$ which rapidly increases as N_μ increases. Therefore the data for Fig. 5.22 was taken from the other curve, N_μ was taken as 2.0 and N_ϵ as zero. A zero power reflection coefficient for $k = 27$ is possible if the inhomogeneous guide is terminated at $z = -0.005$ meters, and $1.425 \leq \mu_r \epsilon_r \leq 1.54$ is used in the homogeneous guide. A perfect match for $k = 29$ can be accomplished by the use of a homogeneous guide with $\mu_r = 2.112$ and $\epsilon_r = 1.065$ only.

The distance at which the inhomogeneous guide should be terminated and a range of mu-epsilon products in the homogeneous guide can be found for a perfect match by using Figs. 5.16 through 5.21.

5.5 Homogeneous System

The reference antenna system to which the inhomogeneous system is compared is a completely homogeneous system. This system is exactly the same as the inhomogeneous system except that the material in the section of waveguide which terminates in the ground plane is homogeneous. Terms μ_r and ϵ_r are equal to $\mu_r(0)$ and $\epsilon_r(0)$. For this system, the power reflection coefficient is found by transforming the aperture impedance found in Figs. 5.2 through 5.5 through a length of waveguide on the Smith Chart. The length of guide used was that necessary to transform the imaginary part of the aperture impedance at the resonant frequency to zero. The guide was then terminated in another homogeneous guide of the same dimensions, but which was loaded with a material whose parameters were such that its characteristic impedance was equal to the real part of the transformed aperture impedance; thus insuring a zero power reflection coefficient at the resonant frequency. With the selection of the material parameters and termination distance, the power reflection coefficient versus frequency was computed using the aperture impedance found by using Figs. 5.2 through 5.5 and the Smith Chart.

5.6 Comparison of the Inhomogeneous and Homogeneous Systems

Figures 5.22 through 5.25 represent power reflection coefficients in the inhomo-

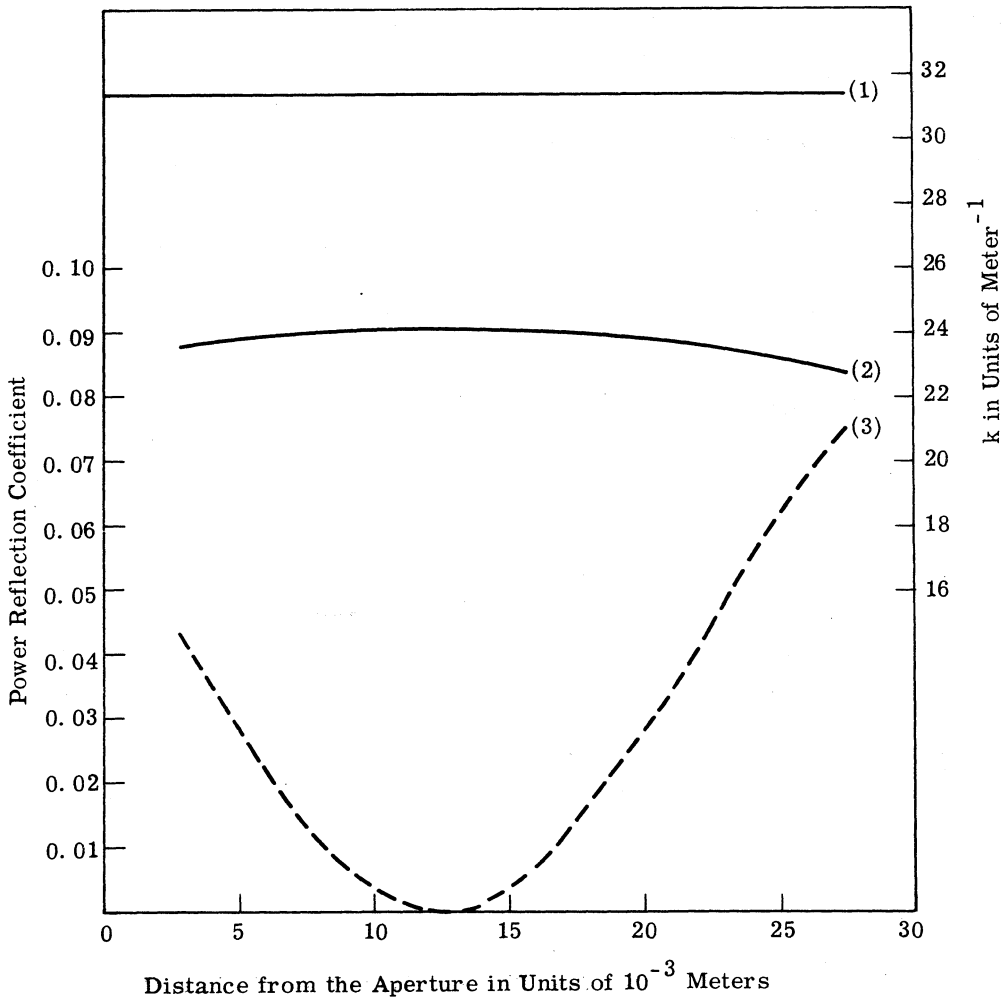

1) Upper frequency limit
(high order modes propagates)

2) Lower frequency limit
(guide is cut off)

3) Minimum power reflection coefficient
$\mu_r(0) = 4.0$, $\epsilon_r(0) = 1.0$
$N_\mu = 2.0$, $N_\epsilon = 0$
$1.623 < \mu_r \epsilon_r < 1.707$

Fig. 5.20. Minimum overall power reflection coefficient and bandwidth vs. termination distance from the aperture for k = 25

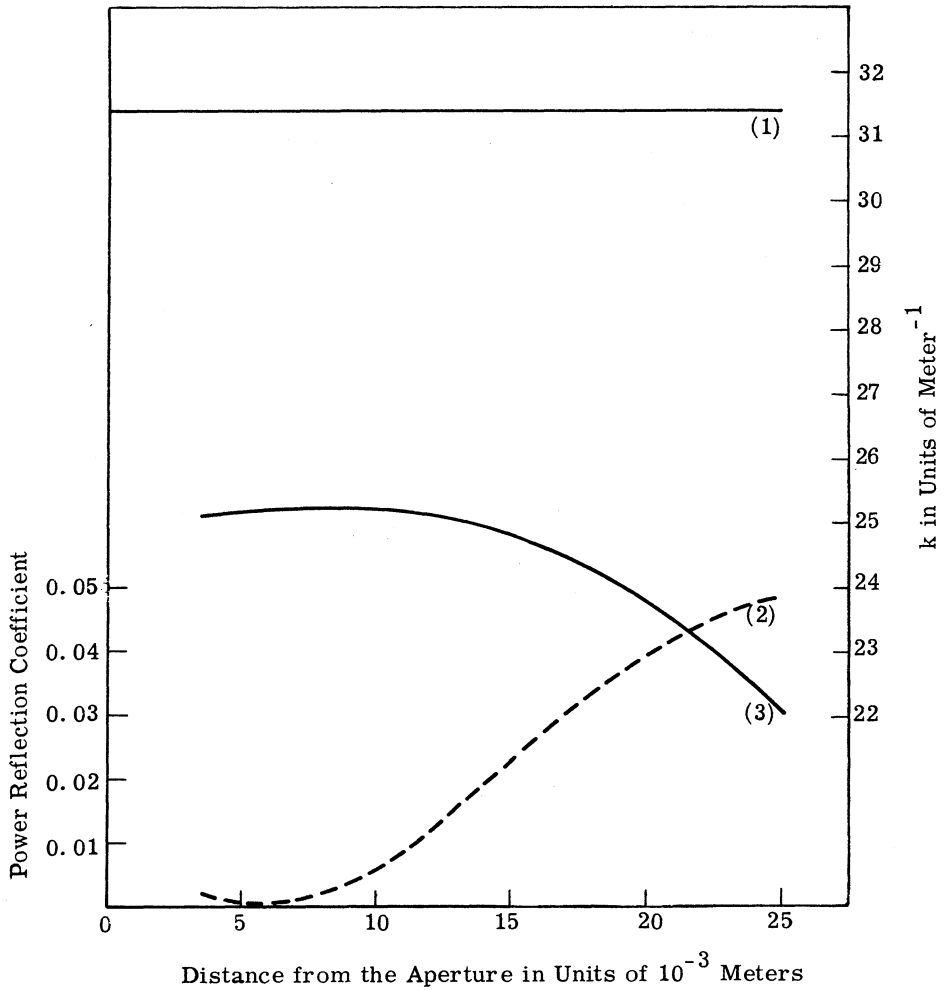

1) Upper frequency limit
(high order mode propagates)

2) Minimum power reflection coefficient

3) Lower frequency limit
(guide is cut off)
$\mu_r(0) = 4.0$, $\epsilon_r(0) = 1.0$
$N_\mu = 2.0$, $N_\epsilon = 0$
$1.425 < \mu_r \epsilon_r < 1.54$

Fig. 5.21. Minimum overall power reflection coefficient and bandwidth vs. termination distance from the aperature of k = 27

geneous guide versus frequency and are calculated by using the material parameters determined from Figs. 5.16 through 5.21. Two cases were calculated; one for the maximum value of the mu-epsilon product, and the other for the minimum value of the mu-epsilon product. Power reflection coefficient versus frequency curves were plotted for a completely homogeneous system on the same figure. Figure 5.22 has $k = 18$ as its resonant frequency. It is apparent that both smaller and larger values of the power reflection coefficient are possible in the inhomogeneous system. If Curves 2 and 3 are used, there is a corresponding reduction of 30 to 50 percent in the power reflection coefficient by using the inhomogeneous system over the homogeneous system. At the very high end of the frequency range, Curve 4 has a lower power reflection coefficient than Curve 2, but through the low and mid frequency ranges, the power reflection coefficients are much greater. Thus for a resonant frequency corresponding to k = 18, the inhomogeneity results in a 30 to 50 percent reduction in power reflection coefficient. Also there is a size reduction of about 29 percent in the inhomogeneous system in the z direction.

It is impossible to have a zero power reflection coefficient in the inhomogeneous system for k = 21 when the optimum aperture parameters are used. The term $\epsilon_r(0)$ is too close to one to be able to terminate the guide far enough back to have a zero power reflection coefficient in the homogeneous guide and still be greater than one.

Figure 5.23 is a plot of power reflection coefficient versus frequency when the data from Fig. 5.18 is used. However, the material parameter for the homogeneous system was chosen so that the power reflection coefficient at k = 21 is zero. It is interesting to note that even though the power reflection coefficient in the inhomogeneous system is not zero for k = 21, that it does drop below that of the homogeneous system. The initial slope of Curves 1 and 4 is negative, and the guide is terminated before the imaginary part of the admittance is equal to zero. As the frequency is increased, the electrical length of the guide is increased, thus the termination distance becomes closer to optimum. This case illustrates a possible method of selecting a termination distance such that at the lowest frequency of operation the homogeneous guide is not too near cut-off and the power reflection coefficient is below some predetermined value. It is apparent from Fig. 5.23 that the inhomogeneous material is still of some value in reducing the over-all power reflection coefficient. There is a size reduction in the z direction of about 55 percent,

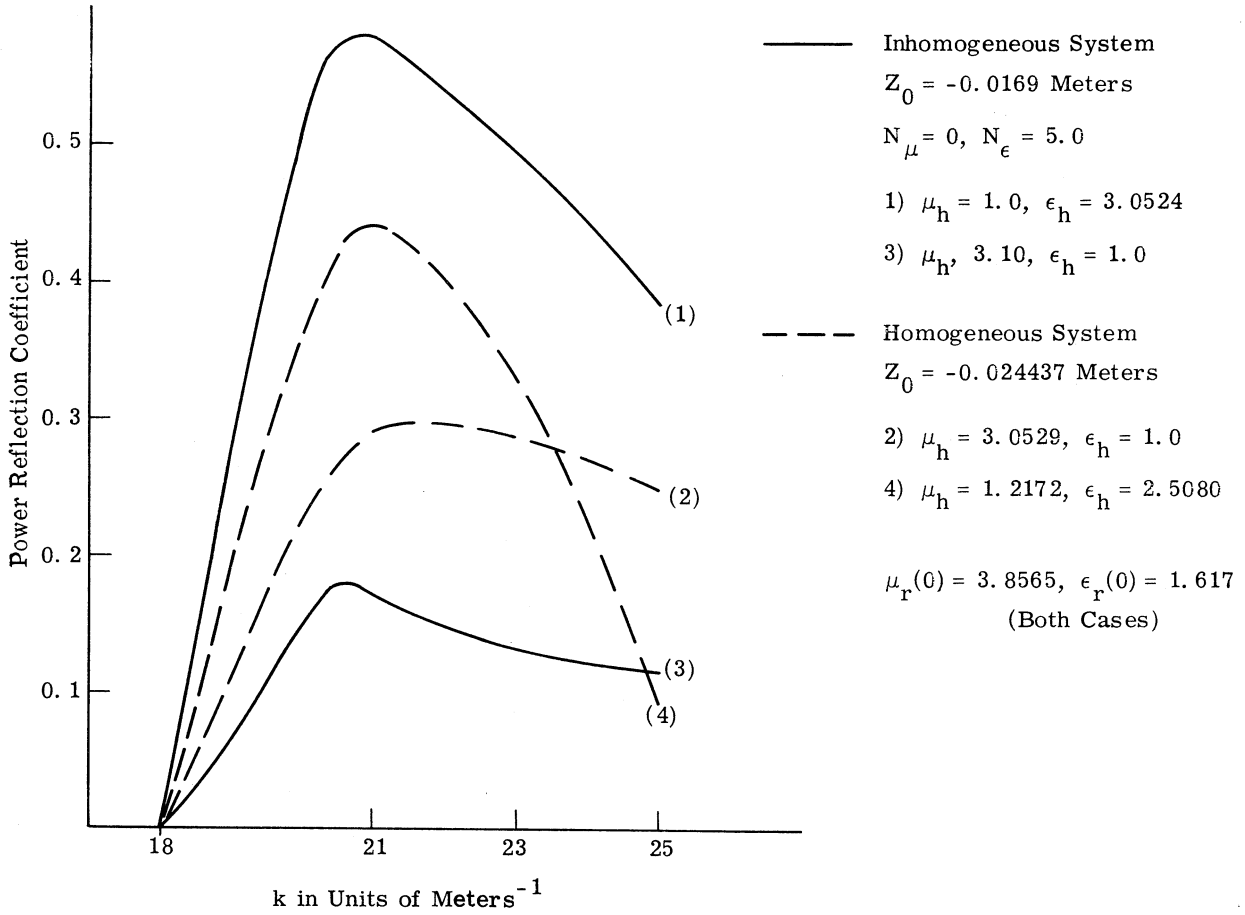

Fig. 5.22 Overall power reflection coefficient vs. free-space wave number for the inhomogeneous and the homogeneous systems resonant at k = 18

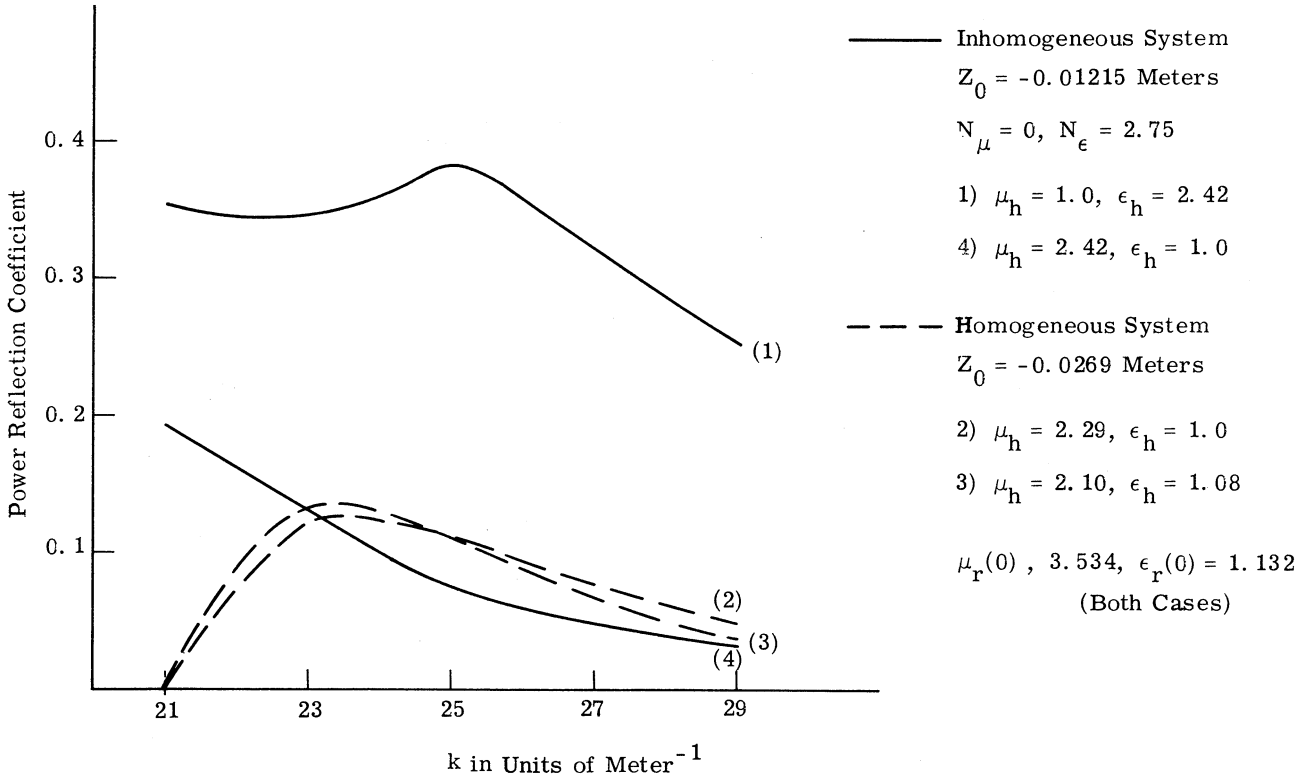

Fig. 5.23 Overall power reflection coefficient vs. free-space wave number for the inhomogeneous and the homogeneous systems resonant at k = 21

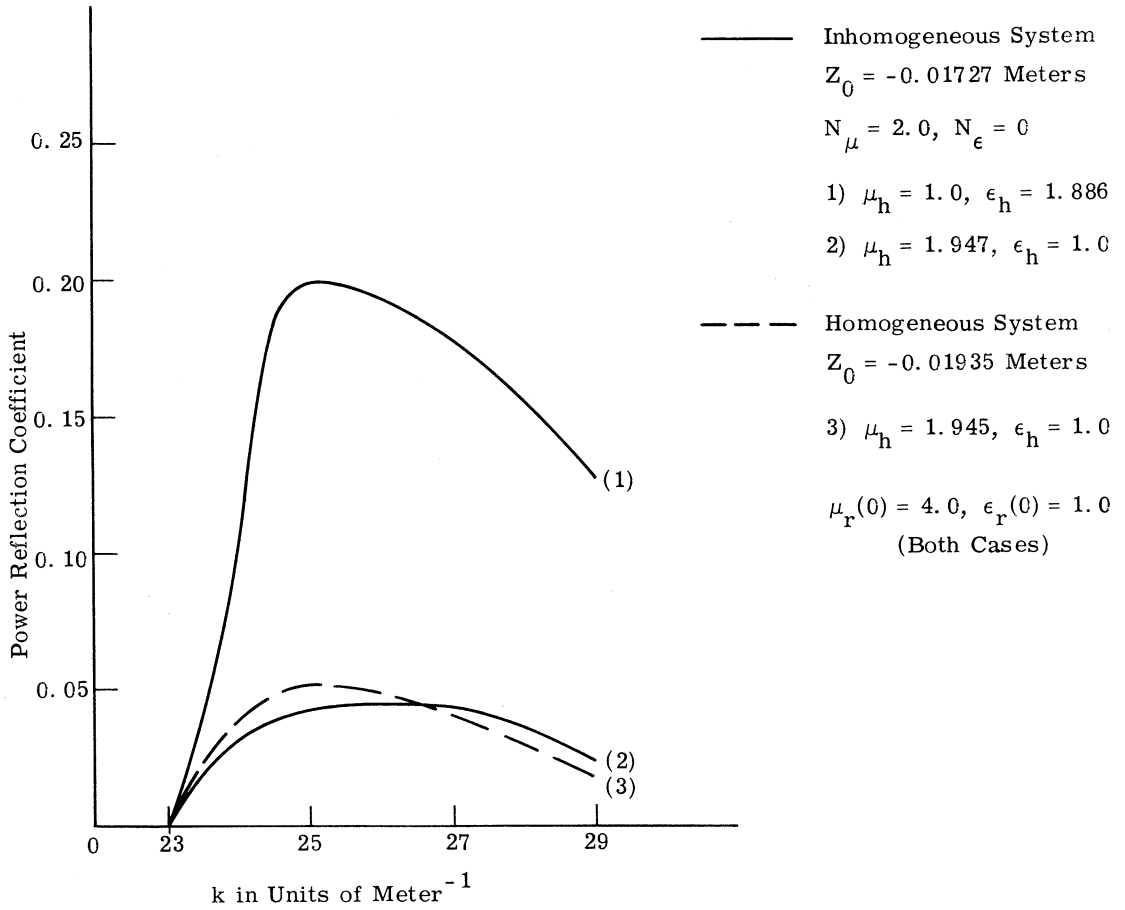

Fig. 5. 24. Overall power reflection coefficient vs. free-space wave number for the inhomogeneous and the homogeneous systems resonant at k = 23

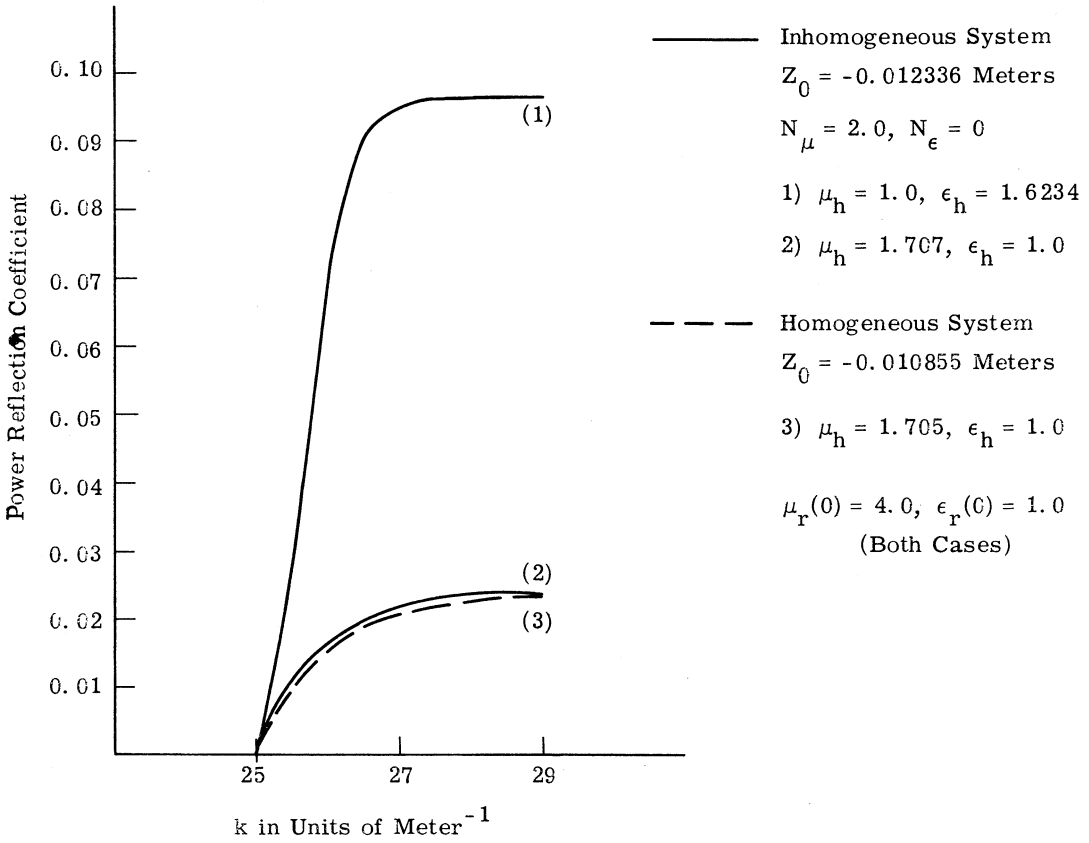

Fig. 5.25. Overall power reflection coefficient vs. free-space wave number for the inhomogeneous and the homogeneous systems resonant at k = 25

but of course, the inhomogeneous system was terminated before optimum. Figures 5.24 and 5.25 represent frequencies where it was impossible to improve the aperture power reflection coefficient by using an inhomogeneous material, (See Fig. 5.15). It is also clear that the inhomogeneity is of no value, and indeed may be a disadvantage with respect to power reflection coefficient versus frequency. For k = 23, there is a size reduction of about 10 percent, but for k = 25, the size is increased by nearly 14 percent. Corresponding figures for k = 27 and k = 29 were not calculated.

Figures 5.26 through 5.29 are plots of the Poynting vector for the material parameters given in Figs. 5.22 through 5.25. The Poynting vector is plotted in two planes on each figure. The $\theta = 0$ plane is defined by the X and Z axis, the $\theta = \frac{\pi}{2}$ plane is defined by Y and Z axis. For each frequency the Poynting vector is normalized to unity along the $\theta = 0$ axis. It is interesting to note that the radiation pattern of the system is very close to a magnetic dipole pointing in the x direction. It is shown in Section 2.3 that an effective magnetic current can be used as the source for the free space fields. This magnetic current is given by $\overrightarrow{M} = \overrightarrow{E} x \hat{n}$, but in the aperture $E_x = 0$. Thus there is only a y directed magnetic current. The aperture magnetic current may be represented in a multiple expansion with the leading term being a dipole. The Poynting vector of a magnetic dipole in the x direction is completely isotropic in the $\theta = \frac{\pi}{2}$ plane and in the $\theta = 0$ plane it has a $\cos^2\theta$ distribution. For frequencies where the aperture is below cut-off with respect to the free-space wavelength, a predominantly dipolar pattern is expected, (See Figs. 5.26 through 5.29).

5.7 Summary of Results

This work has treated the problem of an antenna system filled with inhomogeneous materials, and an exact solution of the aperture fields was set up. The approximations were made for numerical convenience only, but became quite severe as the values of k became less than 18. It was shown that if the frequency is low enough ($k \leq 21$) and the optimum value of $\mu_r(0)$ and $\epsilon_r(0)$ for a given $\mu_r(0)\,\epsilon_r(0)$ product is used then there is an advantage (similar to a flared horn) in using an inhomogeneous material.

Based upon Figs. 5.22 through 5.25, the benefit seems marginal-to-fair for low

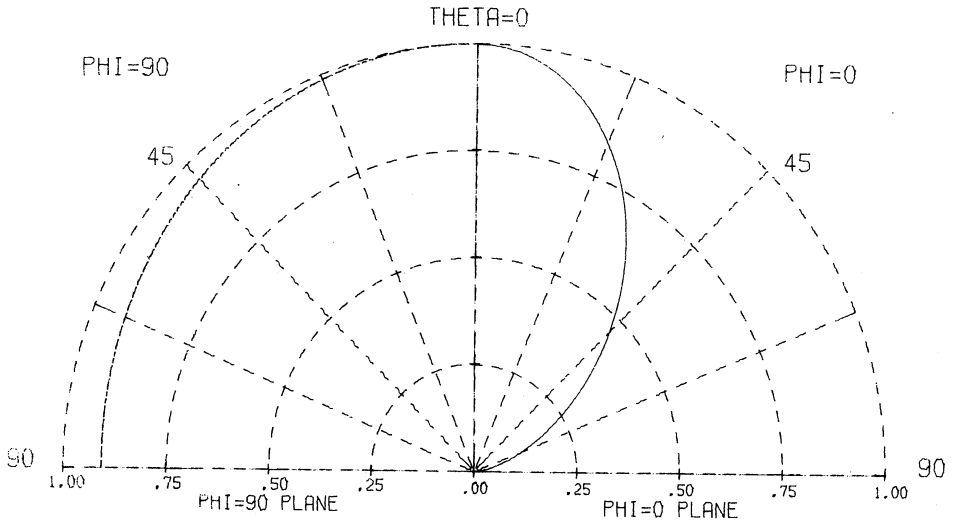

POYNTING VECTOR VS. THETA

K= 18.000 U= 3.8650 E= 1.6170

NU= .000 NE= 5.000

Fig. 5.26. Poynting vector vs. theta for k = 18

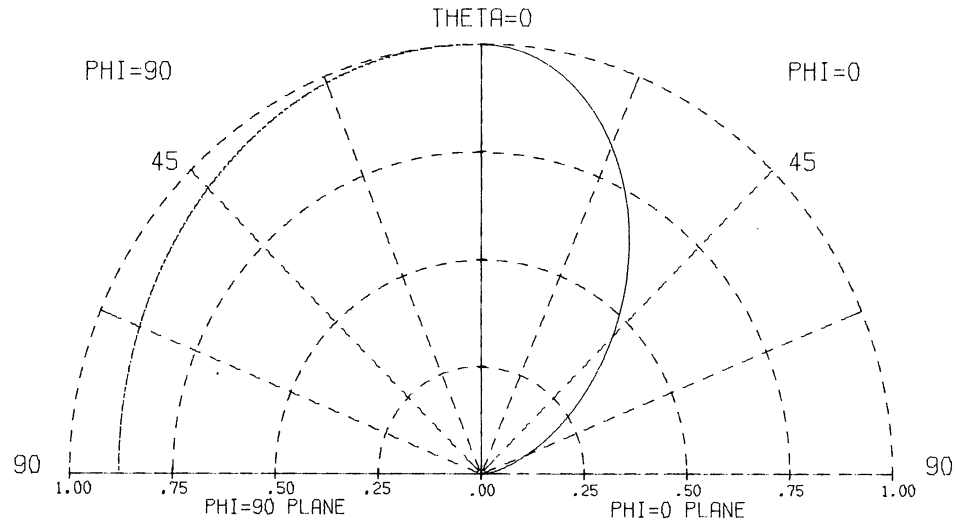

POYNTING VECTOR VS. THETA

K= 21.000 U= 3.5340 E= 1.1320

NU= .000 NE= 2.750

Fig. 5.27. Poynting vector vs. theta for k = 21

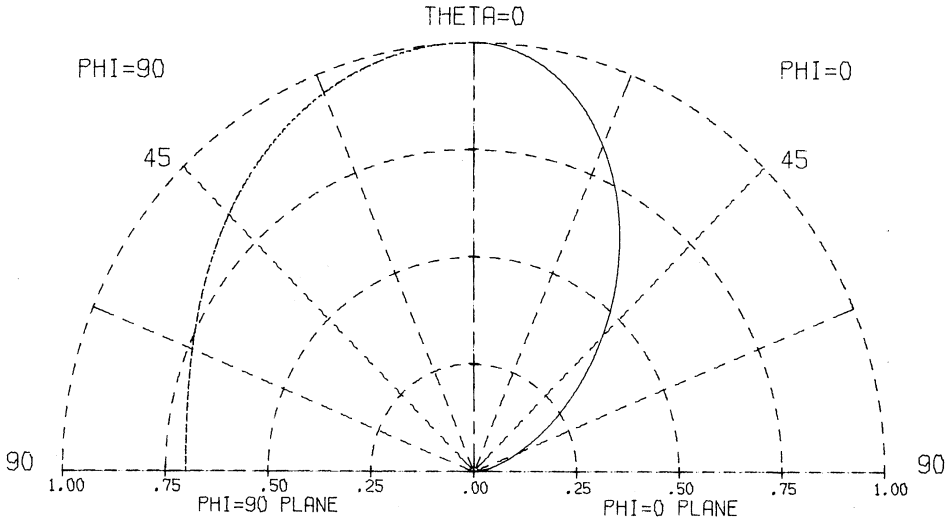

Fig. 5.28. Poynting vector vs. theta for k = 23

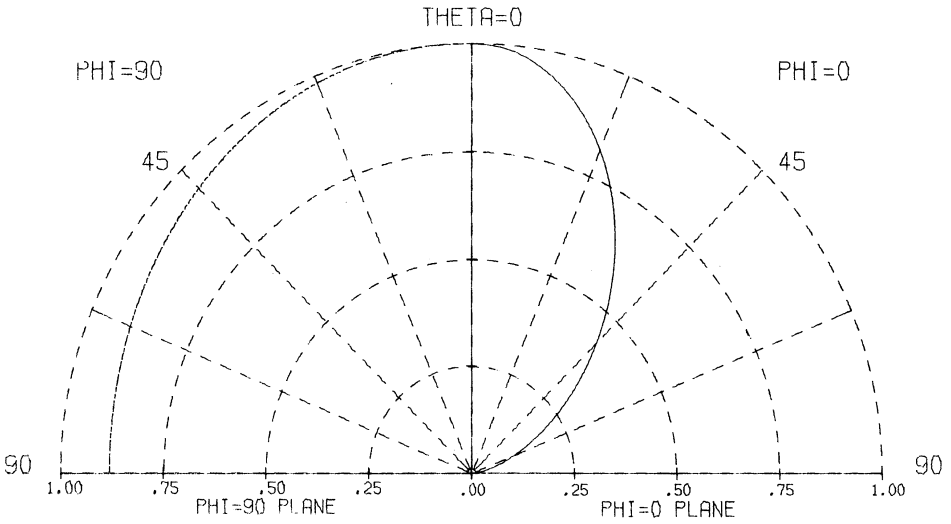

Fig. 5.29. Poynting vector vs. theta for k = 25

frequencies, and non-existent-to-poor at the higher frequencies. For $k = 18$, there is substantial percentage improvement (30 to 50 percent) but throughout the entire region the power reflection coefficient is less than 0.4. For $k = 21$, it was impossible to obtain a zero power reflection coefficient and still maintain a minimum aperture power reflection coefficient. However, even in this case the inhomogeneity improved the over-all bandwidth, but again in the homogeneous system the power reflection coefficient was so small (less than 0.15) that the additional reduction was relatively unimportant. For $k = 23$, the advantage is nonexistent and for $k = 25$ the homogeneous system performs better. Size reduction in the z direction follows the same pattern as a function of frequency. A size reduction in the transverse plane was impossible because the antenna systems that were compared were assumed to be of the same transverse dimension.

The lower frequency limitation of the numerical analysis is determined by the number of higher order modes that are necessary to satisify the boundary condition in the aperture. As the frequency is lowered the matrices must be truncated at larger sizes, which necessitates more computer time.

5.8 Future Work

Future investigation should attempt to extend this analysis to include lower frequency, since the present analysis indicates that the benefits of using inhomogeneous materials are greater at the lower frequencies. In addition it may be feasible to use different aperture material parameters and to terminate the inhomogeneous guide not quite at optimum so that a flatter or more symmetrical response, or perhaps some other desired characteristics, can be obtained.

APPENDIX A

PROOF THAT THE FREE SPACE FIELDS IN INTEGRAL FORM SATISFY MAXWELL'S EQUATIONS AND BOUNDARY CONDITION

The purpose of Appendix A is to show that the fields on the free space side of the aperture, as given in Section 2.3, satisfy both Maxwell's equations and the proper boundary conditions.

For the purpose of this appendix, let the coordinate variables x, y, z be designated r and the coordinate variables η, ξ be designated r'.

By straight forward substitution, it can be shown that the Green's Function, as given in Section 2.3, satisfied the wave equation:

$$\nabla^2 G(r, r') + k^2 G(r, r') = 0 \quad \text{for } r \neq r' \tag{A-1}$$

With the above relationship verified, it can also be shown, by substitution, that Maxwell's curl and divergence equations are satisfied.

However, it is important that fields also satisfy the proper boundary conditions. This can be shown by writing Eq. 2.100 as:

$$E_x(x, y, 0) = \frac{1}{4\pi^2} \int_{\text{aperture}} d\eta\, d\xi \int_{-\infty}^{\infty} dk_x \int_{-\infty}^{\infty} dk_y\, e^{i[k_x(x-\eta) + k_y(y-\xi)]} E_x(\eta, \xi)\, dS(\eta, \xi) \tag{A-2}$$

However,

$$\int_{-\infty}^{\infty} d\alpha\, e^{i\alpha(x - x')} = 2\pi\, \delta(x - x') \tag{A-3}$$

$$\therefore \quad E_x(x, y, 0) = \int_{\text{aperture}} \delta(x - \eta)\, \delta(y - \xi)\, E(\eta, \xi)\, d\eta\, d\xi \tag{A-4}$$

$$E_x(x, y, 0) = \begin{cases} E(x, y, 0) & \text{when } x, \text{ and } y \text{ are in the aperture} \\ \\ 0 & \text{when } x, \text{ and } y \text{ are not in the aperture} \end{cases} \qquad \text{(A-5)}$$

This is the condition necessary, i. e., the E_x field is continuous in the aperture and zero outside. A similar manipulation is carried out on Eq. 2.201, yielding the same result for the E_y field. Thus, the tangential electric fields are continuous and obey the proper boundary conditions over the entire infinite plane.

This and the fact that all the field components satisfy Maxwell's equations is enough to guarantee the proper boundary conditions everywhere.

APPENDIX B

ASYMPTOTIC EXPANSION OF HANKEL FUNCTIONS FOR LARGE ORDER AND ARGUMENT

The purpose of this appendix is to discuss the calculation of the various Hankel functions, which are necessary to determine the mode coefficients.

According the Bateman (Ref. 35), the asymptotic expansion for the Hankel functions of the second kind for large argument and order are given as

$$H_p^{(2)}(x) = \sum_{m=0}^{M-1} \frac{2^{(m+\frac{1}{2})}\,\Gamma(m+\frac{1}{2})\,b_m}{\pi\,(x^2-p^2)^{\frac{1}{2}(m+\frac{1}{2})}}\, e^{-i\left[\sqrt{x^2-p^2} + p\sin^{-1}(\frac{p}{x}) - \frac{\pi}{2}(p+\frac{1}{2}) - m\frac{\pi}{2}\right]} \quad \text{(B-1)}$$

for $x > p >, o,$ and

$$H_p^{(2)}(x) = i \sum_{m=0}^{M-1} \frac{(-1)^m\, 2^{(m+\frac{1}{2})}\,\Gamma(m+\frac{1}{2})\,b_m}{\pi\,(p^2-x^2)^{\frac{1}{2}(m+\frac{1}{2})}}\, e^{\left[\sqrt{p^2-x^2} - p\cosh^{-1}(\frac{p}{x})\right]} \quad \text{(B-2)}$$

for $p > x > o$

where b_m are functions of x and p and are given through $m = 2$.

Thus $H_p^{(2)}(x)$, for $x > p$ represents a traveling wave in the negative direction. (Note: an $e^{-i\omega t}$ time dependence is assumed).

The term $H_p^{(2)}(x)$, for $p > x$, represents an exponentially decaying function as $\frac{p}{x}$ becomes large.

The transition region between the traveling wave and the decaying wave is near $p = x$. For the purpose of determining upper and lower limits of various inequalities, cutoff is assumed to be at $p = x$.

The term $H_p^{(1)}(x)$ is equal to the complex conjugate of $H_p^{(2)}(x)$, and therefore $x > p$ represents a wave traveling in the positive direction.

$$p = \nu_\epsilon = \frac{\sqrt{4\left(\frac{n^2\pi^2}{a^2} + \frac{m^2\pi^2}{b^2}\right) + \frac{4\pi^2 N_\epsilon^2}{k^2}}}{\frac{k}{2\pi}(N_\epsilon + N_\mu)}$$

when associated with the TM modes.

$$p = \nu_\mu = \frac{\sqrt{4\left(\frac{n^2\pi^2}{a^2} + \frac{m^2\pi^2}{b^2}\right) + \frac{4\pi^2 N_\mu^2}{k^2}}}{\frac{k}{2\pi}(N_\epsilon + N_\mu)}$$

when associated with the TE modes.

$$x = \frac{2k_g(0)}{C_g} e^{\frac{1}{2}C_g z} = \frac{4\pi\sqrt{\mu_r(0)\,\epsilon_r(0)}}{N_\epsilon + N_\mu} e^{\left(\frac{N_\mu + N_\epsilon}{4\pi}\right) kz}$$

for either case

$$b_0 = 1,\ b_1 = \frac{1}{8} - \frac{5}{24}\left(1 - \frac{x^2}{p^2}\right)^{-1}$$

$$b_2 = \frac{3}{128} - \frac{77}{576}\left(1 - \frac{x^2}{p^2}\right)^{-1} + \frac{385}{3456}\left(1 - \frac{x^2}{p^2}\right)^{-2}$$

Computer programs were written, using the above results, for the following functions:

HE2. (P1, P2, P3, P4, P5, P6, P7) $\equiv \frac{1}{i} H_{\nu_\mu}^{(2)}(x)$, for $\nu_\mu > x$

HM2. (P1, P2, P3, P4, P5, P6, P7) $\equiv \frac{1}{i} H^{(2)}_{\nu_\epsilon}(x)$, for $\nu_\epsilon > x$

DHE2. (P1, P2, P3, P4, P5, P6, P7) $\equiv \frac{d}{dx}\frac{1}{i}(H^{(2)}_{\nu_\mu}(x))$, for $\nu_\mu > x$

DHM2. (P1, P2, P3, P4, P5, P6, P7) $\equiv \frac{d}{dx}\frac{1}{i}(H^{(2)}_{\nu_\epsilon}(x))$, for $\nu_\epsilon > x$

REH1. (P1, P2, P3, P4, P5, P6, P7) $\equiv \mathrm{Re} H^{(1)}_{\nu_\mu}(x)$, for $\nu_\mu < x$

IMH1. (P1, P2, P3, P4, P5, P6, P7) $\equiv \mathrm{Im}\, H^{(1)}_{\nu_\mu}(x)$, for $\nu_\mu < x$

DREH1. (P1, P2, P3, P4, P5, P6, P7) $\equiv \mathrm{Re}\frac{d}{dx}(H^{(1)}_{\nu_\mu}(x))$, for $\nu_\mu < x$

DIMH1. (P1, P2, P3, P4, P5, P6, P7) $\equiv \mathrm{Im}\frac{d}{dx}(H^{(1)}_{\nu_\mu}(x))$, for $\nu_\mu < x$

P1 $\equiv$ n, P2 $\equiv$ m, P3 $\equiv$ z, P4 $\equiv$ k

P5 $\equiv N_\mu$, P6 $\equiv N_\epsilon$, P7 $\equiv \mu_r(0)\epsilon_r(0)$

For $x > 10$, accuracies are on the order of 1% .

As the material becomes homogeneous, the Hankel functions must go over to plane waves. As C_g goes to zero, the Hankel functions for the TE and TM modes are equal.

$$H^{(2)}_p(x) = \sum_{m=o}^{M-1} C_m\, e^{-i\left[x\sqrt{1-\frac{p^2}{x^2}} + p\sin^{-1}\left(\frac{p}{x}\right) - \frac{\pi}{2}\left(p+\frac{1}{2}\right) - \frac{m\pi}{2}\right]} \qquad \text{(B-3)}$$

where

$$x = \frac{2\omega}{C_g}\sqrt{\mu(z)\,\epsilon(z)}$$

$$p = \frac{2K_c}{C_g} \qquad K_c = \sqrt{\frac{n^2\pi^2}{a^2} + \frac{m^2\pi^2}{b^2}}$$

$$C_m = \frac{2^{(m+\frac{1}{2})}\,\Gamma(m+\frac{1}{2})\,bm}{\pi(x^2 - p^2)^{\frac{1}{2}(m+\frac{1}{2})}}$$

Expand $\sqrt{1 - p^2/x^2}$ and $\sin^{-1}(\frac{p}{x})$ in a Maclaurin series about $C_g = 0$, and retain only the first two terms.

$$\sqrt{1 - \frac{p^2}{x^2}} \cong \left[\sqrt{1 - \frac{p^2}{x^2}} + \frac{C_g z K_c^2}{2\omega^2\,\mu(0)\,\epsilon(0)}\,\frac{1}{\sqrt{1 - \frac{p^2}{x^2}}}\right]_{C_g = 0} \tag{B-4}$$

$$\sin^{-1}(\frac{p}{x}) = \left[\sin^{-1}(\frac{p}{x}) - \frac{C_g z K_c}{2\omega\sqrt{\mu(0)\,\epsilon(0)}}\,\frac{1}{\sqrt{1 - \frac{p^2}{x^2}}}\right]_{C_g = 0} \tag{B-5}$$

$$x \cong \frac{2\omega\sqrt{\mu(0)\,\epsilon(0)}}{C_g}\left(1 - \frac{C_g}{2}z\right)$$

Thus, in the limit as C_g goes to zero

$$H_p^{(2)}(x) \cong H\,e^{-i\sqrt{\omega^2\,\mu(0)\,\epsilon(0) - K_c^2}\,z} \tag{B-6}$$

where

$$H = \sum_{m=0}^{M-1} C_m \Big|_{C_g = 0}\; e^{-i\left[\frac{2\sqrt{\omega^2\,\mu(0)\,\epsilon(0) - K_c^2}}{C_g}\right.}$$

$$\left. + \frac{2K_c}{C_g}\sin^{-1}\left(\frac{K_c}{\omega\sqrt{\mu(0)\,\epsilon(0)}}\right) - \frac{\pi}{2}\left(\frac{K_c}{C_g} + \frac{1}{2}\right) - \frac{m\pi}{2}\right]$$

Therefore, in the limit as C_g goes to zero, that is, as the material becomes homogeneous, the Hankel functions go over to the correct form for a homogeneous guide, but with a rather unusual phase factor. It can be shown that when the mode is cut off, that is, when $p > x$, the Hankel functions go over to a decaying exponential with exponent, $\sqrt{K_c^2 - \omega^2 \mu(0) \epsilon(0)}$. The amplitude factor for this case is also a negative exponential which goes as $\frac{1}{C_g}$. Therefore, in the limit as the material becomes homogeneous, all field quantities must be renormalized by a factor that goes as e^{1/C_g}.

APPENDIX C

EVALUATION OF $I_{nm}^{\alpha\beta}$

The term $I_{nm}^{\alpha\beta}$, as originally defined in Chapter 3, is given as

$$I_{nm}^{\alpha\beta} = \int_{-\infty}^{\infty} \frac{(k_x^2 - k^2)\, a_n^{(1)} a_\alpha^{(2)} a_m^{(3)} a_\beta^{(4)}\, dk_x dk_y}{\sqrt{k^2 - (k_x^2 + k_y^2)}} \qquad \text{(C-1)}$$

Using Eq. 3.10 through Eq. 3.15, $I_{nm}^{\alpha\beta}$ can be written as

$$I_{nm}^{\alpha\beta} = \epsilon_{nm}^{\alpha\beta} \frac{256}{a^2 b^2} \left(\frac{n\pi}{a}\right)\left(\frac{\alpha\pi}{a}\right) \int_{-\infty}^{\infty} \frac{k_y^2 (k_x^2 - k^2) \sin^2\left(\frac{k_x a}{2} + \frac{n\pi}{2}\right) \sin^2\left(\frac{k_y b}{2} + \frac{m\pi}{2}\right) dk_x dk_y}{\sqrt{k^2 - (k_x^2 + k_y^2)}\left(k_x^2 - \frac{n^2\pi^2}{a^2}\right)\left(k_x^2 - \frac{\alpha^2\pi^2}{a^2}\right)\left(k_y^2 - \frac{m^2\pi^2}{b^2}\right)\left(k_y^2 - \frac{\beta^2\pi^2}{b^2}\right)} \qquad \text{(C-2)}$$

where

$$\epsilon_{nm}^{\alpha\beta} \begin{cases} 0 \text{ when } \alpha + n = \text{odd integer} \\ 0 \text{ when } \beta + m = \text{odd integer} \\ \frac{1}{2} \text{ when } \beta = 0, \text{ or } m = 0, \text{ but not both} \\ \frac{1}{4} \text{ when } \beta = 0,\ m = 0 \\ 1 \text{ otherwise} \end{cases}$$

(Note: $I_{nm}^{\alpha\beta}$ is symmetric in the α, n and β, m pairs.)

That is,

$$I_{nm}^{\alpha\beta} = I_{n\beta}^{\alpha m} = I_{\alpha m}^{n\beta} = I_{\alpha\beta}^{nm}$$

A proper selection of branch cuts must be made for the square root in the

denominator of C-2. From Eq. 2.100, it can be shown that for the outgoing wave on the free space side of the aperture, $\sqrt{k^2 - (k_x^2 + k_y^2)}$ must be greater than zero for $(k_x^2 + k_y^2) < k^2$, and equal to $i\sqrt{(k_x^2 + k_y^2) - k^2}$ for $(k_x^2 + k_y^2) > k^2$. It is the condition of outward traveling waves that determine the proper branches of the square root. Since the argument of $\sqrt{k_x^2 - (k_x^2 + k_y^2)}$ is independent of the sign of either k_x or k_y, it is convenient to rewrite the integral in the form

$$I_{nm}^{\alpha\beta} = K_{nm}^{\alpha\beta} \int_0^\infty dx \int_0^\infty dy \frac{y^2(x^2 - 1)\sin^2\left(\frac{kax}{2} + \frac{n\pi}{2}\right)\sin^2\left(\frac{kby}{2} + \frac{m\pi}{2}\right)}{\sqrt{1 - (x^2 + y^2)}\left(x^2 - \frac{n^2\pi^2}{a^2k^2}\right)\left(x^2 - \frac{\alpha^2\pi^2}{a^2k^2}\right)\left(x^2 - \frac{m^2\pi^2}{b^2k^2}\right)\left(y^2 - \frac{\beta^2\pi^2}{b^2k^2}\right)} \tag{C-3}$$

where

$$K_{nm}^{\alpha\beta} = \epsilon_{nm}^{\alpha\beta}\left(\frac{256}{a^2b^2}\right)\left(\frac{n\pi}{a}\right)\left(\frac{\alpha\pi}{a}\right)\frac{4}{k^3}$$

$$x = \frac{k_x}{k} \qquad y = \frac{k_y}{k}$$

$$\text{Arg}\left(\sqrt{1 - (x^2 + y^2)}\right) = \begin{cases} 0 & \text{when } (x^2 + y^2) < 1 \\ \frac{\pi}{2} & \text{when } (x^2 + y^2) > 1 \end{cases}$$

The region in the x - y plane is then divided up into eight subregions, and the integral is evaluated separately in each region.

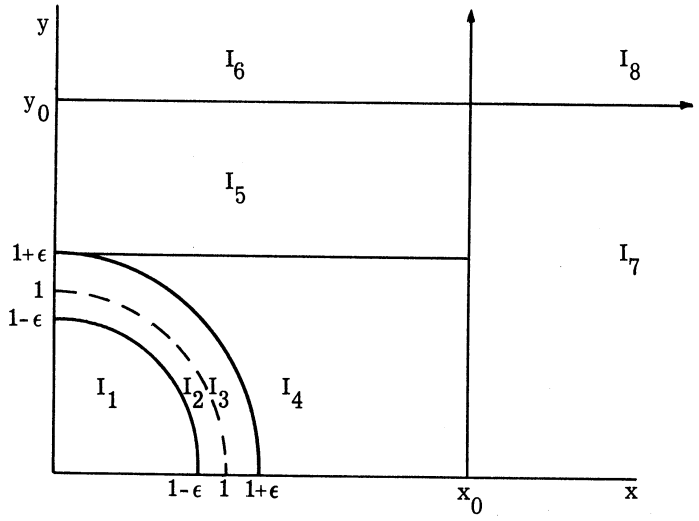

Fig. C.1. Regions of integration of the integrals $I_1 - I_8$

The term ϵ is chosen to allow an acceptable error in the region near the singularity with an acceptable error.

Define I_1 through I_8 such that

$$I_{nm}^{\alpha\beta} = K_{nm}^{\alpha\beta} \sum_{\ell=1}^{8} I_\ell$$

The real part of Eq. C-1 is contained in the region for which $(x^2 + y^2) \leq 1$, whereas the imaginary part of Eq. C-1 is contained in the remainder of the quarterplane.

$$I_1 = \int_0^{1-\epsilon} dy \frac{y^2 \sin^2\left(\frac{kby}{2} + \frac{m\pi}{2}\right)}{\left(y^2 - \frac{m^2\pi^2}{b^2k^2}\right)\left(y^2 - \frac{\beta^2\pi^2}{b^2k^2}\right)} \int_0^{\sqrt{(1-\epsilon)^2 - y^2}} dx \frac{(x^2 - 1)\sin^2\left(\frac{kax}{2} + \frac{n\pi}{2}\right)}{\sqrt{1 - (x^2 + y^2)}\left(x^2 - \frac{n^2\pi^2}{a^2k^2}\right)\left(x^2 - \frac{\alpha^2\pi^2}{a^2k^2}\right)} \tag{C-4}$$

$$I_2 \cong \sqrt{\epsilon} \int_0^{\frac{\pi}{2}} d\phi \frac{\sin^4\phi \sin^2\left(\frac{ak}{2}\cos\phi + \frac{n\pi}{2}\right)\sin^2\left(\frac{kb}{2}\sin\phi + \frac{m\pi}{2}\right)}{\left(\cos^2\phi - \frac{n^2\pi^2}{a^2k^2}\right)\left(\cos^2\phi - \frac{\alpha^2\pi^2}{a^2k^2}\right)\left(\sin^2\phi - \frac{m^2\pi^2}{b^2k^2}\right)\left(\sin^2\phi - \frac{\beta^2\pi^2}{b^2k^2}\right)} \tag{C-5}$$

where

$$x = r\cos\phi$$

$$y = r\sin\phi$$

Integration over the r variable was carried out by hand with the approximation that ϵ was small compared to 1. I_1 and I_2 were evaluated with the aid of a computer, using a library integration subroutine (See Appendix D).

In the limit as n, α, m, and β become larger, it is possible to evaluate I_1 and I_2 by hand. This calculation was performed, and the results were compared with computer results using various values of ϵ. It was found that for $\epsilon = 0.005$, the error was a minimum, being less than $\frac{1}{2}$ percent. A computer program was written in the form of an external function for the evaluation of the real part of $I_{nm}^{\alpha\beta}$. The function was called REI (n, α, m, β, k).

The term I_3 is of the same form as I_2 except that it is multiplied by -i.

$$I_4 = -i \int_1^{1+\epsilon} dy \frac{y^2 \sin^2\left(\frac{kby}{2} + \frac{m\pi}{2}\right)}{\left(y^2 - \frac{m^2\pi^2}{b^2k^2}\right)\left(y^2 - \frac{\beta^2\pi^2}{b^2k^2}\right)} \int_{\sqrt{(1+\epsilon)^2 - y^2}}^{x_0} dx \frac{(x^2 - 1)\sin^2\left(\frac{kax}{2} + \frac{n\pi}{2}\right)}{\sqrt{x^2 + y^2 - 1}\left(x^2 - \frac{n^2\pi^2}{a^2k^2}\right)\left(x^2 - \frac{\alpha^2\pi^2}{a^2k^2}\right)}$$

(C-6)

x_0 is determined by either n or α, whichever is larger.

$$x_0 = \begin{cases} 5\frac{n\pi}{ak} \\ 5\frac{\alpha\pi}{ak} \end{cases} \quad \text{whichever is larger}$$

ϵ is the same as was used for I_2.

$$I_5 = -i \int_{1+\epsilon}^{y_0} dy \frac{y^2 \sin^2\left(\frac{kby}{2} + \frac{m\pi}{2}\right)}{\left(y^2 - \frac{m^2\pi^2}{b^2k^2}\right)\left(y^2 - \frac{\beta^2\pi^2}{b^2k^2}\right)} \int_0^{x_0} dx \frac{(x^2 - 1)\sin^2\left(\frac{kax}{2} + \frac{n\pi}{2}\right)}{\sqrt{x^2 + y^2 - 1}\left(x^2 - \frac{n^2\pi^2}{a^2k^2}\right)\left(x^2 - \frac{\alpha^2\pi^2}{a^2k^2}\right)}$$

(C-7)

y_0 is determined by either m or β, whichever is larger.

$$y_0 = \begin{cases} 10 & \text{when } m = \beta = 0 \\ 5\frac{m\pi}{bk} & \\ 5\frac{\beta\pi}{bk} & \text{whichever is larger} \end{cases}$$

$$I_6 \cong -i\frac{1}{2} \int_0^{x_0} dx \frac{(x^2 - 1)\sin^2\left(\frac{kax}{2} + \frac{n\pi}{2}\right)}{\left(x^2 - \frac{n^2\pi^2}{a^2k^2}\right)\left(x^2 - \frac{\alpha^2\pi^2}{a^2k^2}\right)} \int_{y_0}^{\infty} \frac{dy}{y^2\sqrt{y^2 + (x^2 - 1)}} \qquad \text{(C-8)}$$

The integration over y has been simplified by the proper choice of y_0, i.e.,

$$y^2 \geq \begin{cases} 25\,\dfrac{m^2\pi^2}{b^2k^2} \\ \\ 25\,\dfrac{\beta^2\pi^2}{b^2k^2} \end{cases} \quad \text{whichever is larger}$$

$\sin^2\left(\frac{kby}{2} + \frac{m\pi}{2}\right)$ has been replaced by $\frac{1}{2}$. Therefore, it is possible to neglect $\frac{m^2\pi^2}{b^2k^2}$ and $\frac{\beta^2\pi^2}{b^2k^2}$ with respect to y in this region.

$$I_6 \cong -i\,\frac{1}{2}\int_0^{x_0} dx\,\frac{\sin^2\left(\frac{kax}{2} + \frac{n\pi}{2}\right)\left(\sqrt{y_0^2 + (x^2 - 1)} - y_0\right)}{y_0\left(x^2 - \frac{n^2\pi^2}{a^2k^2}\right)\left(x^2 - \frac{\alpha^2\pi^2}{a^2k^2}\right)} \qquad \text{(C-9)}$$

$$I_7 \cong -i\,\frac{1}{2}\int_0^{y_0} dy\,\frac{y^2\sin^2\left(\frac{kby}{2} + \frac{m\pi}{2}\right)\left(\sqrt{x_0^2 + (y^2 - 1)} - x_0\right)}{x_0\,(y^2 - 1)\left(y^2 - \frac{m^2\pi^2}{b^2k^2}\right)\left(y^2 - \frac{\beta^2\pi^2}{b^2k^2}\right)} \qquad \text{(C-10)}$$

The approximation that $\frac{n^2\pi^2}{a^2k^2}$ and $\frac{\alpha^2\pi^2}{a^2k^2}$ could be neglected with respect to x^2 and that $\frac{kby}{2} >> \frac{m\pi}{2}$ was used in Eq. C-10. The reasons are the same as those used in Eq. C-9.

$$I_8 \cong -i\,\frac{1}{4}\int_{y_0}^{\infty}\int_{x_0}^{\infty} \frac{dx\,dy}{x^2\,y^2\sqrt{x^2 + y^2}} \qquad \text{(C-11)}$$

$$I_8 \cong -i\,\frac{1}{12}\left[\frac{(x_0^2 + y_0^2)^{\frac{3}{2}} - x_0^2}{x_0^3\,y_0^3} - \frac{1}{x_0^3}\right] \qquad \text{(C-12)}$$

The usual approximations were used in Eq. C-12.

A computer program in the form of an external function was used to evaluate I_3 through I_8, and then used to evaluate the imaginary part of $I_{nm}^{\alpha\beta}$. The function was called IMI, (n, α, m, 2, k).

Therefore, the real and imaginary parts of $I_{nm}^{\alpha\beta}$ were written as external functions for use on the digital computer.

The library integration subroutine, (Appendix D), has two degrees of flexibility to obtain the needed degree of accuracy. The first is the number of subintervals in which the integration over any other variable of integration can be divided. This number is completely arbitrary but cannot be negative or zero. The second is the number of Gaussian points to be used in the numerical evaluation. This number is limited to a maximum of eight. However, when the entire eight points are used, the accuracy is such that any function that can be approximated by a polynomial of order 15 or less will be integrated with zero error.

For the evaluation of $I_{nm}^{\alpha\beta}$, eight Gaussian points were used in all cases. Where the region of integration was large, a sufficient number of subintervals was used. The error involved should be much less than one percent.

APPENDIX D

COMPUTER INTEGRATION SUBROUTINE

The purpose of this appendix is to discuss the computer library subroutine that is used for the evaluation of multiple integrals.

The subroutine is called ITINT and its purpose is to compute:

$$\int_{A}^{B_0} F_0(X_0) \int_{A_1(X_0)}^{B_1(X_0)} F_1(X_0, X_1) \cdots \int_{A_{k-1}(X_0, \cdots, X_{k-2})}^{B_{k-1}(X_0, \cdots, X_{k-2})} F_{k-1}(X_0, \cdots X_{k-1}) \, dX_{k-1} \cdots dX_0$$

for any integer, $k \geq 1$, by Gaussian quadrature.

A value for the L-th integral in the above expression is computed from the sum

$$\int_{A_L}^{A_L+H} F_L \, dX_L + \int_{A_L+H}^{A_L+2H} F_L \, dX_L + \cdots + \int_{A_L+(N_L-1)H}^{A_L+N_LH} F_L \, dX_L$$

Where N_L may be a function of $X_0, \ldots, X_{L-1}$ and $H = \dfrac{B_L - A_L}{N_L}$

where

$$\int_{A_L+TH}^{A_L+(T+1)H} F_L \, dX_L$$

is approximated from M_L evaluations of F_L on the interval $A_L + TH < X < A_L + (T+1)H$; $1 \leq M_L \leq 8$.

Numerical integration by Gaussian quadrature is accomplished by the following method:

$$\int_{-1}^{1} f(x)\,dx = \sum_{i=1}^{n} \omega_i\, f(x_i) + R_n$$

where

x_i is the i^{th} zero of $P_n(x)$

$$\omega_i = \frac{2}{(1 - x_i)^2}\, P_n'(x_i) \qquad \text{(D-1)}$$

$$R_n = \frac{2^{2n+1}\,(n!)^4}{(2n+1)[(2n)!]^3}\, f^{(2n)}(\xi)\,;\ -1 < \xi < 1$$

The integral over the interval $-1 \leq \chi \leq 1$ may be generalized to an arbitrary interval, by a simple change of variable.

$$\int_{a}^{b} f(y)\,dy = \frac{b-a}{2} \sum_{i=1}^{n} \omega_i\, f(y_i) + R_n \qquad \text{(D-2)}$$

$$y_i = \left(\frac{b-a}{2}\right) x_i + \left(\frac{b+a}{2}\right)$$

where

ω_i and x_i are given above.

Thus, this method is exact for any polynomial of order less than 2n.

APPENDIX E

INTEGRATION BY THE METHOD OF STATIONARY PHASE

The purpose of this appendix is to discuss the use of the Method of Stationary Phase to evaluate the integrals representing the far-field components of the radiated fields.

Copson (38) has treated $F(\nu) = \int_a^b e^{i\nu f(x)} \phi(x)\, dx$ (E-1)

under the following condition:

(a) f(z) and $\phi(z)$ are analytic functions of the complex variable z, regular in a simply connected open region D, containing the segment $a \leq x \leq b$ of the real axis.

(b) f(z) is real on the real axis.

If $f'(x) \neq 0$

$$0 \leq x \leq b$$

$$F(\nu) = \int_a^b e^{i\nu f(x)} \phi(x)\, dx = \frac{\phi(b)\, e^{i\nu f(b)}}{i\nu f'(b)} - \frac{\phi(a)\, e^{i\nu f(a)}}{i\nu f'(a)} + 0\left(\frac{1}{\nu^2}\right) \qquad \text{(E-2)}$$

The above expression may be verified by integration by parts with $F(\nu)$ in the following form:

$$F(\nu) = \frac{1}{i\nu} \int_a^b \frac{\phi(x)}{f'(x)} \frac{d}{dx} e^{i\nu f(x)}\, dx \qquad \text{(E-3)}$$

If $f'(x_0) = 0$, i. e., if the phase has a stationary point at x_0, and $f''(x_0) \neq 0$, then

$$I(\nu) = \int_{x_0}^b e^{i\nu f(x)} \phi(x)\, dx = \sqrt{\frac{\pi}{2\nu f''(x_0)}}\, e^{i\nu f(x) + \frac{i\pi}{4}} + 0\left(\frac{1}{\nu}\right) \qquad \text{(E-4)}$$

for $f''(x_0) > 0$

$$I(\nu) = \sqrt{\frac{\pi}{-2\nu f''(x_0)}}\ \phi(x_0)\, e^{i\nu f(x_0) - \frac{i\pi}{4}} + 0\left(\frac{1}{\nu}\right) \qquad \text{(E-5)}$$

$$\text{for } f''(x_0) < 0$$

If the stationary point is at the upper limit of integration, then the results are the same except that all functions are evaluated at the upper limit instead of the lower limit. If

$$f'(x_0) = f''(x_0) = 0 \quad \text{and} \quad f'''(x_0) \neq 0$$

then it can be shown that the leading term of $I(\nu)$ is $0\left(\frac{1}{\nu^{\frac{1}{3}}}\right)$.

Thus, the leading term of $F(\nu)$ as $\nu \to +\infty$ will always be from the stationary phase point of highest order.

The integrals of current interest may always be written as

$$F(\nu) \cong 2\sqrt{\frac{\pi}{2\nu\,|f''(x_0)|}}\ \phi(x_0) e^{i\nu f(x_0) \pm i\frac{\pi}{4}} \qquad \text{(E-6)}$$

where the (+) sign is used for $f''(x_0) > 0$ and the (-) sign when $f''(x_0) < 0$.

The general form of the integrals needed to express the radiated fields is:

$$I = \int_{s(k)} \Phi(k_x, k_y)\, e^{kR[\,k_x \sin\theta\cos\phi + k_y \sin\theta \sin\phi + \cos\theta\sqrt{k^2 - (k_x^2 + k_y^2)}\,z\,]}\, dk_x dk_y$$

$$= \int_{-k}^{k} dk_x\, e^{iRk_x \sin\theta\cos\phi} \int_{-\sqrt{k^2 - k_x^2}}^{\sqrt{k^2 - k_x^2}} \Phi(k_x, k_y)\, e^{iR[\,k_y \sin\theta \sin\phi + \cos\theta\sqrt{k^2 - (k_x^2 + k_y^2)}\,]}\, dk_y \qquad \text{(E-7)}$$

Let

$$I(k_x, R) = \int_{-\sqrt{k^2 - k_x^2}}^{\sqrt{k^2 - k_x^2}} \Phi(k_x, k_y) e^{iR[k_y \sin\theta \cos\phi + \cos\theta \sqrt{k^2 - (k_x^2 + k_y^2)}]} dk_y \qquad \text{(E-8)}$$

The term $I(k_x, R)$ is now in the form $F(R)$, except that the phase is not analytic at the end points of integration. At these points, the square root contains a branch point. However, the branch cuts need never lie in the domain D.

The general formalism will be followed, the justification of such will be shown via the results, when applied to integrals of known form.

The phase is stationary for

$$k_y^0 = \frac{\sqrt{k^2 - k_x^2} \sin\theta \sin\phi}{\sqrt{1 - \sin^2\theta \cos^2\phi}} \qquad \text{(E-9)}$$

Note that

$$0 \leq \left| \frac{\sin\theta \cos\phi}{\sqrt{1 - \sin^2\theta \cos^2\phi}} \right| \leq 1 \qquad \text{(E-10)}$$

Thus the stationary point always lies within the region of integration.

$$f_y''(k_y^0) = \frac{-(1 - \sin^2\theta \cos^2\phi)^{\frac{3}{2}}}{\sqrt{k^2 - k_x^2} \cos^2\theta} \qquad \text{(E-11)}$$

Note

$$|f_y''(k_y^0)| > 0 \qquad \text{(E-12)}$$

$$I(k_x, R) = 2\sqrt{\frac{\pi}{2R|f_y''(k_y^0)|}} \Phi(k_x, k_y^0) e^{iRf_y(k_y^0) - i\frac{\pi}{4}} \qquad \text{(E-13)}$$

$$\therefore \quad I = \sqrt{\frac{2\pi}{R}} \frac{\cos\theta \; e^{-i\frac{\pi}{4}}}{(1 - \sin^2\theta \cos^2\phi)^{\frac{3}{4}}}$$

(E-14)

$$\int_{-k}^{k} (k^2 - k_x^2)^{\frac{1}{4}} \Phi(k_x, k_y^0) \, e^{iR\left[k_x \sin\theta \cos\phi + \sqrt{k_x^2 - k^2} \; \sqrt{1 - \sin^2\theta \cos^2\phi} \right]} dk_y$$

Following the same procedure:

$$k_x^0 = k \sin\theta \cos\phi \tag{E-15}$$

$$0 \leq \left| \sin\theta \cos\phi \right| \leq 1 \tag{E-16}$$

$$f_x''(k_x^0) = \frac{-1}{k(1 - \sin^2\theta \cos^2\phi)} \tag{E-17}$$

After the cancelling and rearranging of terms

$$I = \frac{-2i\pi k \cos\theta}{R} \Phi(k_x^0, k_y^0) \, e^{ikR} \tag{E-18}$$

where

$$k_x^0 = k \sin\theta \cos\phi \tag{E-15}$$

$$k_y^0 = k \sin\theta \sin\phi \tag{E-19}$$

As a partial justification of the results of the Method of Stationary Phase to integration of the type shown above, consider the free-space Green's function in integral form, Eq. 2.

$$G = \frac{(2) \, e^{i|R-r'|k}}{4\pi|R-r'|} = \frac{i}{4\pi^2}$$

(E-20)

$$\int_{-\infty}^{\infty} dk_x \, dk_y \, \frac{e^{i\left[k_x(x - \eta) + k_y(y - \xi) + \sqrt{k^2 - (k_x^2 + k_y^2)} \, z \right]}}{\sqrt{k^2 - (k_x^2 + k_y^2)}}$$

Let $r' = 0$ and $R \to \infty$

$$G = \frac{e^{ikR}}{2\pi R} = \frac{i}{4\pi^2} \tag{E-21}$$

$$\int_{s(k)} dk_x\, dk_y \; \frac{e^{\,iR[\,k_x \sin\theta \cos\phi + k_y \sin\theta \sin\phi + \cos\theta \sqrt{k^2 - (k_x^2 + k_y^2)}\,]\, z}}{\sqrt{k^2 - (k_x^2 + k_y^2)}}$$

Therefore

$$\Phi(k_x, k_y) = \frac{1}{\sqrt{k^2 - (k_x^2 + k_y^2)}} \tag{E-22}$$

$$\Phi(k_x^0, k_y^0) = \frac{1}{\sqrt{k^2(1 - \sin^2\theta \cos^2\phi - \sin^2\theta \sin^2\phi)}} = \frac{1}{k \cos\theta} \tag{E-23}$$

$$\therefore \quad G = \frac{e^{ikR}}{2\pi R} = \frac{i}{4\pi^2} \left(\frac{-2i\pi k \cos\theta}{R}\right) \frac{1}{k \cos\theta}\, e^{ikR} = \frac{e^{ikR}}{2\pi R} \tag{E-24}$$

Therefore, the method gives the correct results in this case. The required symmetry of the radiated field is examined, it is found that they exhibit the required symmetry. Therefore, if the method above is in error, it must be in amplitude and not a function of angles. However, the calculation of the Poynting vector over the radiated field yields the correct results. Therefore it is assumed that the form for the integral is correct, even though the phase factor is not analytic at the end point of integration.

REFERENCES

1. M. Islam, "A Theoretical Treatment of Low-Frequency Loop Antennas with Permeable Cores," IRE Trans. PGAP, March 1963, pp. 162-169.

2. R. E. Burgess, "Iron-Cored Loop Receiving Aerial," Wireless Engineer, June 1946, pp. 172-178.

3. J. Herman, "Thin Wire Loop and Thin Biconical Antennas in Finite Media," Diamond Ord. Fuze Lab. Tech. Rept. No. TR-462, May 1957.

4. O. R. Cruzan, "Radiation Properties of a Thin Wire Loop Antenna Embedded in a Spherical Medium," IRE Trans. PGAP, Oct. 1959, pp. 345-352.

5. Saburo Adachi, "Impedance Characteristics of a Uniform Current Loop Having a Spherical Core," Ohio State Univ. Res. Foun. Rept. No. 662-26, April 1959.

6. C. T. Tai, "Radiation From a Uniform Circular Loop Antenna in the Presence of a Sphere," Stanford Res. Inst. Tech. Rept. No. 32, 1952.

7. D. M. Grimes, "Miniaturized Resonant Antenna Using Ferrites," J. Appl. Phys., Vol. 29, No. 3, March 1958, p. 401.

8. C. Polk, "Resonance and Supergain Effects in Small Ferromagnetically or Dielectrically Loaded Biconical Antennas," IRE Trans. PGAP, Dec. 1959.

9. L. Lewin, Advanced Theory of Waveguides, Iliffe and Sons, Ltd., London, 1951.

10. H. Levine and C. H. Papas, "Theory of the Circular Diffraction Antenna," J. Appl. Phys., Jan. 1951, pp. 29-43.

11. J. W. Galejs and T. W. Thompson, "Admittance of a Cavity-Backed Annular Slot Antenna," IRE Trans. PGAP, Nov. 1962, pp. 671-678.

12. J. W. Galejs, "Admittance of a Rectangular Slot Which is Backed by a Rectangular Cavity," IRE Trans. PGAP, March 1963, pp. 119-126.

13. J. E. Storer, Variational Solution to the Problem of the Symmetrical Cylindrical Antenna, Cruft Lab. Rept. TR 101, Harvard Univ., 1952.

14. M. H. Cohen, T. H. Crowley, and C. A. Levis, The Aperture Admittance of a Rectangular Waveguide Radiating Into Half Space, Ohio State Univ. Res. Foun. Rept. 339-22 of Nov. 1951.

15. V. H. Rumsey, "Traveling Wave Slot Antennas," J. Appl. Phys., Nov. 1953, pp. 1358-1365.

16. M. H. Cohen, "The Normal Modes of Cavity Antennas," Doctoral Dissertation, Ohio State Univ., 1952.

17. J. S. S. Kerr, "The Radiation Impedance of a Flanged Rectangular Waveguide," Doctoral Dissertation, Univ. of Ill., 1951.

REFERENCES (Cont.)

18. C. C. Nash, "The Input Impedance of a Rectangular Aperture Antenna," Doctoral Dissertation, Univ. of Ill., 1949.

19. V. Counter, Miniature Cavity Antennas, Microwave Laboratory, Stanford Univ., Rept. No. 105, Jan. 1950.

20. R. J. Tector, The Cavity-Backed Slot Antenna, Electrical Engineering Research Lab., University of Illinois, Technical Report No. 26.

21. A. T. Adams, The Rectangular Cavity Slot Antenna with Homogeneous Isotropic Loadin Cooley Electronics Laboratory Technical Report No. 147, University of Michigan, Ann Arbor, Michigan, March 1964.

22. D. J. Angelakos and M. M. Korman, "Radiation from Ferrite-Filled Aperture," Proc. IRE, Vol. 44, 1956, pp. 1463-1468.

23. G. Tyras and G. Held, "Radiation from a Rectangular Waveguide Filled with Ferrite," Microwave Theory and Techniques, MTT-6, 1958, pp. 268-277.

24. J. C. Palais, Impedance and Radiation Characteristics of a Ferrite Obstacle in the Aperture of a Rectangular Waveguide, Cooley Electronics Laboratory Technical Report No. 146, University of Michigan, Ann Arbor, Michigan, August 1964.

25. H. M. Barlow and J. Brown, "Radio Surface Waves," Oxford Univ. Press, 1962.

26. H. Levine and J. Schwinger, "On the Radiation of Sound from an Unflanged Circular Pipe," Phys. Rev., Feb. 1948, pp. 383-406.

27. B. Noble, Methods Based on the Wiener-Hopf Technique, Pergamon Press, Inc., N. Y., 1953.

28. L. A. Vajnshtehn, Propagation in Semi-Infinite Waveguides, Six papers translated by J. Schmoys, New York Univ., Inst. of Math. Sci., Rept. No. EM-63.

29. A. E. Heins, "The Scope and Limitations of the Method of Wiener and Hopf," Communications on Pure and Applied Mathematics, Vol. IX, 1956, pp. 447-461.

30. R. Mittra, "The Finite Range Wiener-Hopf Integral Equation and Boundary Value Problem in a Waveguide," IRE Transactions on Antennas and Propagation, Dec. 1959, pp. 5244-5254.

31. L. R. Walker and N. Wax, "Non-Uniform Transmission Lines and Reflection Coefficients," J. Appl. Phys., Vol. 17, 1946, pp. 1043-1045.

32. J. G. Gurley, "Impedance Matching by Means of Nonuniform Transmission Lines," Trans. of the IRE, PGAP-4, 1952, pp. 107-109.

33. R. W. Klopfenstein, "A Transmission Line Taper of Improved Design," Proc. IRE, 1956, pp. 31-35.

34. R. E. Collin, "The Optimum Tapered Transmission Line Matching Section," Proc. IRE, 1956, pp. 539-548.

35. Magnus Erdélyi and Tricomi Oberhettinger, Higher Transcendental Functions, Vol. 2, McGraw-Hill, N. Y., 1953.

36. R. F. Harrington, Time Harmonic Electromagnetic Fields, McGraw-Hill, N. Y., 1961.

37. H. Levine and J. Schwinger, "On the Theory of Diffraction by an Aperture in an Infinite Plane Screen · I," Physical Review, Vol. 74, No. 8, 1948, pp. 958-974.

38. E. T. Copson, Asymptotic Expansions, Cambridge, England: Cambridge Tracts in Mathematics and Mathematical Physics, 1965.

DISTRIBUTION LIST

No. of Copies	
20	Defense Documentation Center Attn: DDC-IRS Cameron Station (Bldg. 5) Alexandria, Virginia 22314
1	Office of Assistant Secretary of Defense (Research and Engineering) Attn: Technical Library, Rm. 3E1065 Washington, D. C. 20301
1	Bureau of Ships Technical Library Attn: Code 312 Main Navy Building, Rm. 1528 Washington, D. C. 20325
1	Chief, Bureau of Ships Attn: Code 454 Department of the Navy Washington, D. C. 20360
2	Director U. S. Naval Research Laboratory Attn: Code 2027 Washington, D. C. 20390
1	Commanding Officer and Director U. S. Navy Electronics Laboratory Attn: Library San Diego, California 92101
1	Commander U. S. Naval Ordnance Laboratory Attn: Technical Library White Oak, Silver Spring, Maryland 20910
1	Rome Air Development Center (EMTLD) Attn: Documents Library Griffiss Air Force Base New York 13440
1	Systems Engineering Group (SEPIR) Wright-Patterson Air Force Base Ohio 45433
2	Electronic Systems Division (ESTI) L. G. Hanscom Field Bedford, Massachusetts 01731

No. of Copies	
3	Commanding Officer U. S. Army Combat Developments Command Communications-Electronics Agency Fort Monmouth, New Jersey 07703
1	Commanding Officer U. S. Army Sec Agcy Combat Dev Actv Arlington Hall Station Arlington, Virginia 22212
1	Harry Diamond Laboratories Attn: Library Connecticut Avenue and Van Ness Street Washington, D. C. 20438
2	Commanding General, U. S. Army Security Agency, Arlington Hall Station Arlington, Virginia 22207 Attn: IALOG and IARD
1	Chief, Mountain View Office Electronic Warfare Lab., USAECOM P. O. Box 205 Mountain View, California 94042
1	Chief, Intelligence Materiel Dev Office Electronic Warfare Lab.,USAECOM Fort Holabird, Maryland 21219
1	Chief Missile Electronic Warfare Tech Area EW Lab, USA Electronics Command White Sands Missile Range, N. M. 88002
1	Chief, Willow Run Office CSTA Lab. USAECOM P. O. Box 618 Ann Arbor, Michigan 48107
1	USAECOM Liaison Officer MIT, BLDG 26, Rm. 131 77 Massachusetts Avenue Cambridge, Massachusetts 02139

DISTRIBUTION LIST (Cont.)

No. of Copies	
2	Chief of Research and Development Department of the Army Washington, D. C. 20315
2	Commanding General U. S. Army Materiel Command Attn: R & D Directorate Washington, D. C. 20315
1	USAECOM Liaison Office U. S. Army Electronic Proving Ground Fort Huachuca, Arizona 85613
16	Commanding General U. S. Army Electronics Command Fort Monmouth, N. J. 07703 Attn: AMSEL-EW " WL-D " WL-S (3 copies) " WL-N " WL-C " WL-E " HL-CT-DD " RD-MAT " RD-MAF " RD-MAF-2 " RD-GFR " XL-D " RD-LNA " KL-TM
1	USAECOM Liaison Officer Aeronautical Systems Division Attn: ASDL-9 Wright-Patterson AF Base, Ohio 45433
1	USAECOM Liaison Officer Rome Air Development Center Attn: EMPL Griffiss AF Base, New York 13440
1	Stanford Electronics Laboratories Stanford University Stanford, California Attn: Dr. D. G. Grace
1	Dr. T. W. Butler, Director Cooley Electronics Laboratory The University of Michigan Ann Arbor, Michigan 48105
10	Cooley Electronics Laboratory The University of Michigan Ann Arbor, Michigan 48105

UNCLASSIFIED
Security Classification

DOCUMENT CONTROL DATA - R&D
(Security classification of title, body of abstract and indexing annotation must be entered when the overall report is classified)

1. ORIGINATING ACTIVITY (Corporate author) Cooley Electronics Laboratory The University of Michigan Ann Arbor, Michigan	2a. REPORT SECURITY CLASSIFICATION Unclassified 2b. GROUP

3. REPORT TITLE

Analysis of an Aperture Antenna System Loaded with an Inhomogeneous Dielectric

4. DESCRIPTIVE NOTES (Type of report and inclusive dates)

7695-12-T (TR 180) - May 1967

5. AUTHOR(S) (Last name, first name, initial)

Bitler, J. Samuel

6. REPORT DATE	7a. TOTAL NO. OF PAGES	7b. NO. OF REFS
May 1967	134	38

8a. CONTRACT OR GRANT NO.	9a. ORIGINATOR'S REPORT NUMBER(S)
DA 28-043-AMC-01870(E) b. PROJECT NO. 1 PO 21101 AO42.01.02 c. d.	7695-12-T 9b. OTHER REPORT NO(S) (Any other numbers that may be assigned this report) ECOM-01870-180

10. AVAILABILITY/LIMITATION NOTICES

Distribution of this report is unlimited.

11. SUPPLEMENTARY NOTES	12. SPONSORING MILITARY ACTIVITY
	U. S. Army Electronics Command Electronic Warfare Lab., AMSEL-WL-S Fort Monmouth, N. J. 07703

13. ABSTRACT An analysis is made of an aperture system loaded with an inhomogeneous dielectric. The system consists of two parts. The first part is a section of rectangular waveguide extending from negative infinity along the z-axis to a distance z_0 back from an infinite, perfectly conducting ground plane, whose normal is also in the z direction. This section of waveguide is filled with a homogeneous dielectric. The second part is a section of rectangular waveguide of the same dimensions extending from z_0 to an aperture in the ground plane. This section of waveguide is filled with an inhomogeneous dielectric. The dielectric is characterized by a permeability and permittivity that varies exponentially with distance from the aperture.

At first the waveguide containing the inhomogeneous dielectric was considered to extend to negative infinity. A set of modes was found to satisfy Maxwell's equations and the required aperture symmetries when the field incident at the aperture was a conventional TE_{10} mode. The fields on the free-space side of the aperture were written in integral form using the free-space Green's Function as a kernel and the aperture electric field as its source.

DD FORM 1 JAN 64 1473

UNCLASSIFIED
Security Classification

14. KEY WORDS	LINK A		LINK B		LINK C	
	ROLE	WT	ROLE	WT	ROLE	WT

INSTRUCTIONS

1. ORIGINATING ACTIVITY: Enter the name and address of the contractor, subcontractor, grantee, Department of Defense activity or other organization *(corporate author)* issuing the report.

2a. REPORT SECURITY CLASSIFICATION: Enter the overall security classification of the report. Indicate whether "Restricted Data" is included. Marking is to be in accordance with appropriate security regulations.

2b. GROUP: Automatic downgrading is specified in DoD Directive 5200.10 and Armed Forces Industrial Manual. Enter the group number. Also, when applicable, show that optional markings have been used for Group 3 and Group 4 as authorized.

3. REPORT TITLE: Enter the complete report title in all capital letters. Titles in all cases should be unclassified. If a meaningful title cannot be selected without classification, show title classification in all capitals in parenthesis immediately following the title.

4. DESCRIPTIVE NOTES: If appropriate, enter the type of report, e.g., interim, progress, summary, annual, or final. Give the inclusive dates when a specific reporting period is covered.

5. AUTHOR(S): Enter the name(s) of author(s) as shown on or in the report. Enter last name, first name, middle initial. If military, show rank and branch of service. The name of the principal author is an absolute minimum requirement.

6. REPORT DATE: Enter the date of the report as day, month, year; or month, year. If more than one date appears on the report, use date of publication.

7a. TOTAL NUMBER OF PAGES: The total page count should follow normal pagination procedures, i.e., enter the number of pages containing information.

7b. NUMBER OF REFERENCES: Enter the total number of references cited in the report.

8a. CONTRACT OR GRANT NUMBER: If appropriate, enter the applicable number of the contract or grant under which the report was written.

8b, 8c, & 8d. PROJECT NUMBER: Enter the appropriate military department identification, such as project number, subproject number, system numbers, task number, etc.

9a. ORIGINATOR'S REPORT NUMBER(S): Enter the official report number by which the document will be identified and controlled by the originating activity. This number must be unique to this report.

9b. OTHER REPORT NUMBER(S): If the report has been assigned any other report numbers *(either by the originator or by the sponsor)*, also enter this number(s).

10. AVAILABILITY/LIMITATION NOTICES: Enter any limitations on further dissemination of the report, other than those imposed by security classification, using standard statements such as:

(1) "Qualified requesters may obtain copies of this report from DDC."

(2) "Foreign announcement and dissemination of this report by DDC is not authorized."

(3) "U. S. Government agencies may obtain copies of this report directly from DDC. Other qualified DDC users shall request through _____."

(4) "U. S. military agencies may obtain copies of this report directly from DDC. Other qualified users shall request through _____."

(5) "All distribution of this report is controlled. Qualified DDC users shall request through _____."

If the report has been furnished to the Office of Technical Services, Department of Commerce, for sale to the public, indicate this fact and enter the price, if known.

11. SUPPLEMENTARY NOTES: Use for additional explanatory notes.

12. SPONSORING MILITARY ACTIVITY: Enter the name of the departmental project office or laboratory sponsoring *(paying for)* the research and development. Include address.

13. ABSTRACT: Enter an abstract giving a brief and factual summary of the document indicative of the report, even though it may also appear elsewhere in the body of the technical report. If additional space is required, a continuation sheet shall be attached.

It is highly desirable that the abstract of classified reports be unclassified. Each paragraph of the abstract shall end with an indication of the military security classification of the information in the paragraph, represented as *(TS), (S), (C), or (U)*.

There is no limitation on the length of the abstract. However, the suggested length is from 150 to 225 words.

14. KEY WORDS: Key words are technically meaningful terms or short phrases that characterize a report and may be used as index entries for cataloging the report. Key words must be selected so that no security classification is required. Identifiers, such as equipment model designation, trade name, military project code name, geographic location, may be used as key words but will be followed by an indication of technical context. The assignment of links, rules, and weights is optional.